5-2015

Ontogenesis in the Cranium of Alligator mississippiensis Based on Disarticulated Cranial Elements

William Henry Harris
East Tennessee State University

Ontogenesis in the Cranium of *Alligator mississippiensis* Based on Disarticulated Cranial Elements

---

A thesis

presented to

the faculty of the Department of Geosciences

East Tennessee State University

In partial fulfillment

of the requirements for the degree

Master of Science in Geosciences

---

by

William H. Harris

May 2015

Blaine W. Schubert, Chair

Steven C. Wallace

Jim I. Mead

Keywords: Landmark Morphometrics, *Alligator*, Cranium, Ontogenesis

ABSTRACT

Ontogenesis in the Cranium of *Alligator mississippiensis*

Based on Disarticulated Cranial Elements

by

William H. Harris

The American alligator, *Alligator mississippiensis*, is a large extant archosaur and member of the Order Crocodilia. Crocodilian ontogeny has been studied in great detail, the skull being of particular interest. One aspect of the skull left unstudied is how individual cranial elements change through ontogeny independent of one another. This study observed morphological change in a growth series of 34 specimens of *A. mississippiensis* from ETSU Vertebrate Paleontology Lab collections. The premaxilla, maxilla, nasal, jugal, frontal, and parietal were analyzed using landmark morphometrics. The frontal, jugal, and parietal showed more allometric growth with the orbits reducing in size posteriorly. The premaxilla, maxilla, and nasal showed more isometric growth. This suggests the common observation that the snout elongates with age is mistaken. The cranium showed allometric growth in very early in life but more isometric growth after that. Unique to this study, the premaxilla showed almost no shape change throughout ontogeny.

ACKNOWLEDGEMENTS

I would first like to thank my professors, who also make up my committee: Dr. Blaine Schubert, Dr. Steven Wallace, and Dr. Jim Mead; for reading my thesis and helping me through the research as well as the writing. I'd like to thank Gene Pritchett for donating the specimens to ETSU. Thank you to everyone at the ETSU Natural History Museum; Brett for making the collection available and everyone else for making my GA work during this time so pleasant. Of course thanks to my parents, they have given me endless support throughout these last three years. I surely would have had a rougher time, and may not have made it, without even the knowledge that I could always count on them for help. Thank you to Sandy for helping me with my images in Photoshop. Finally, I want to thank all my friends who were always there to help me stay sane during it all. Both friends close and long distance who supported me all the way through this, Ana Sampson especially. I'm not going to list everyone here in TN but everybody form D&D and movie nights, you know who you are. Without those times of pure fun this would have been an unachievable goal for me.

TABLE OF CONTENTS

LIST OF TABLES

Table

LIST OF FIGURES

Figure

CHAPTER 1

INTRODUCTION

The American alligator, *Alligator mississippiensis*, is a large member of the Order Crocodilia, which includes crocodiles, caimans, and the gharial. This alligator is also the largest extant member of its genus, the only other extant member being the Chinese alligator, *A. sinensis*. *Alligator mississippiensis* has been heavily studied. Reasons for such focus on this species include: their large increase in size from juvenile to adult (Neill 1971; Dodson 1975; McIlhenny 1987; Brisbin 1988; Jacobsen and Kushlan 1989; Gignac 2010; Gignac and Erickson 2014); ease of obtaining specimens, compared to other crocodilians, for study (Dodson 1975); extreme shifts in diet throughout ontogeny (Erickson et al. 2003; Gignac 2010; Gignac and Erickson 2014); accompanied by the fact that they are a large extant archosaur which makes them ideal stand-ins for looking at fossil archosaurs, such as dinosaurs (Dodson, 1975; Brochu 1996; Farlow et al. 2005; Rayfield et al. 2007; Snyder 2007; Bonnan et al. 2008; Holliday and Witmer 2008; Tsai and Holliday 2011).

The research presented here focuses primarily on osteological ontogeny. Previous studies have looked at the ontogeny of both the postcranial (Dodson 1975; Farlow et al. 2005; Bonnan et al. 2008; Vickaryous and Hall. 2008) and cranial aspects of alligators (Mook 1921a; Mook 1921b; Dodson 1975; Woodward et al. 1995; Erickson et al. 2003; Erickson et al. 2004; Sadleir 2009; Gignac 2010; Holliday 2011; Tsai and Holliday 2011). The skull is highly informative because crocodilians rely so heavily on their jaws to interact with their environment (Gignac 2010). Cranial studies have dealt with all extant crocodilians (e.g. Mook 1921a; Mook 1921b; Brongersma 1941; Greer 1974; Brisbin 1988; Portier 1994; Busbey 1995; Erickson et al. 2004;

Wu et al. 2006; Hall and Pierce et al. 2008; Platt et al. 2009). These studies show that the snout elongates and narrows from hatchlings to adults, and the teeth become blunter compared to their sharp juvenile forms (Mook 1921a; Mook 1921b; Dodson 1975; Erickson et al. 2003; Sadleir 2009). A high degree of morphological divergence was also found between wild and captive-reared alligators, with the jaws of the captive animals being shorter and broader than their wild counterparts, showing a high degree of plasticity commonly found in crocodilians (Busbey 1995; Erickson et al. 2004; Pierce et al. 2008). However, in all ontogenetic cranial studies to date, only the articulated skull was used, never the isolated bones. It seems plausible that disarticulated cranial elements could yield a clearer picture of how the different portions of the skull are changing though ontogeny. It is surmised that this approach could have important implications for better understanding the growth, ecomorphology, and evolution of *A. mississippiensis*. These two premises form the foundation of the study presented here.

By implementing landmark analysis, specific bones of the cranium were examined for ontogenetic and allometric change in *A. mississippiensis*. The results were used to test the hypotheses:

1) That isolated cranial elements tested will show evidence of morphological change through ontogeny;
2) That isolated cranial elements will show differing degrees of allometric change through ontogeny;
3) The morphological change demonstrated will differ from results provided by previous analyses of complete crania.

CHAPTER 2

MATERIALS AND METHODS

A series of isolated cranial bones was selected to represent focal areas of the skull, which included: bones constituting the rostrum—premaxilla, maxilla, and nasal; and three bones from the mid and posterior of the skull—jugal, frontal, and parietal. Rostral bones were selected due to their importance in food acquisition while the more posterior elements were selected to gain insight into the proportional changes through ontogeny between the anterior and posterior of the cranium. Whenever possible right-side elements were used, if none were available the left-side element was photographed and the image inverted for analysis. All specimens came from the collections of the ETSU Vertebrate Paleontology Lab (ETVP), held at the General Shale Brick Natural History Museum and Visitor Center in Gray, TN.

Specimens included complete skeletons to partial crania, all disarticulated as much as fusion would allow. In total, 34 specimens were used in the study, these consisted of 29 premaxillae, 34 maxillae, 20 nasals, 32 jugals, 27 frontals, and 21 parietals. All specimens were from wild populations in Georgia and were collected by Gene Pritchett, a nuisance alligator trapper who donated the carcasses to the ETVP Collections. The only exceptions are the smallest specimens, (ETVP 7197 and ETVP 7198) which come from farms, and the large complete-skull specimen (NVPL 265), which was collected by S. Wallace in Arkansas.

Photography

All of the bones were photographed in dorsal and ventral view except for the jugal and nasal, in which only one view provided the majority of possible landmarks. Photograph were taken using a Panasonic DMC-FH25 digital camera mounted on a stand and set to intelligent auto. Each bone was placed on a felt or sand surface with a scale bar and label beside it.

Premaxilla, maxilla, and nasal were positioned so that the medial sutures were parallel with the bottom of the camera frame. For the dorsal view of the premaxilla and maxilla, the palate was laid flat on the photography surface while the ventral view was achieved by propping up the lateral edge so that the palate was level. For the dorsal view of the nasal, it was simply laid dorsal side up. Jugal was placed exterior side down with the medial edge of the maxillary scarf joint (the anterior portion that overlaps the posterior of the maxilla) positioned parallel to the bottom of the frame (only the interior surface was photographed). Frontal was aligned so its midline was parallel to the bottom of the camera frame, placed flat on its ventral surface for the dorsal image, and balanced on the orbital margins for the ventral image. Parietal was positioned with the parietal-frontal suture parallel with the bottom of the frame. For the dorsal image, it was propped up so the cranial table surface was level, and for the ventral image, it was laid flat on its exterior surface. Image numbers and letters were used to differentiate the specimens since elements of one skull would share a collections number. For instance, 7205PML869 represents collections number ETVP 7205, premaxilla (PM), left element (L), and photo 869, in case more than one premaxilla was stored with this collections number. Specimen numbers are in the measurement graphs in Appendix A and the photographs will be stored in the ETVP Collections.

Measurements

Each bone was measured to place them in Size Groups (SG) representing ontogenetic growth stages (Fig. 1). These categories do not represent known age groups. Due to the variable growth rate of crocodilians, exact age is difficult to ascertain and will not be dealt with in this study (Jacobsen and Kushlan 1989). However, these SGs do represent developmental stages that are separated by size. Measurements were obtained using an IP66 & IP67 ABS Coolant Proof Caliper (150 mm) and a Fowler Heavy Duty Electronic Digital Caliper (600 mm) and are

presented in Appendix A. Each bone was measured three times and the average taken to account for any measurement errors. To create the SGs the total range of measurements for each bone was divided into five equal ranges and the bones were placed in each range accordingly (Table 1 and 2). The nasal was the only bone that did not occupy all SGs, no bones of SG2 were available.

Landmarks

Landmarks were digitally placed on the photographs using the program tpsDig (Rohlf 2009a). Once all landmarks were placed the resulting files of each SG were combined using tpsUtil (Rohlf 2009b). Files were then superimposed with the tpsSuper program and converted to Shape Variables using the Procrustes fit function (Rohlf 2009c). First a file was created for each SG, for the use in the thin plate splines, and finally all were superimposed and resized together into a master file, for use in the statistical analyses. Finally the master file was reformatted into a Microsoft Excel 2013 spreadsheet and saved for analysis. These steps were followed for both the dorsal and ventral views of each bone. Many of the landmarks followed Sadleir (2009), looking at articulated crania (Fig. 2, 3, 4, 5, 6, 7, 8, 9, 10, and 11). Terminology follows Holliday (2011) and Kardong and Zalisko (2012). Landmarks were placed in an attempt to account for the overall shape, an outline of the bone, as well as critical features. Following Bookstein (1991) Type I landmarks are points at the intersections of multiple tissues, usually where three or more bones meet; Type II landmarks are maximum points of curvature and tips of excursions or other features; and Type III are points described as farthest, closest, perpendicular, tangential, or similar adjectives with reference to some other feature or point. Here, primarily Type II and Type III landmarks were used. No Type I landmarks were used since only individual bones were being observed.

Table 1: Bone Size Group (SG) Ranges. All measurements are in mm.

Bone	Size Ranges	SG1	SG2	SG3	SG4	SG5
Premax	10.81-76.47	10.81-23.94	23.95-37.07	37.08-50.20	50.21-63.33	63.34-76.47
Maxilla	33.88-241.11	33.88-75.33	75.34-116.78	116.79-158.23	158.24-199.68	199.67-241.11
Nasal	22.06-218.52	22.06-61.35	61.36-100.64	100.65-139.93	139.94-179.22	179.23-218.52
Jugal	30.02-195.10	30.02-63.04	63.05-96.06	96.07-129.08	129.09-162.10	153.84-195.10
Frontal	25.45-139.15	25.45-48.19	48.20-70.93	70.94-93.67	93.68-116.41	116.41-139.15
Parietal	12.53-52.92	12.53-21.41	21.42-29.29	29.30-37.17	37.18-45.05	45.06-52.92

Premax=premaxilla

Table 2: Numbers of Specimens of each Skeletal Element in each Size Group (SG).

Distribution	Size Groups				
Bone	SG1	SG2	SG3	SG4	SG5
Premaxilla	2	3	7	14	3
Maxilla	2	2	15	12	3
Nasal	2	0	6	8	4
Jugal	2	5	5	15	5
Frontal	2	2	9	11	3
Parietal	2	1	6	9	3

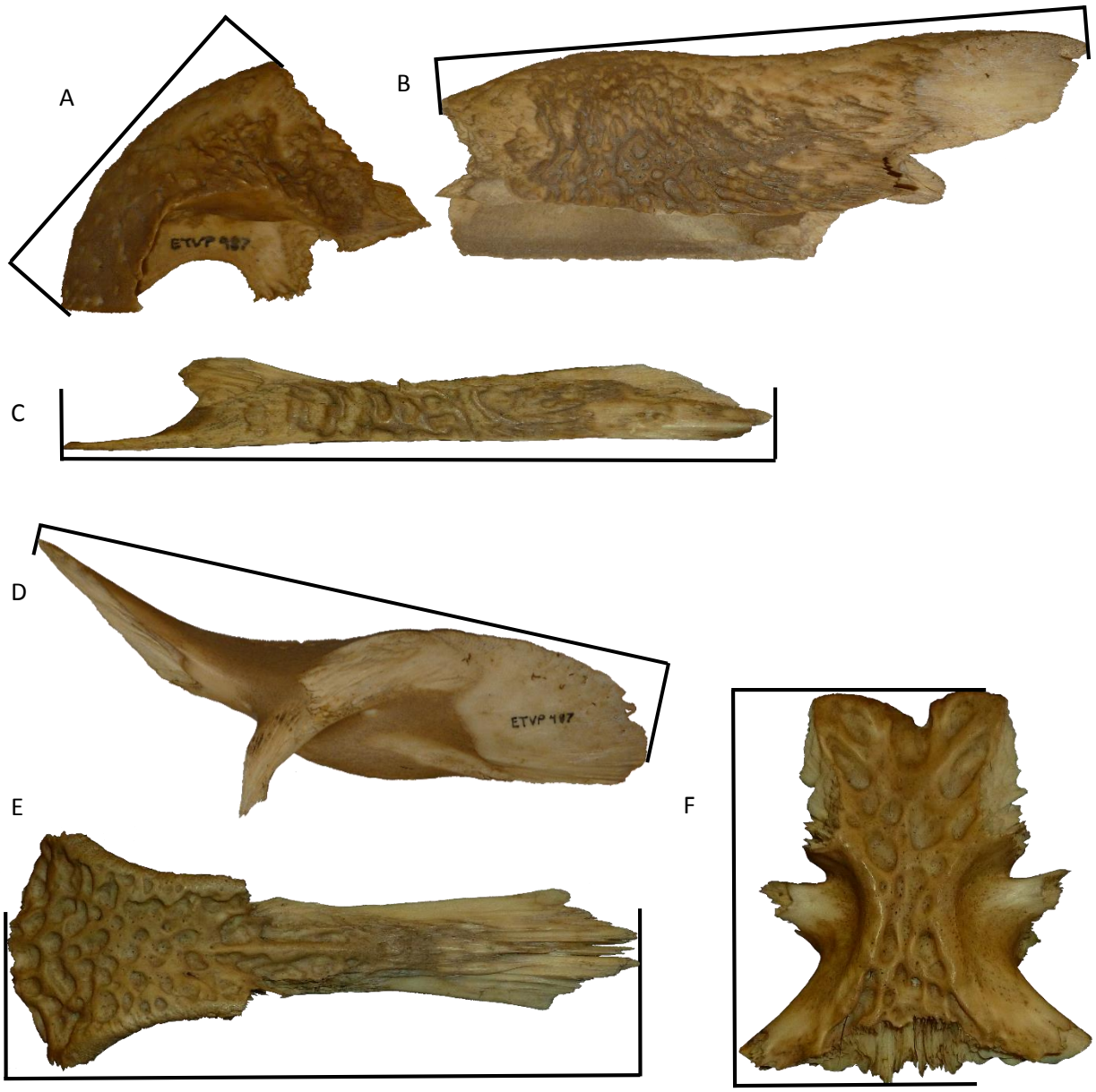

Figure 1 – Measurements of cranial bones: **A**, Premaxilla was measured from the anterior-most point of the premaxilla along the anterior premaxillary suture, to the lateral-most point of the premaxilla-maxilla suture (Specimen 487PM702). **B**, Maxilla was measured from the lateral-most edge of the maxilla-premaxilla suture to the posterior-most point of the maxilla-ectopterygoid suture (Specimen 3235M327). **C**, Nasal measured from the anterior extent of the nasal medial suture, tip of the internarial strut to the posterior extent of the nasal (Specimen 487N136). **D**, Jugal was measured from the most posterior point of the quadratojugal suture to the anterior-most point of the jugal (Specimen 3235J437). **E**, Frontal was measured with the edges of the caliper jaws flat against the posteromedial-most point of the frontal-parietal suture and flat against the anterioventral extent of the frontal-nasal suture (Specimen 487F133). **F**, Parietal was measured with the edges of the caliper jaws flat against the frontal-parietal suture and flat against the posterior edge (Specimen 487P144).

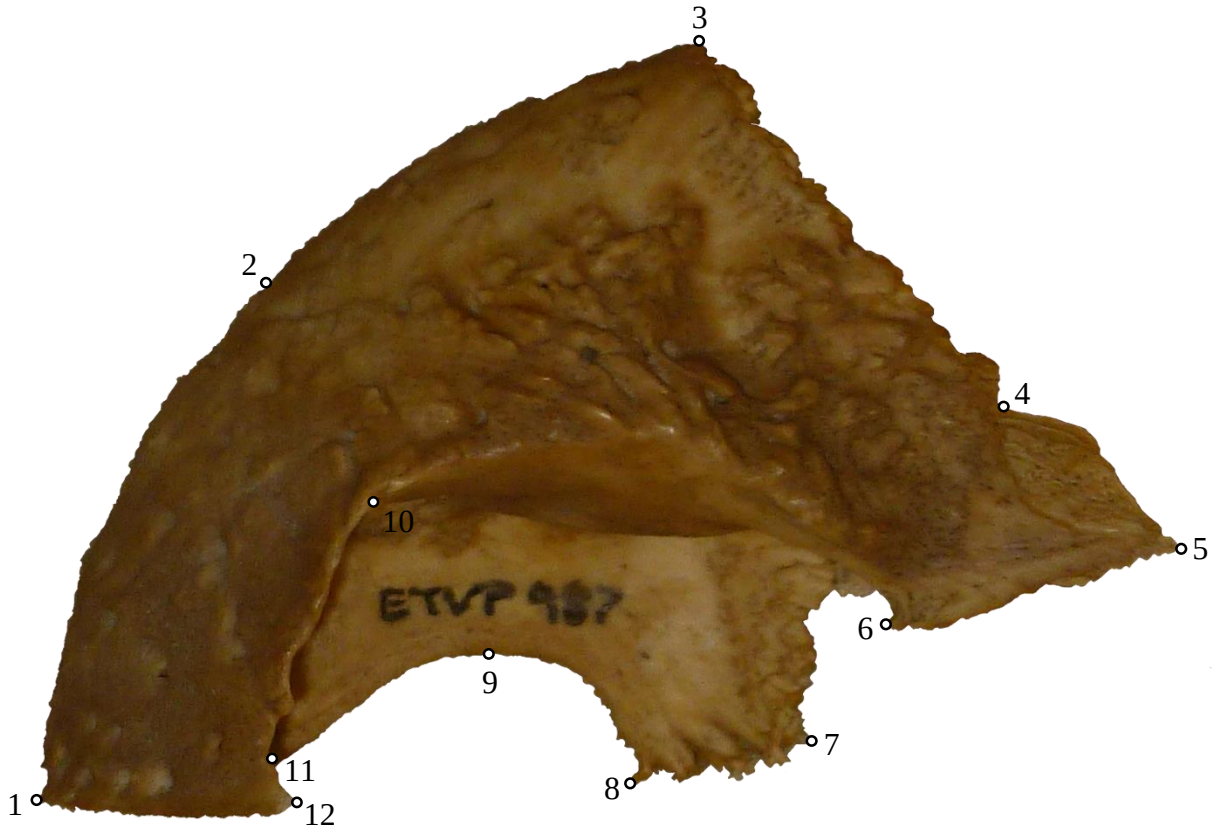

Figure 2 – Premaxilla landmarks in dorsal view (Specimen 487PM702, SG4): (1) Anterior-most point of the premaxilla along the anterior premaxillary suture. (2) The point at the anterior edge of the premaxilla perpendicular to a point equidistant from landmarks 1 and 3. (3) Lateral-most point of the premaxilla-maxilla suture. (4) The anterolateral extent of the ascending process. (5) Posterior extent of the premaxilla-nasal-maxilla suture. (6) The anteromedial extent of the premaxilla-nasal suture. (7) Posterior extent of the palatal process premaxillary suture. (8) Anterior extent of the palatal process premaxillary suture. (9) Lateral-most point of the nares ventral fenestra. (10) The point of the anterior edge of the nares dorsal fenestra that is closest to the anterior edge of the premaxilla. (11) Anteromedial-most point of the nares dorsal fenestra. (12) Posterior extent of the premaxillary internarial strut. Following Bookstein (1991), landmarks classify as: Type II = 1, 3, 5, 6, 7, 8, 11, 12; and Type III = 2, 4, 9, 10.

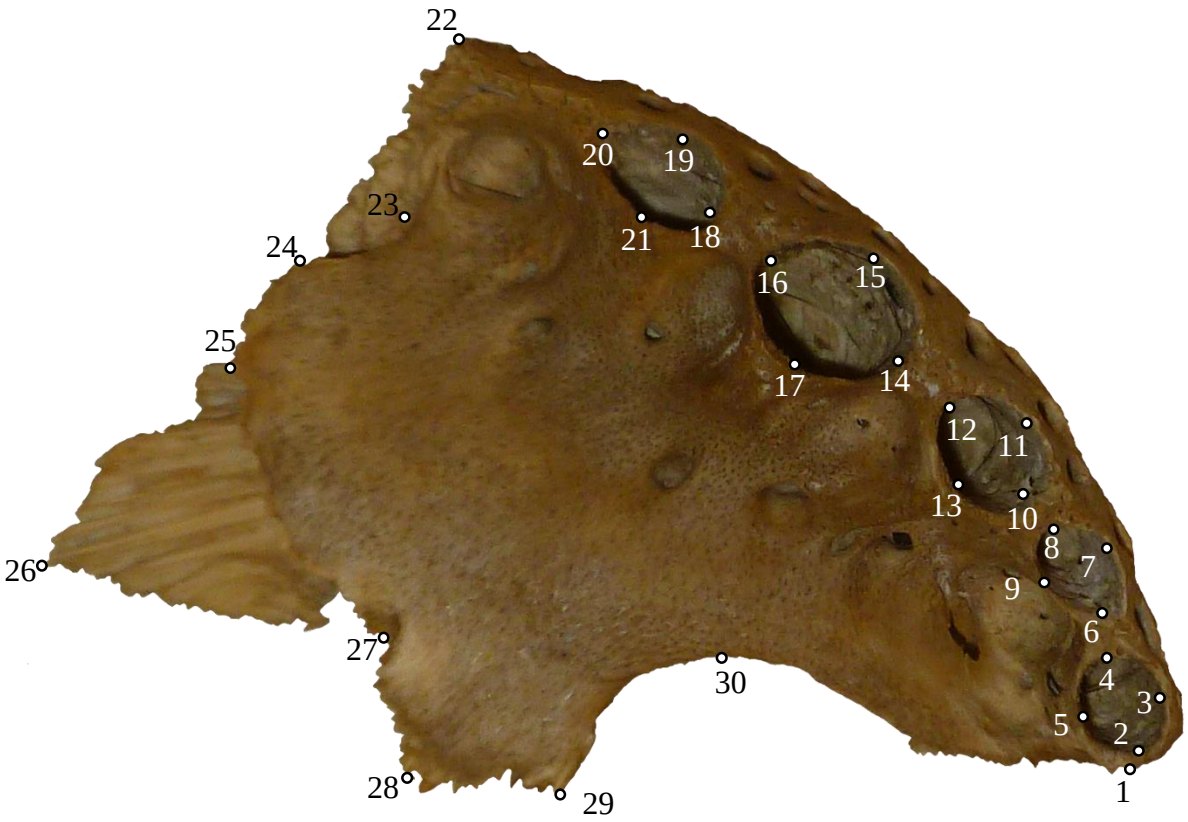

Figure 3 – Premaxilla landmarks in ventral view (Specimen 487PM705, SG4): (1) Anterior-most point of the premaxilla along the anterior premaxillary suture. (2) Mesial interproximal edge of the 1st (2), 2nd (6), 3rd (10), 4th (14), and 5th (18) alveoli of the premaxilla. Lateral margin of the tooth row and orthogonal to the center of the 1st (3), 2nd (7), 3rd (11), 4th (15), and 5th (19) alveoli of the premaxilla. Distal interproximal edge of the 1st (4), 2nd (8), 3rd (12), 4th (16), and 5th (20) alveoli of the premaxilla. Lingual margin of the tooth row and orthogonal to the center of the 1st (5), 2nd (9), 3rd (13), 4th (17), and 5th (21) alveoli of the premaxilla. (22) Lateral-most point of the premaxilla-maxilla suture. (23) Apex of the lateral concave curve of the premaxilla-maxilla suture. (24) Lateral edge of the lateral convex curve of the premaxilla-maxilla suture. (25) Posterior-most point of the secondary palate along the premaxilla-maxilla suture. (26) Posterior extent of the premaxilla-nasal-maxilla suture. (27) Apex of the medial concave curve of the premaxilla-maxilla suture. (28) Posterior extent of the palatal process premaxillary suture. (29) Anterior extent of the palatal process premaxillary suture. (30) Lateral-most point of the nares ventral fenestra. Following Bookstein (1991), landmarks classify as: Type II = 1, 2, 4, 6, 8, 10, 12, 14, 16, 18, 20, 22, 23, 26, 28, 29; and Type III = 3, 5, 7, 9, 11, 13, 15, 17, 19, 21, 24, 25, 30.

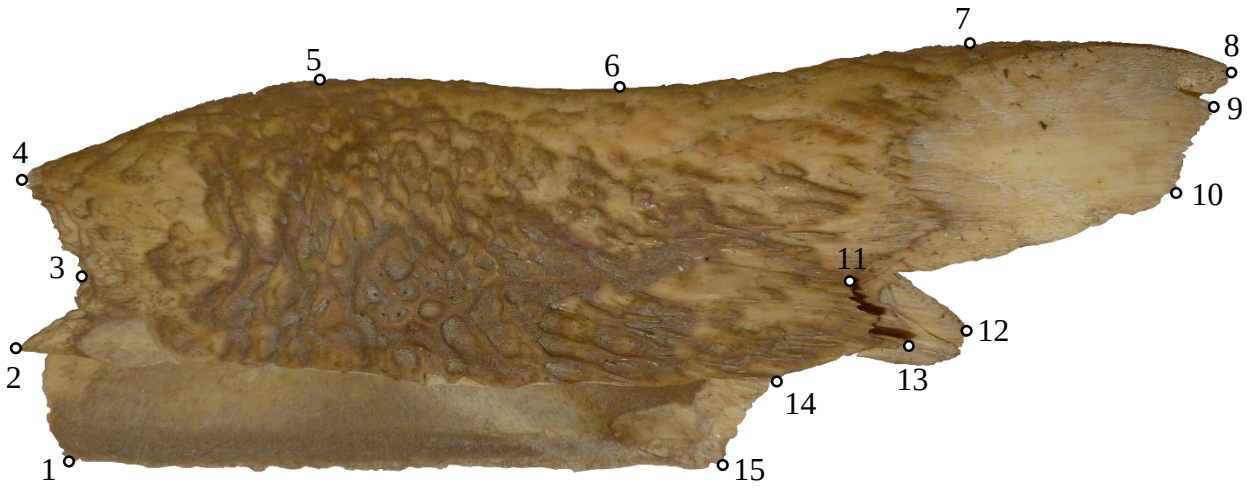

Figure 4 – Maxilla landmarks in dorsal view: Specimen 487M699, SG4. (1) The anterior-most point of the maxillary medial suture. (2) Anterior-most point of the nasal cavity and premaxilla suture. (3) Posterior point in the curve of the maxilla-premaxilla suture. (4) Lateral-most edge of the maxilla-premaxilla suture. Landmarks 5, 6, and 7 are placed along the lateral edge of the maxilla perpendicular to points spaced evenly along a line drawn between landmarks 4 and 8. (8) Posterior-most point of the maxilla-ectopterygoid suture. (9) Posterior-most point of the maxilla-jugal-ectopterygoid suture. (10) Ventral point of the maxilla-lachrymal-jugal suture. (11) Anterior-most point of the dorsal edge of the maxilla-lachrymal suture. (12) Posterior point of the palatine-maxilla suture. (13) Posterior point of the maxilla-prefrontal-lachrymal suture. (14) Anterior point of the maxilla-prefrontal-nasal suture. (15) The posterior-most point of the maxillary medial suture. When LM 8 was not visible it was placed beside LM 9. Following Bookstein (1991), landmarks classify as: Type II = 1, 2, 3, 4, 8, 9, 10, 11, 13, 14, 15; and Type III = 5, 6, 7, 12.

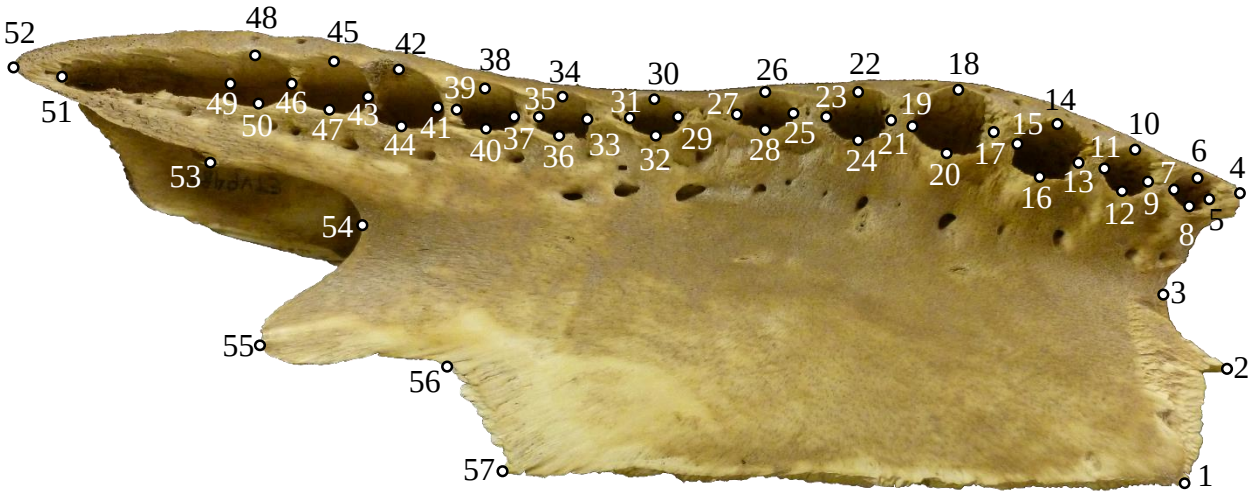

Figure 5 – Maxilla landmarks in ventral view: Specimen 487M833, SG4. (1) Anterior of the maxillary suture. (2) The anterior-most point of the nasal cavity and premaxilla suture. (3) Posterior point in the curve of the maxilla-premaxilla suture. (4) Lateral-most edge of the maxilla-premaxilla suture. Mesial interproximal edge of the 1st(5), 2nd(9), 3rd(13), 4th(17), 5th(21), 6th(25), 7th(29), 8th(33), 9th(37), and 10th(41) alveoli of the maxilla. Lateral margin of the tooth row and orthogonal to the center of the 1st(6), 2nd(10), 3rd(14), 4th(18), 5th(22), 6th(26), 7th(30), 8th(34), 9th(38), 10th(42), 11th(45), and 12th(48) alveoli of the maxilla. Distal interproximal edge of the 1st(7), 2nd(11), 3rd(15), 4th(19), 5th(23), 6th(27), 7th(31), 8th(35), 9th(39), and 12th(49) alveoli of the maxilla. Lingual margin of the tooth row and orthogonal to the center of the 1st(8), 2nd(12), 3rd(16), 4th(20), 5th(24), 6th(28), 7th(32), 8th(36), 9th(40), 10th(44), 11th(47), and 12th(50) alveoli of the maxilla. (43) Interproximal point of the 10th and 11th alveoli of the maxilla. (46) Interproximal point of the 11th and 12th alveoli of the maxilla. (51) Posterior limit of tooth row. (52) Posterior limit of maxilla. (53) The anteromedial limit of the maxilla-ectopterygoid suture along the lateral margin of the suborbital fenestra. (54) The anterior limit of the suborbital fenestra. (55) Posterior point of the palatine-maxilla suture. (56) Apex of the curve of the palatine-maxilla suture. (57) Posterior of the maxillary suture. If interproximal edges were not present then both LM were placed at interproximal region. Following Bookstein (1991), landmarks classify as: Type II = 1, 2, 4, 5, 7, 9, 11, 13, 15, 17, 19, 21, 23, 25, 27, 29, 31, 33, 35, 37, 39, 41, 43, 46, 49, 52, 53, 55, 56, 57; and Type III = 3,6, 8, 10, 12, 14, 16, 18, 20, 22, 24, 26, 28, 30, 32, 34, 36, 38, 40, 42, 44, 45, 47, 48, 50, 54.

Figure 6 – Nasal landmarks: Specimen 487N136, SG4. (1) Anterior extent of the nasal medial suture, tip of the internarial suture. (2) The posterior-most point of the nares on the anterior edge of the nasal-premaxilla suture. (3) The anterior extent of the nasal-premaxilla suture. (4) The posterolateral extent of the nasal-premaxilla suture. (5) The posterior extent of the nasal-premaxilla suture. (6) The posterior extent of the nasal-premaxilla suture process. Landmarks 7 and 8 were placed at points at the lateral edge of the nasal-premaxilla suture perpendicular to points spaced evenly between landmarks 6 and 9. (9) Posterior extent of the nasal. (10) Posterior extent of the nasal medial suture. Following Bookstein (1991), landmarks classify as: Type II = 1, 4, 5, 6, 9, 10; and Type III = 2, 3, 7, 8.

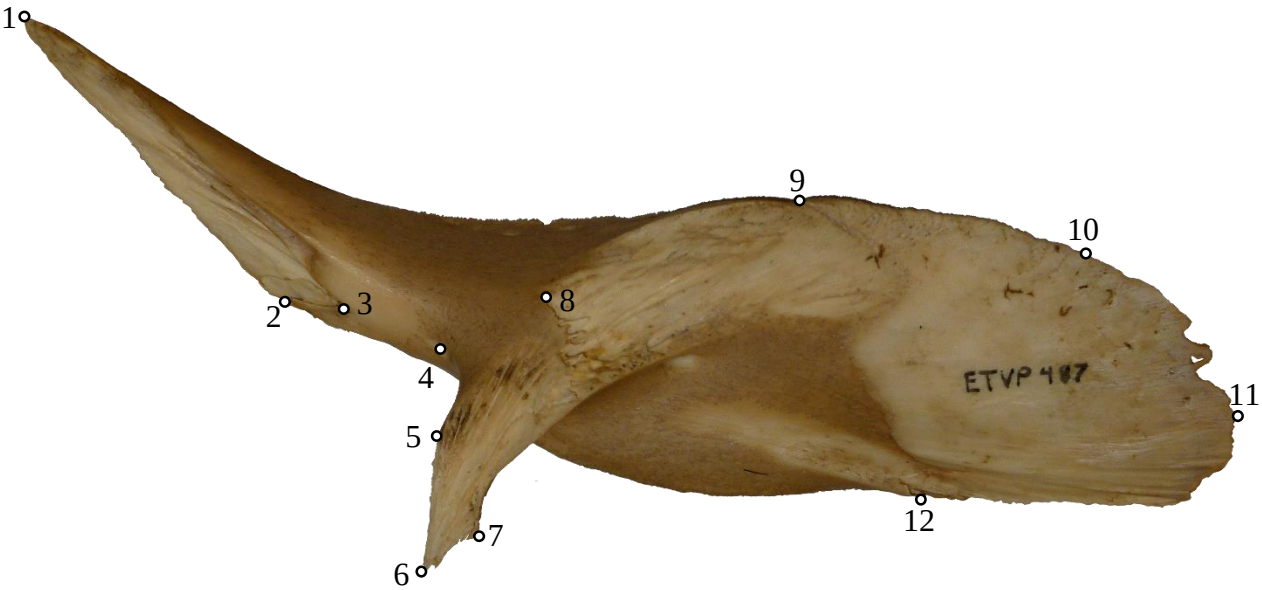

Figure 7 – Jugal landmarks: Specimen 487J804, SG4. (1) Most posterior point of the quadratojugal suture. (2) Anterior point of the quadratojugal suture along the medial edge. (3) Most anterior point of the quadratojugal suture. (4) Center of foramen posterior the postorbital bar. (5) Posterior-most extent of postorbital suture. (6) Distal-most point of postorbital suture. (7) Ventral-most point of postorbital suture. (8) Posterior-most point of the ectopterygoid suture. (9) Posterolateral extent of jugal-maxilla suture where it meets the ectopterygoid suture. (10) The point at the lateral edge of the jugal-maxilla perpendicular to a point equidistant from landmarks 9 and 11. (11) The anterior-most point of the Jugal. (12) Posterolateral limit of the lachrymal suture. When the tip of the anterior portions were missing the curve was followed and predicted where LM 11 would have fallen. Following Bookstein (1991), landmarks classify as: Type II = 1, 2, 3, 4, 5, 6, 7, 9, 12; and Type III = 8, 10, 11.

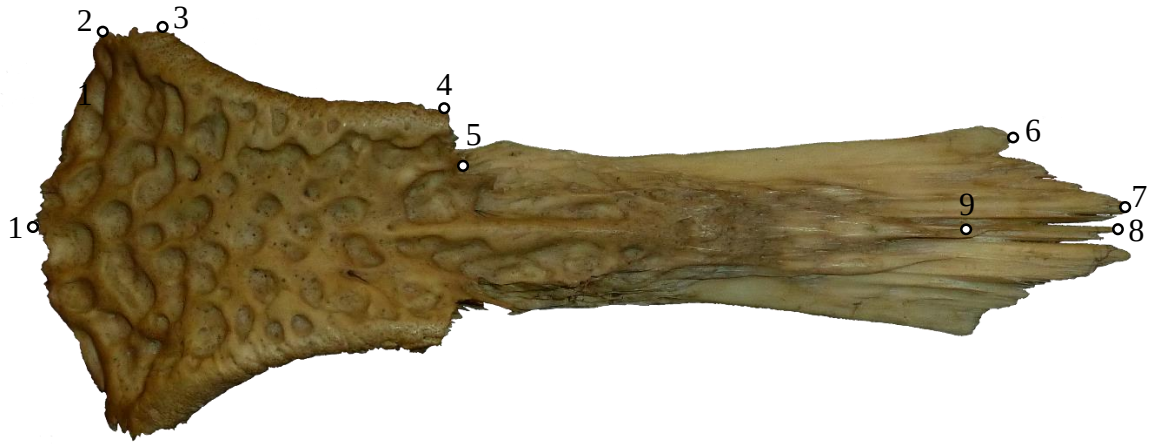

Figure 8 – Frontal landmarks in dorsal view: Specimen 487F133, SG4. Points were only placed on half of the bone to capture shape. (1) Posteromedial-most point of the frontal-parietal suture. (2) Posterodorsal extent of the postorbital-frontal suture. (3) Posterior extent of the orbital margin. (4) Anterior extent of the orbital margin. (5) Posteromedial point of the frontal-prefrontal suture. (6) Lateral extent of the frontal-nasal suture. (7) Anterioventral extent of the frontal-nasal suture. (8) Anterodorsal extent of the frontal-nasal suture. (9) Anteromedial extent of the frontal-nasal suture. Following Bookstein (1991), landmarks classify as: Type II = 2, 3, 4, 5, 7, 9; and Type III =1, 6, 8.

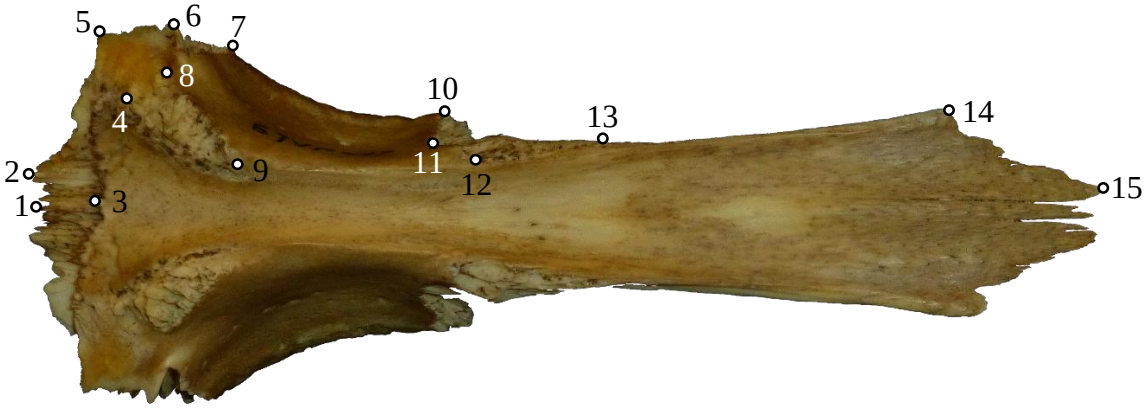

Figure 9 – Frontal landmarks in ventral view: Specimen 487F135, SG4. Points were only placed on half of the bone to capture shape. (1) Posteromedial-most point of the frontal-parietal suture. (2) The posterior-most point of the frontal-parietal suture. (3) Ventral anteromedial-most point of the frontal-parietal suture. (4) Posterior extent of the frontal-laterosphenoid suture. (5) Lateral extent of the frontal-parietal suture. (6) Anterioventral extent of the frontal-postorbital suture. (7) Point at the meeting of the Anterodorsal extent of the frontal-postorbital suture and the posterior extent of the orbital margin. (8) Lateral extent of the frontal-laterosphenoid suture. (9) Anterior extent of the frontal-laterosphenoid suture. (10) Anterior extent of the orbital margin. (11) Posterior extent of the frontal-prefrontal suture within the orbit. (12) Medial-ventral extent of the frontal-prefrontal suture. (13) Anterioventral extent of the frontal-prefrontal suture. (14) Lateral extent of the frontal-nasal suture. (15) Anterioventral extent of the frontal-nasal suture. Following Bookstein (1991), landmarks classify as: Type II = 5, 6, 7, 10, 11, 13, 14, 15; and Type III = 1, 2, 3, 4, 8, 9, 12.

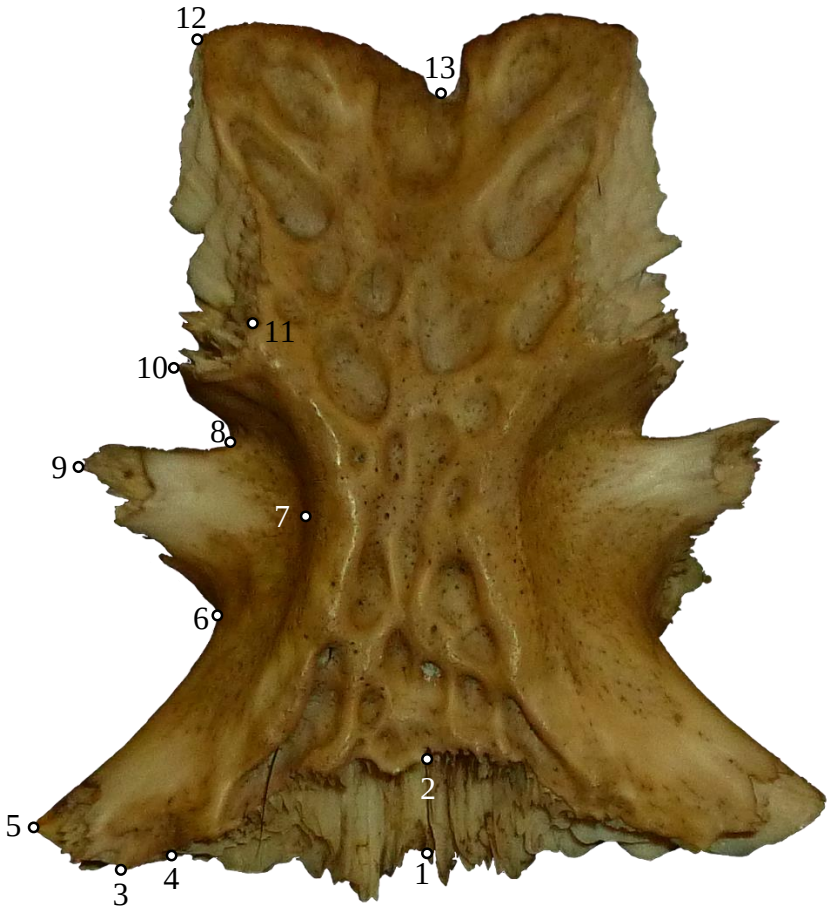

Figure 10 – Parietal landmarks in dorsal view: Specimen 487P144, SG4. Points were only placed on half of the bone to capture shape. (1) Anteromedial-most point of the frontal-parietal suture. (2) Dorsal posteromedial-most point of the frontal-parietal suture. (3) The dorsolateral extent of the frontal-parietal suture. (4) Posterior extent of the dorsotemporal fenestra. (5) Lateral extent of the parietal-postorbital suture. (6) Medioventral-most point of the dorsotemporal fossa. (7) Medial-most point of the dorsotemporal fenestra. (8) Medial-most point of the tempoorbital foramen. (9) Lateral extent of the parietal-squamosal suture anterior to the tempoorbital foramen. (10) Lateral extent of the parietal-squamosal suture posterior to the tempoorbital foramen. (11) Medial extent of the parietal-squamosal suture. (12) Posterior extent of the parietal-squamosal suture. (13) Posteromedial-most point of the parietal. Following Bookstein (1991), landmarks classify as: Type II = 3, 4, 5, 8, 9, 10, 12; and Type III = 1, 2, 6, 7, 11, 13.

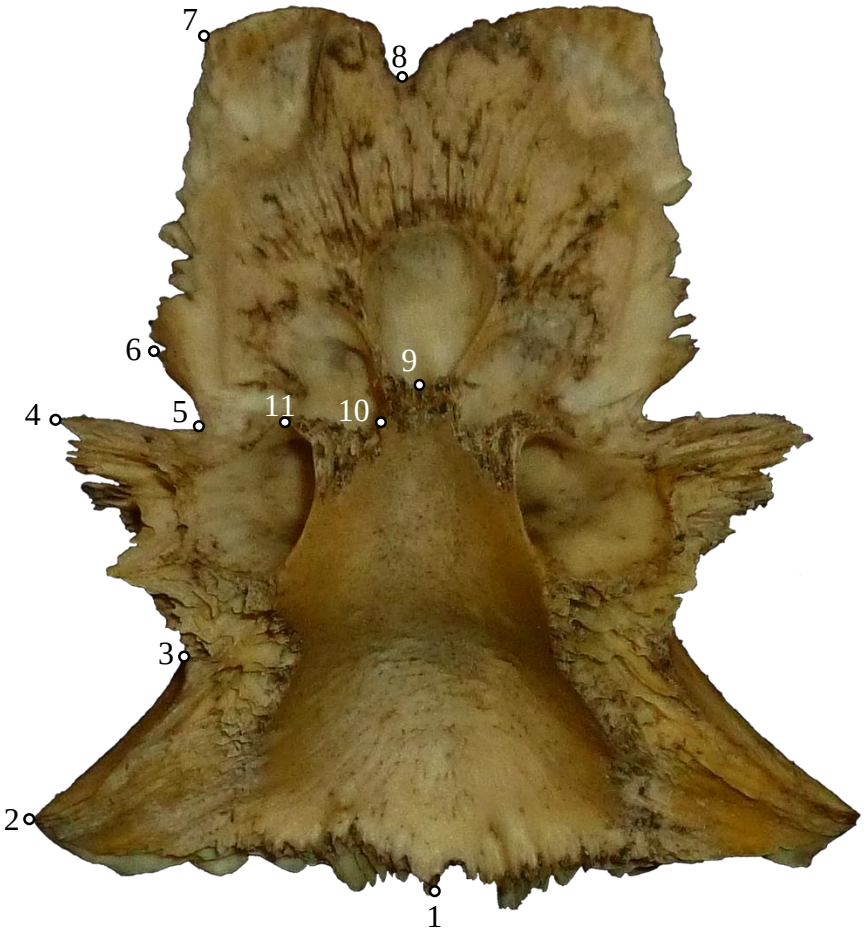

Figure 11 – Parietal landmarks in ventral view: Specimen 487P146, SG4. Points were only placed on half of the bone to capture shape. (1) Anteromedial-most point of the frontal-parietal suture. (2) Lateral extent of the parietal-postorbital suture. (3) Medioventral-most point of the dorsotemporal fossa. (4) Lateral extent of the parietal-squamosal suture anterior to the tempoorbital foramen. (5) Medial-most point of the tempoorbital foramen. (6) Lateral extent of the parietal-squamosal suture posterior to the tempoorbital foramen. (7) Posterior extent of the parietal-squamosal suture. (8) Posteromedial-most point of the parietal. (9) Anterior extent of medial foramen of the middle ear cavity. (10) Medial extent of posterolateral foramen of the middle ear cavity. (11) Posterior extent of lateral foramen of the middle ear cavity. Following Bookstein (1991), landmarks classify as: Type II = 2, 4, 5, 6, 7; and Type III = 1, 3, 8, 9, 10, 11.

Analysis

Landmark data were analyzed and graphed using the statistics software SPSS 16.0 (SPSS Inc. 2007). With this, Principal Component Analyses (PCA), Discriminant Analyses (DA), as well as stepwise DA were run on the landmark data. Due to the large size gap between SG1 and SG2, and the large separation in all of the graphs between the two, the analyses were run again but with SG1 removed to be sure it was not skewing the results.

Thin plate splines were then created to visualize the shape change between the SGs. Since groups were being compared instead of individual specimens the SG files were appended, using tpsUtil, to create one averaged set of landmarks to compare for each in the splines (Rohlf 2009b). Both grid and vector views were created, using the program tpsSplin, to be able to more easier see overall shape change and individual landmark movement respectively(Rohlf 2009d).

CHAPTER 3

RESULTS

Statistical Analysis

Of the PCA and DA analyses, the PCAs proved most informative in terms of deciphering ontogenetic change. As in the thin plate splines, the PCAs show similar differentiation of the size groups. The DA, stepwise, and analysis without SG1 are not described here since they did not add any contrasting information and are therefore provided in the Appendix. The PCA results are discussed here briefly by looking at the first three factors in graph form for all the bones. Circles have been drawn around the SGs in the graphs to more easily keep track them in morphospace.

Premaxilla—The PCA for the dorsal view of the premaxilla described 29.018% of the total variance along the first PCA factor score (PC1), 21.973% along second PCA factor score (PC2), and 10.267% along third PCA factor score (PC3), meaning 61.258% of the total variance was accounted for in the graphs of PC1 vs. PC2 and PC1 vs. PC3. All of the SGs overlapped along all three axes. The only point that separated from the other groups was a single specimen in SG1 in the far positive along PC1 and one specimen in SG2 in the positive along PC2. The rest of the SGs were mixed among each other thoroughly. So there was slight separation of SG1 and SG2 but the rest of the SGs were indistinguishable for the premaxilla.

The PCA for the ventral view of the premaxilla described 31.832% of the total variance along PC1, 16.489% along PC2, and 12.424% along PC3, meaning 60.745% of the total variance was accounted for in the graphs of PC1 vs. PC2 and PC1 vs. PC3. SG1 was completely separate in PC1 vs. PC2, with one point extending far into the negative along PC1, and the other along PC2. SG2, SG3 and SG 4 all overlapped each other with SG2 in the center of the grouping, SG 5

only overlapped SG4. SG1 separated completely along PC1 but overlapped with all but SG5 along PC3.

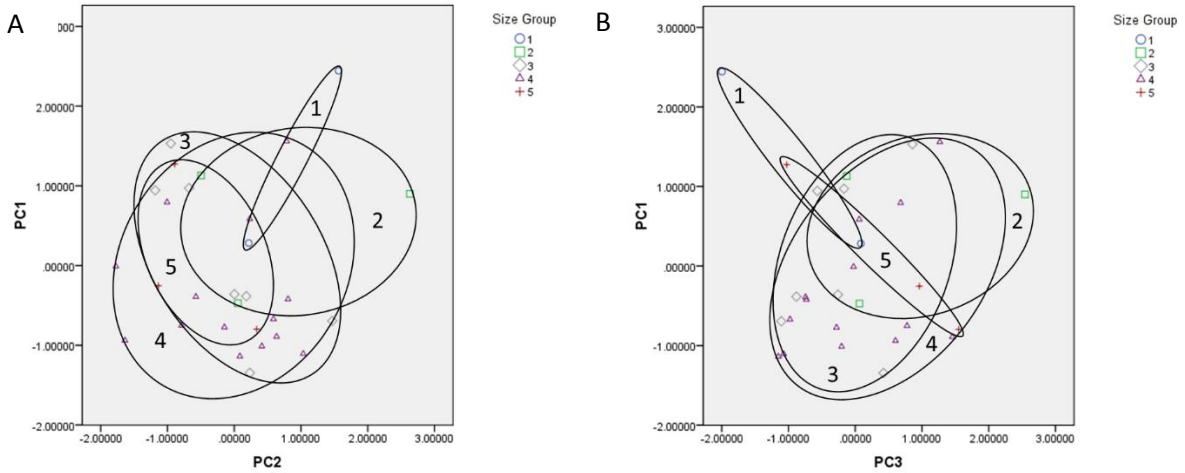

Figure 12 – Premaxilla Dorsal View: **A**, PC1 vs. PC2 and **B**, PC1 vs. PC3.

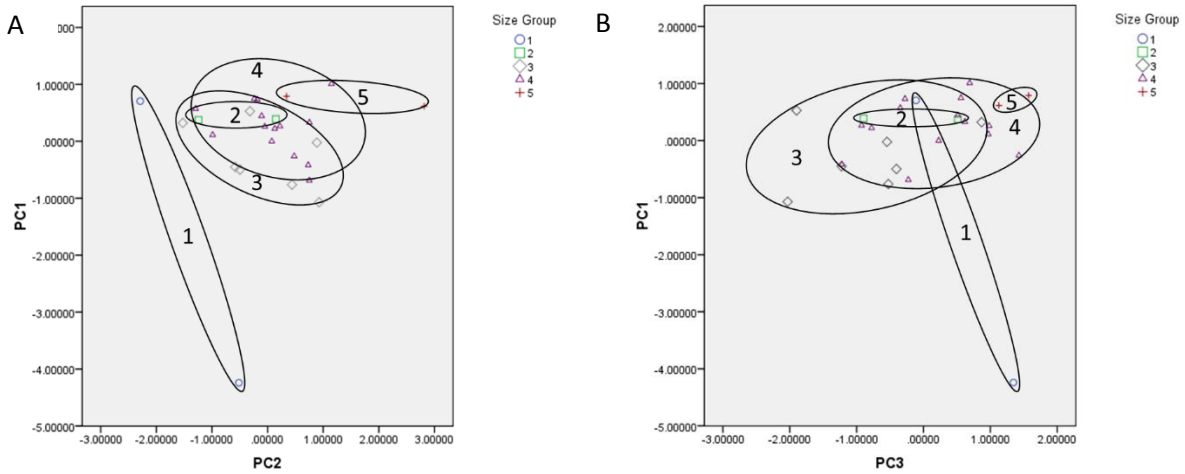

Figure 13 – Premaxilla Ventral View: **A**, PC1 vs. PC2 and **B**, PC1 vs. PC3

Maxilla—The PCA for the dorsal view of the maxilla described 53.277% of the total variance along PC1, 11.548% along PC2, and 9.149% along PC3, meaning 73.974% of the total variance was accounted for in the graphs of PC1 vs. PC2 and PC1 vs. PC3. SG1 was completely separated from the other SGs, falling out in the positive along PC1. SG 2 also separated out in the graph of

PC1 vs. PC2. Along PC1 the rest of the SGs descended by size, with some overlap. SG5 was the exception in that it was among SG4 along PC1 and PC3 but separate along PC2. PC2 also showed the same sort of separation by size, with the SGs increasing in size in the positive direction. In PC3 they all stacked in the middle of the axis along the zero line.

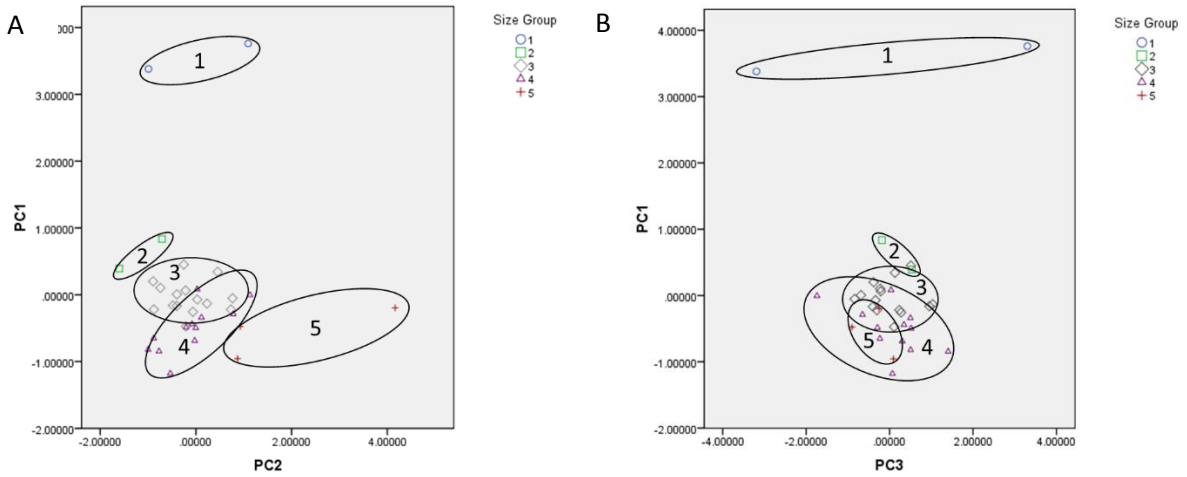

Figure 14 – Maxilla Dorsal View: **A**, PC1 vs. PC2 and **B**, PC1 vs. PC3

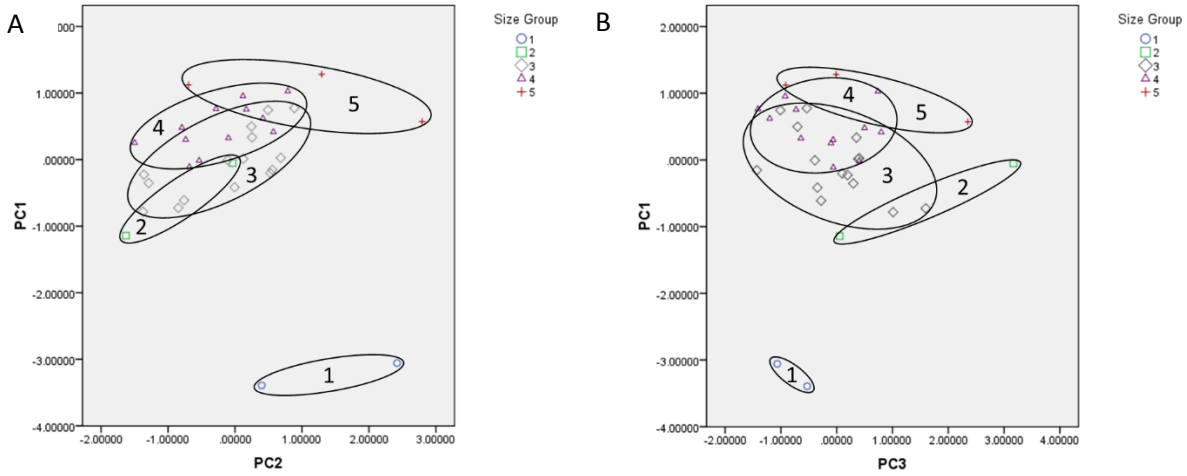

Figure 15 – Maxilla Ventral View: **A**, PC1 vs. PC2 and **B**, PC1 vs. PC3

The PCA for the ventral view of the maxilla described 28.673% of the total variance along PC1, 16.722% along PC2, and 11.133% along PC3, meaning 56.529% of the total variance

was accounted for in the graphs of PC1 vs. PC2 and PC1 vs. PC3. PC1 showed a similar pattern of the SGs increasing in size, this time in the positive direction. SG1 was completely separate from the other SGs in the far negative of PC1. The other SGs definitely separated in increasing size but still overlapped quite a bit, with each overlapping with the SG above it in the series at least, most overlapping at least two others. There wasn't much descriptive placement along PC2 or PC3.

Nasal—The PCA for the nasal described 30.178% of the total variance along PC1, 21.573% along PC2, and 18.041% along PC3, meaning 69.793% of the total variance was accounted for in the graphs of PC1 vs. PC2 and PC1 vs. PC3. SG1 was the only one to place out from the other SGs, falling out in the positive along PC1, the positive in PC2, and negative again in PC3. The placement along PC2 and PC3 of SG1 was what separated it from the other SGs. SG3 and SG4 overlapped in the extreme, with SG3 falling almost completely within the boundaries of SG4. SG5 fell to the negative along PC1 but still overlapped with SG3 and SG4 slightly.

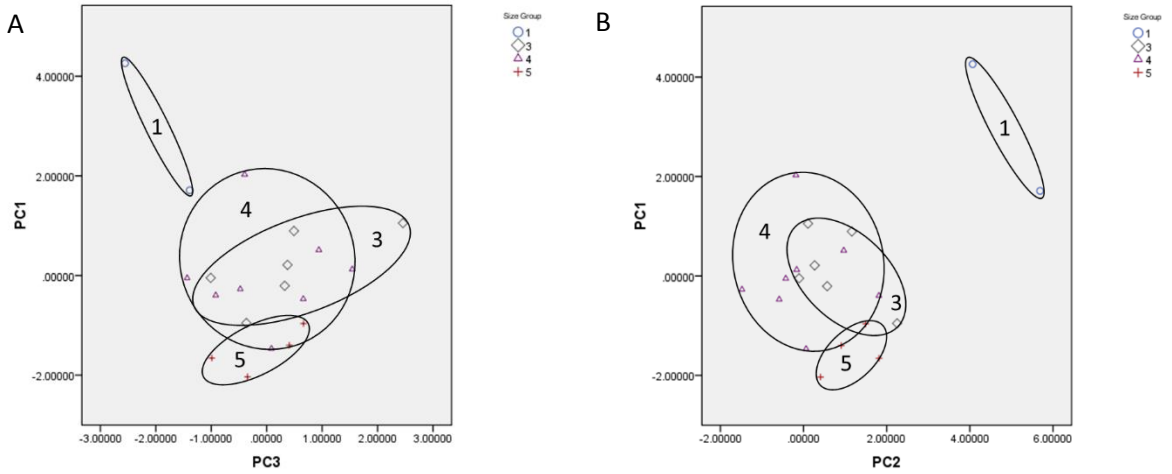

Figure 16 – Nasal: **A**, PC1 vs. PC2 and **B**, PC1 vs. PC3

Jugal—The PCA for the jugal described 40.818% of the total variance along PC1, 14.892% along PC2, and 11.433% along PC3, meaning 67.143% of the total variance was accounted for in the graphs of PC1 vs. PC2 and PC1 vs. PC3. SG1 and SG5 both separated out from the other

three SGs and fell out on opposite ends of PC1, SG1 in the positive and SG5 in the negative. SG2 fell out just to the positive of the zero line along PC1, overlapping SG3 and SG4 slightly. SG3 and SG4 both fell on the zero line of PC1 overlapping almost completely. The only separation between them was that SG3 was more in the negative along PC2 and PC3 and SG4 was more in the positive.

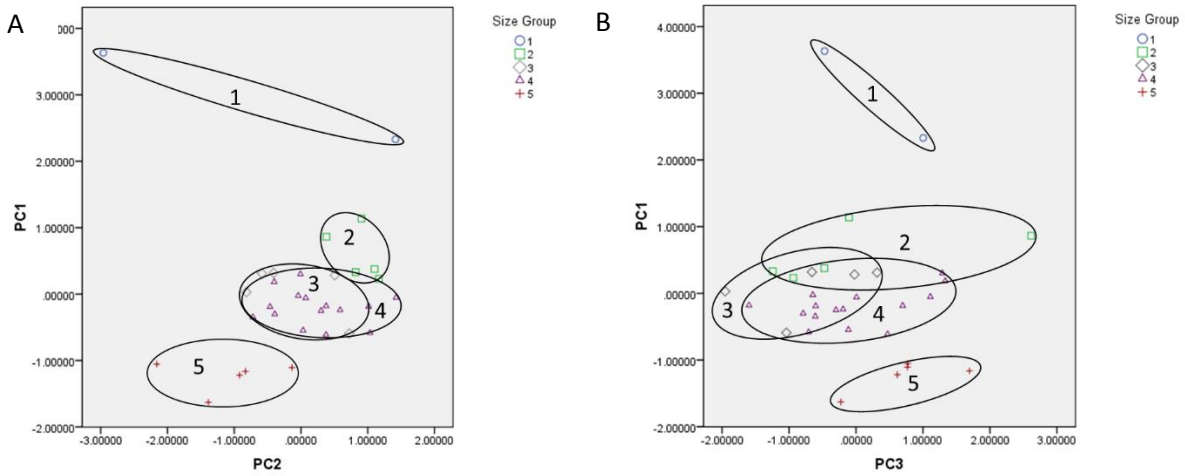

Figure 17 – Jugal: **A**, PC1 vs. PC2 and **B**, PC1 vs. PC3

Frontal—The PCA for the dorsal view of the frontal only had two components, the first described 77.972% of the total variance along PC1 and 22.028% along PC2, so 100.00% of the total variance was accounted for in the graph of PC1 vs. PC2. There was seemingly no pattern to the placement of the SGs in the graph. SG1 was separate from the other SGs while the rest were all overlapping SG4. SG2, SG3, and SG5 were all within the spread of SG4, which extended into the positive and negative of PC1 along the zero line of PC2. SG2 was separate from SG3 and SG5, which overlapped each other slightly. Along PC1 there was no pattern of size increase, with SG2 at the same level as SG4 and SG5, but some could be seen along PC2. SG4 extended past SG2 along PC2 but the rest of the SGs increased in size in the positive direction.

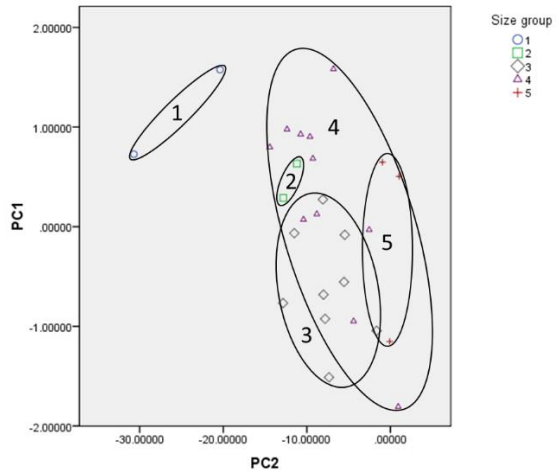

Figure 18 – Frontal Dorsal View: PC1 vs. PC2

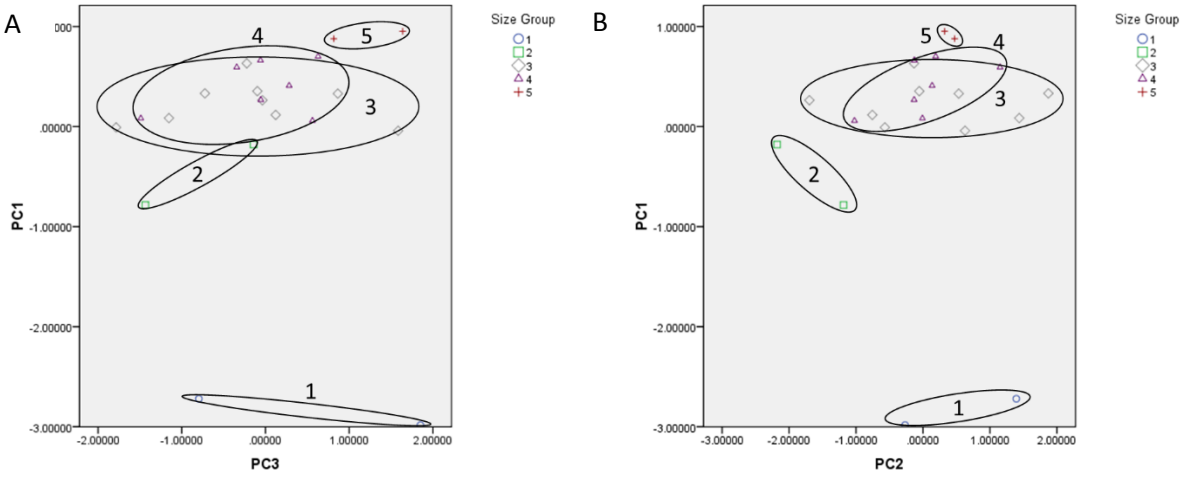

Figure 19 – Frontal Ventral View: **A**, PC1 vs. PC2 and **B**, PC1 vs. PC3

The PCA for the ventral view of the frontal described 43.768% of the total variance along PC1, 11.814% along PC2, and 7.593% along PC3, meaning 63.175% of the total variance was accounted for in the graphs of PC1 vs. PC2 and PC1 vs. PC3. The SGs separated out much more than in the dorsal view. SG1 and SG5 were completely separated in both graphs, with SG1 in the negative of PC1 and SG5 in the positive. SG2 separated in the PC1 vs. PC2 graph and slightly overlapped SG3 on the negative edge in the PC1 vs. PC3 graph. SG3 and SG4 overlapped a great

degree, with SG4 falling out slightly in the positive of PC1. Along PC1 the SGs showed a pattern of increasing size moving in the positive direction.

Parietal—The PCA for the dorsal view of the parietal described 30.373% of the total variance along PC1, 15.804% along PC2, and 14.513% along PC3, meaning 60.691% of the total variance was accounted for in the graphs of PC1 vs. PC2 and PC1 vs. PC3. The SGs fell out in a very interesting spread for the parietal. Along PC1, SG1 and SG2 both separated out in the negative direction, with SG1 more negative than SG2. SG3, SG4, and SG5 all fell just negative of the zero line on PC1, with SG4 the most negative and a point of SG3 the most positive. SG5 fell in the middle of SG3 and overlapped it and SG4.

The PCA for the ventral view of the parietal described 53.871% of the total variance along PC1, 14.565% along PC2, and 6.799% along PC3, meaning 75.236% of the total variance was accounted for in the graphs of PC1 vs. PC2 and PC1 vs. PC3. In the ventral view only SG1 was separated from the other SGs, once again in the negative of PC1. Along PC3, SG2 separated from the others but along PC2 it was in the middle of SG3 and SG5. There was a rough pattern along PC1 of the SGs increasing in size in the positive direction but all still overlapped each other. SG5 had a large spread and encompassed all the SGs except for SG1 in the PC1 vs. PC2 graph. Along PC3, SG3 and SG4 had a wide spread and almost perfectly overlapped, with SG5 just crossing them along the PC1 axis.

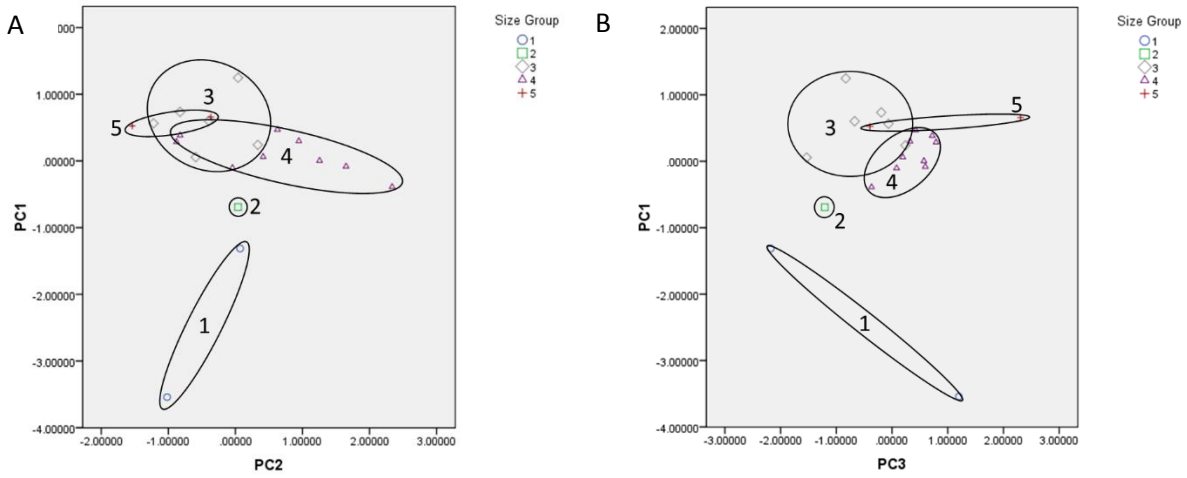

Figure 20 – Parietal Dorsal View: **A**, PC1 vs. PC2 and **B**, PC1 vs. PC3

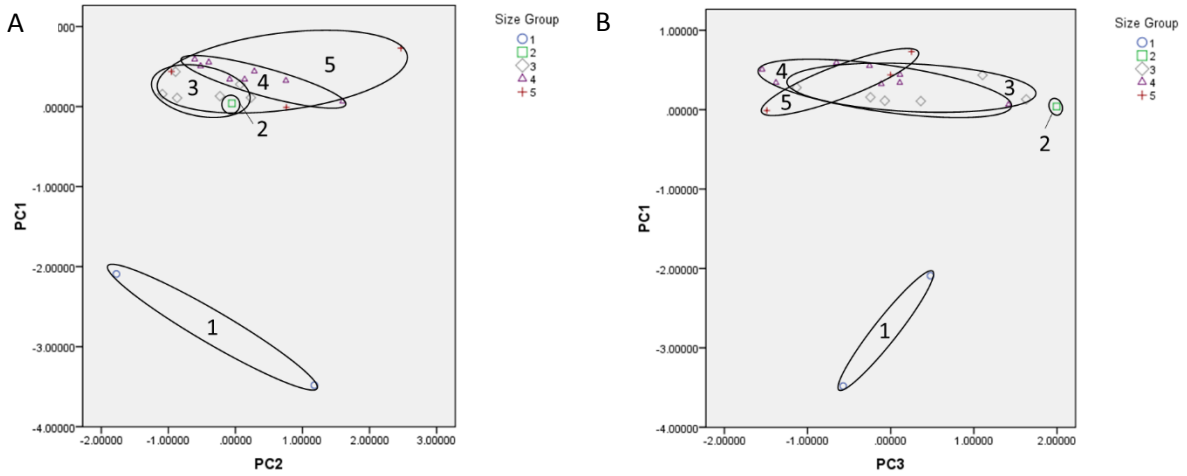

Figure 21 – Parietal Ventral View: **A**, PC1 vs. PC2 and **B**, PC1 vs. PC3

Thin Plate Spline

Premaxilla—The premaxilla showed very little shape change overall (Fig. 22). There was initial movement of the nares and ascending process between the First Size Group (SG1) and the Second Size Group (SG2). The lateral – and posterior-most points of the nares ventral fenestra moved anteriorly, also lengthening the palatal process. The ascending process also lengthened with the posterior point moving further posteriorly. The nares ventral fenestra constricted anteroposteriorly between SG2 and SG3 with otherwise minimal movement. The movement of

the landmarks in the larger SGs was minimal, the spline for SG3 and SG4 showed almost no movement of the landmarks. There was still evidence of the nares constricting, but very reduced. The only notable change between SG4 and SG5 was the palatal process, once again lengthened a small amount.

There seems to have been slightly more activity in the ventral view of the premaxilla but only between SG1 and SG2 (Fig. 23). The same changes were seen in the ventral nares fenestra, palatal process, and ascending process as were seen in the ventral view. The new changes exhibited in this view were in the tooth row. The 3rd, 4th, and 5th tooth alveoli enlarged and the lateral-most point of the premaxilla-maxilla suture moved posteromedially. After these initial changes, the landmarks showed the same lack of movement as the ventral view. The landmarks in the spline for SG2 and SG3 showed minute shifts but for many, no definite direction could not be discerned. The lateral portion of the premaxilla-maxilla suture did show slight anteromedial movement. The anterior of the palatal process moved posteriorly, actually shortening the premaxillary suture. Only two landmarks showed noticeable movement between SG3 and SG4—the posterior extent of the premaxilla-nasal-maxilla suture moved posteriorly and the lateral-most point of the premaxilla-maxilla suture moved anterolaterally. There was an increase in landmark movement across the premaxilla between SG4 and SG5. The 2nd, 4th, and 5th tooth alveoli all increased in diameter. The lateral portion of the premaxilla-maxilla suture continued its anterior movement. The posterior point of the palatal process moved further posteriorly, resuming the lengthening of the premaxillary suture. The ascending process lengthened posteromedially.

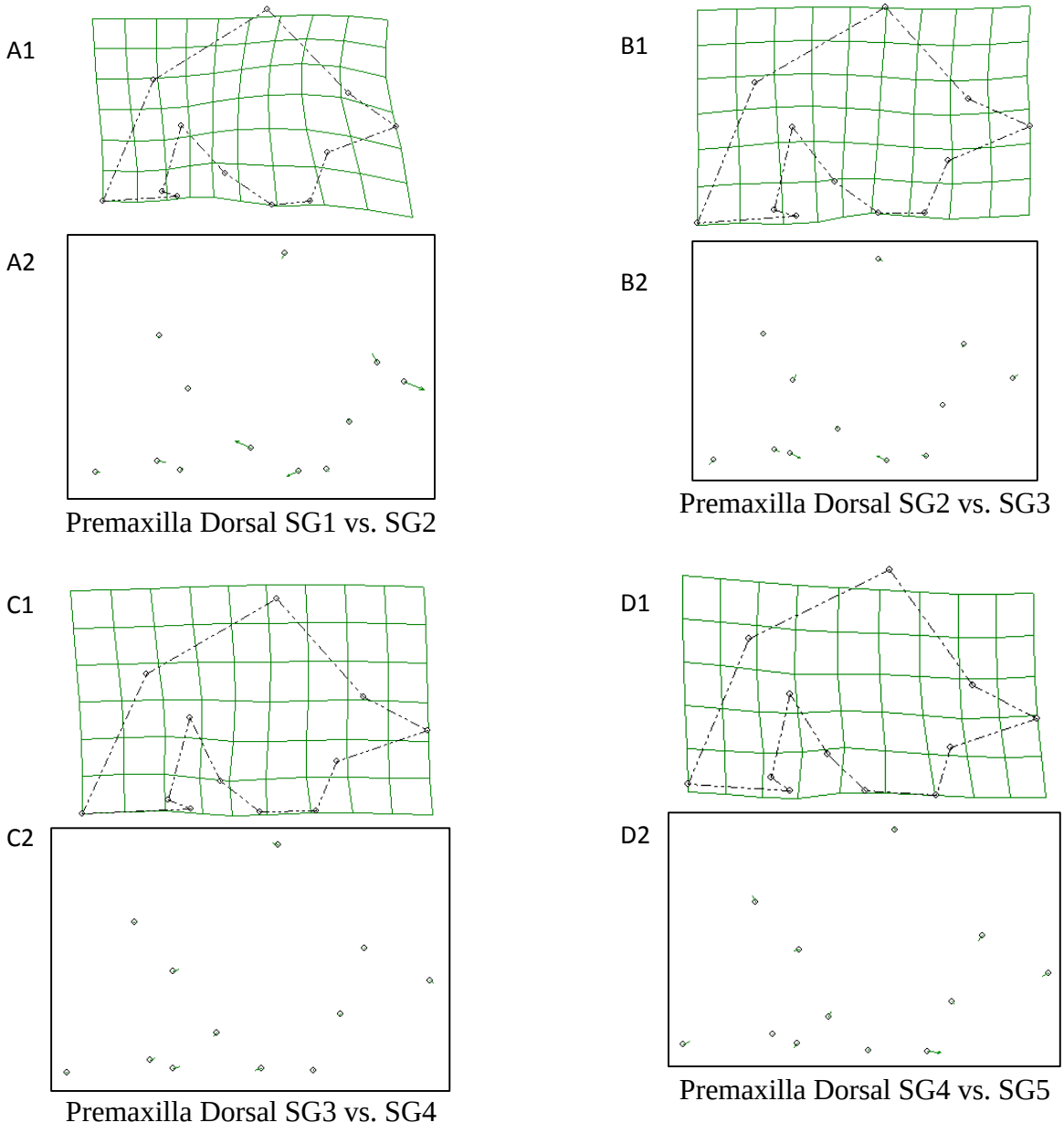

Figure 22 – Premaxilla Dorsal View Thin Plate Splines. Spline comparing SG1 and SG2 in (A1) grid and (A2) vector format. Spline comparing SG2 and SG3 in (B1) grid and (B2) vector format. Spline comparing SG3 and SG4 in (C1) grid and (C2) vector format. Spline comparing SG4 and SG5 in (D1) grid and (D2) vector format.

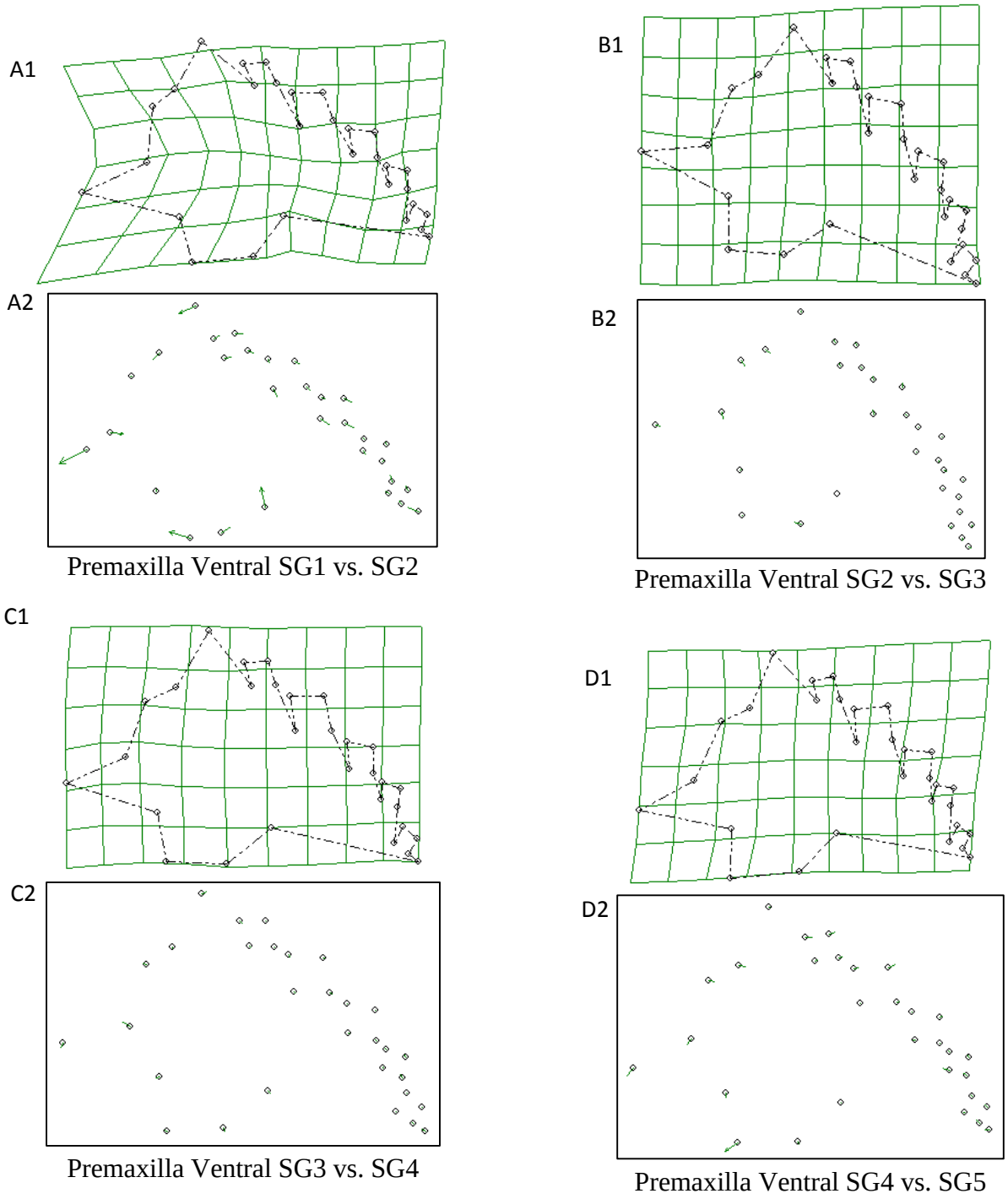

Figure 23 – Premaxilla Ventral View Thin Plate Splines. Spline comparing SG1 and SG2 in (A1) grid and (A2) vector format. Spline comparing SG2 and SG3 in (B1) grid and (B2) vector format. Spline comparing SG3 and SG4 in (C1) grid and (C2) vector format. Spline comparing SG4 and SG5 in (D1) grid and (D2) vector format.

Maxilla—The dorsal view of the maxilla showed a similar pattern as the premaxilla with slightly more overall shape change occurring throughout ontogeny (Fig. 24). Once again the majority of the change happened between SG1 and SG2. Every single landmark showed noticeable movement, meaning the maxilla showed more change during this stage than the rest of the bones. The landmarks along the lateral edge and anterior of the maxilla moved anteriorly. The posteromedial points along the maxilla-lachrymal suture moved posterolaterally, showing the lengthening and narrowing of the rostrum. The posterior of the lateral edge also moved medially, contributing to the mediolateral narrowing of the maxilla. The maxillary suture elongated anteroposteriorly and appeared to be moving laterally (this was merely due to the mediolateral narrowing of the maxilla). Between SG2 and SG3 the lateral edge continued to move anteriorly but at a highly reduced rate. The posterior movement of the lachrymal suture also continued and was the most dramatic movement of this stage. The maxillary suture elongated, but only slightly. There was almost no movement between SG3 and SG4; only slight posterior movement of the lachrymal suture was noticeable. There was actually an increase in movement between SG4 and SG5, with the lateral-edge landmarks moving anterolaterally. The lachrymal suture increased its movement posteromedially while the maxillary suture continued to elongate.

In the ventral view of the maxilla the pattern was the same as the dorsal view (Fig. 24). A great deal of landmark movement was seen in the spline for SG1 and SG2. Similar to the dorsal view of the maxilla, the landmarks at the posterior of the (maxilla, along the palatine-maxilla suture, and suborbital fenestra) moved posteriorly and again appeared to move laterally, narrowing the maxilla. The maxillary suture again elongated with the posterior point moving posterolaterally in the spline. The posterolateral points also moved medially. The teeth showed

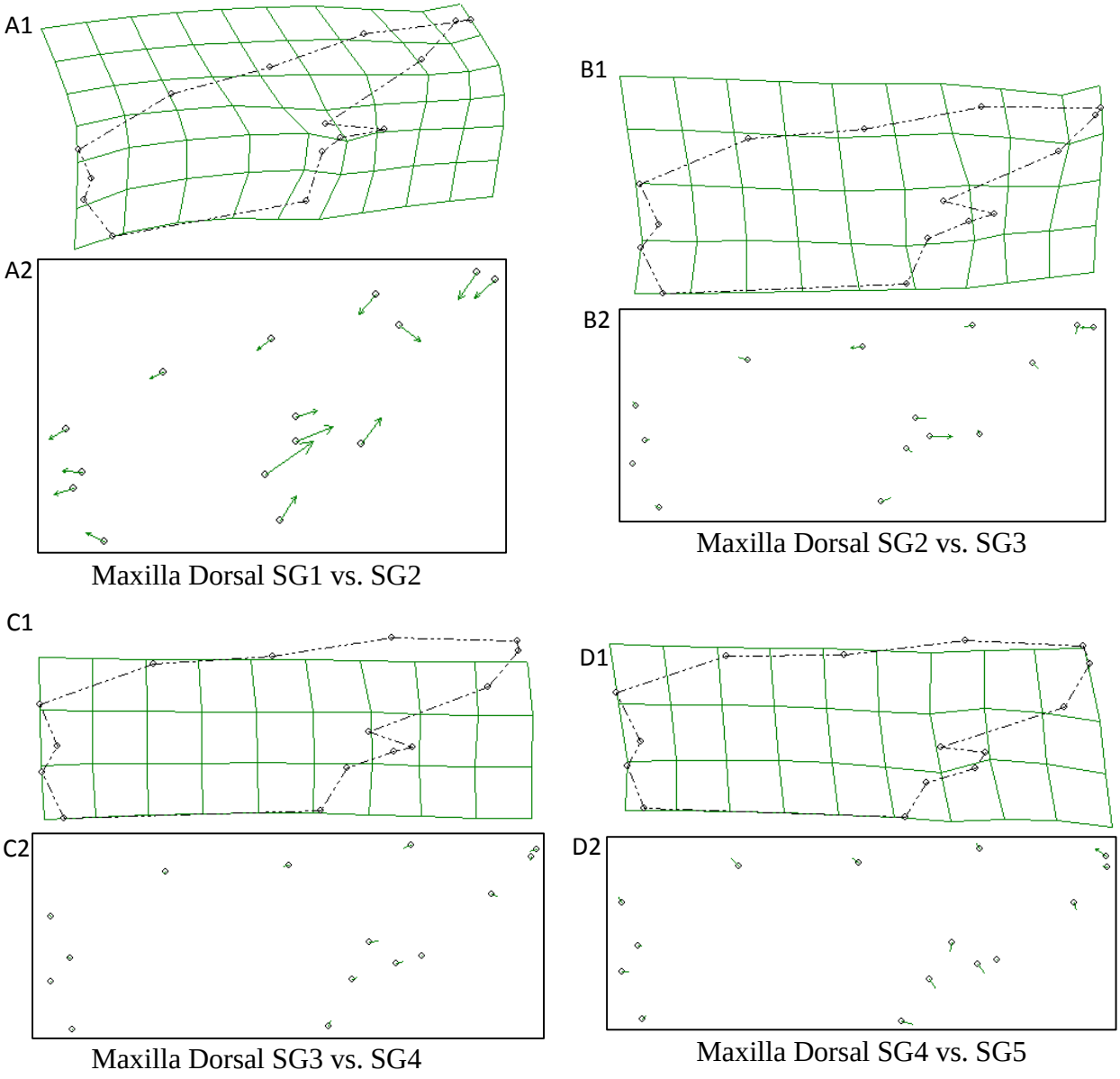

Figure 24 – Maxilla Dorsal View Thin Plate Splines. Spline comparing SG1 and SG2 in (A1) grid and (A2) vector format. Spline comparing SG2 and SG3 in (B1) grid and (B2) vector format. Spline comparing SG3 and SG4 in (C1) grid and (C2) vector format. Spline comparing SG4 and SG5 in (D1) grid and (D2) vector format.

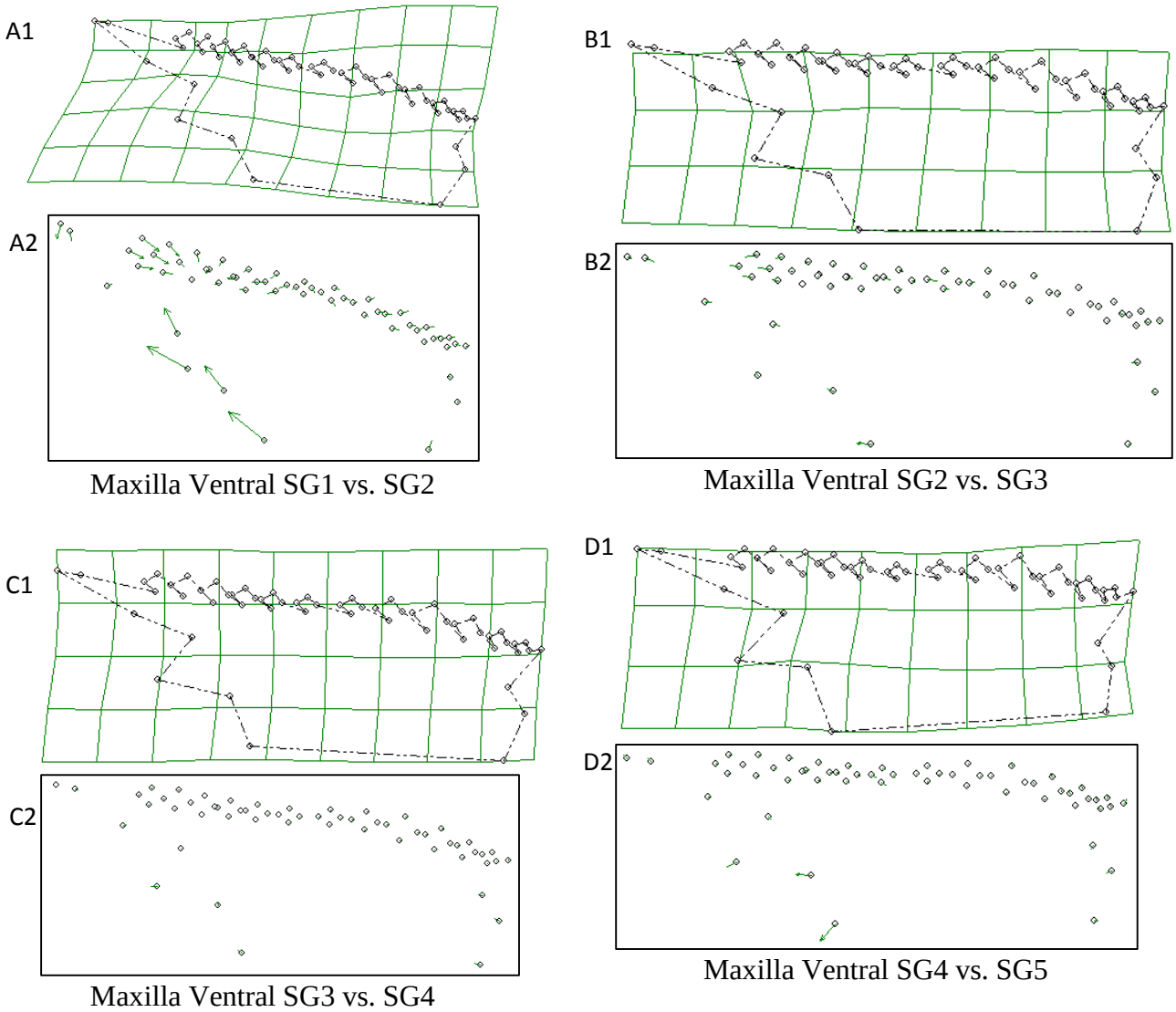

Figure 25 – Maxilla Ventral View Thin Plate Splines. Spline comparing SG1 and SG2 in (A1) grid and (A2) vector format. Spline comparing SG2 and SG3 in (B1) grid and (B2) vector format. Spline comparing SG3 and SG4 in (C1) grid and (C2) vector format. Spline comparing SG4 and SG5 in (D1) grid and (D2) vector format.

extreme changes between these SG1 and SG2. The anterior tooth alveolis, the first five, all showed anterior movement and an increase in diameter. The sixth tooth alveoli also increased in diameter but anteroposteriorly. The posterior tooth alveolis, the last six that received landmarks, all showed a decrease in diameter and all moved toward the ninth tooth alveoli, with the alveoli further from it showing the most movement. Between SG2 and SG3 there was continual

movement of the tooth alveoli landmarks. Many of the posterior alveoli, the 6th, 7th, 11th, and 12th, showed a decrease in diameter with the final marked alveoli once again showing the largest decrease. The posterior of the tooth row also moved anteriorly, shortening it. There were slight anterior movements of the suborbital fenestra. The maxillary suture lengthened at its posterior end. Besides slight posterior movement of the premaxilla-maxilla suture and posterior point of the palatine-maxilla suture, there was no discernable movement among any of the other landmarks between SG3 and SG4. This lack of change continued from SG4 to SG5 except for the posterior movements at the posteromedial corner of the maxilla. The posterior of the maxillary suture moved posteromedially in the spline, widening the posterior of the maxilla. The palatine-maxilla suture also moved posteriorly.

Nasal—The nasal showed movement on all landmarks between SG1 and SG3 (Fig. 26). The nasal narrowed mediolaterally overall, with the internarial suture and posterior extent of the nasal landmarks moving laterally while the lateral edge of the nasal moved medially. The points between the nasal-premaxilla suture and the posterior of the nasal also moved posteriorly, showing a flattening of the maxilla-nasal suture. The nasal-premaxilla suture's lateral points moved medially while the posterior extent of the nares moved anterolaterally. There was almost no landmark movement between SG3 and SG4, other than some slight shifts on the lateral edge. Increased movement was seen from SG4 to SG5. The posterior of the nasal extended further posteriorly. The nasal-premaxilla suture narrowed anteroposteriorly with the anterior and posterior edges moving toward its center.

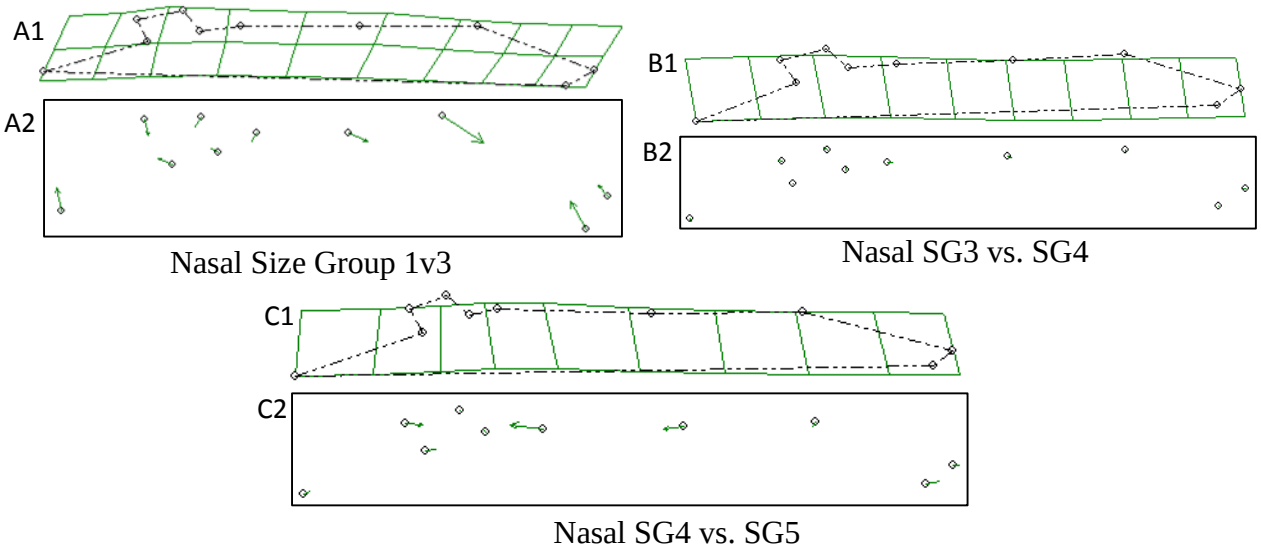

Figure 26 – Nasal Thin Plate Spline. Spline comparing SG1 and SG2 in (A1) grid and (A2) vector format. Spline comparing SG2 and SG3 in (B1) grid and (B2) vector format. Spline comparing SG3 and SG4 in (C1) grid and (C2) vector format.

Jugal—The jugal showed slightly more consistent shape change (Fig. 27). The postorbital process lengthened medially from SG1 to SG2 while the quadratojugal process angled more laterally. The maxillary process began to expand mediolaterally, with the anterior point shifting laterally, forming more of an oval shape than the juvenile blade shape. The ectopterygoid suture shifted and expanded anteromedially. The maxillary process continued to expand slightly mediolaterally during the shift from SG2 to SG3. The anterior point of the quadratojugal suture along the medial edge moved anteriorly and the postorbital bar lengthened further at its end. Other than that there was no movement of the landmarks at the center of the bone. Between SG3 and SG4 there was very little change. The anterior of the ectopterygoid suture moved further anteriorly and the posterior edge of the postorbital bar moved medially. The main shift in the landmarks from SG4 to SG5 was that the maxillary process further expanded mediolaterally.

A1

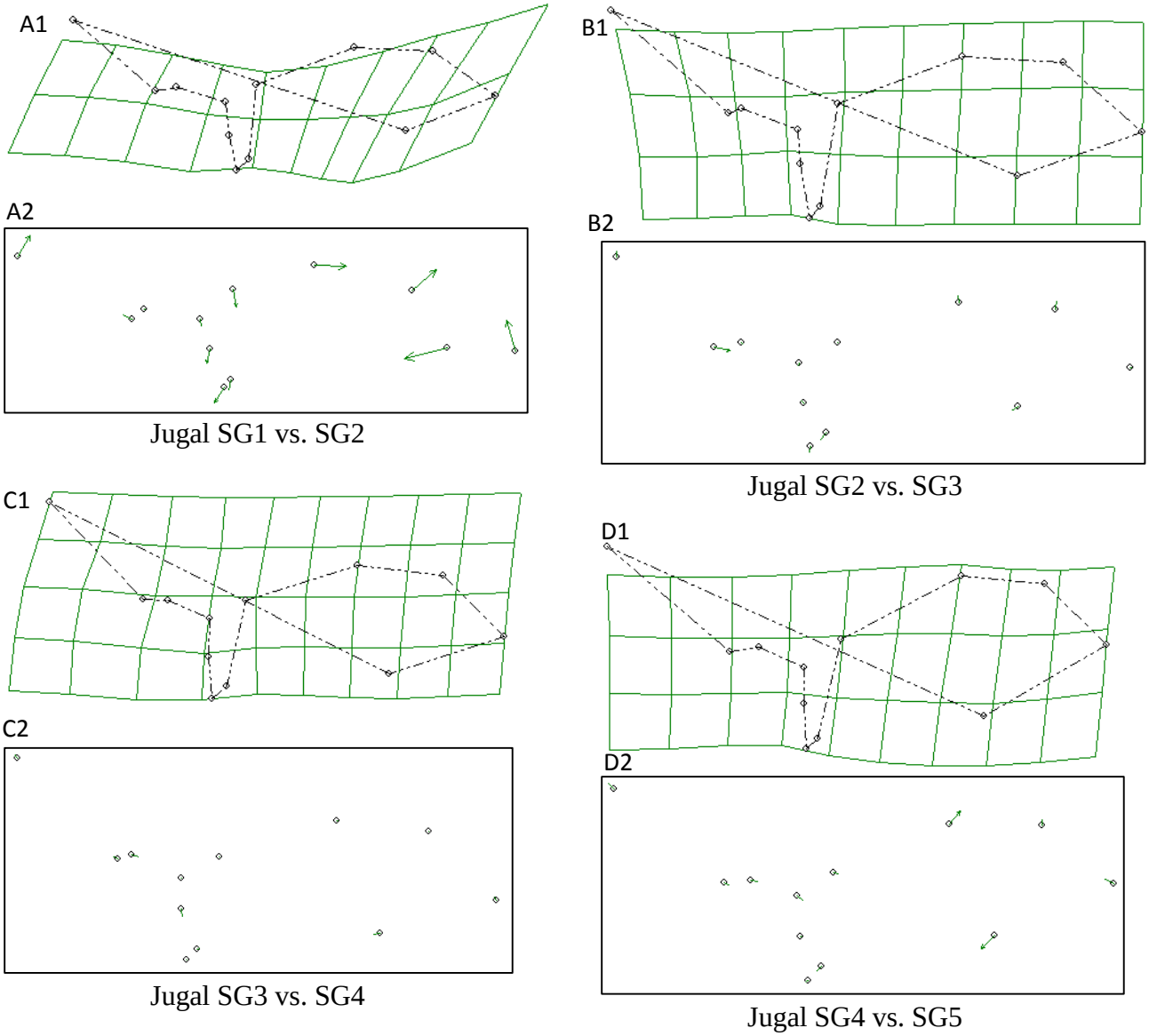

Figure 27 – Jugal Thin Plate Spline. Spline comparing SG1 and SG2 in (A1) grid and (A2) vector format. Spline comparing SG2 and SG3 in (B1) grid and (B2) vector format. Spline comparing SG3 and SG4 in (C1) grid and (C2) vector format. Spline comparing SG4 and SG5 in (D1) grid and (D2) vector format.

Frontal—The majority of the landmark movement was at the posterior of the frontal from SG1 to SG2 (Fig. 28). The orbital margin shortened anteroposteriorly, the posterior point moved anteromedially, and the anterior point (as well as the frontal-prefrontal suture) moved posterolaterally. The postorbital-frontal suture also moved anteromedially while the landmark at

the posteromedial of the frontal moved anterolaterally, narrowing the posterior of the frontal. The anterior points moved further anterior. The anterior of the orbital margin and frontal-prefrontal continued their posterior movement from SG2 to SG3 as well as the medial points continued their anterior movement. All landmark movement was reduced between these SGs. Other than slight posterolateral movement of the frontal-prefrontal suture there was no significant movement of landmarks between SG3 and SG4. The orbital margin decreased in length noticeably from SG4 to SG5. All movements were the in same directions as previous splines except for the anteromedial point which moved posteriorly.

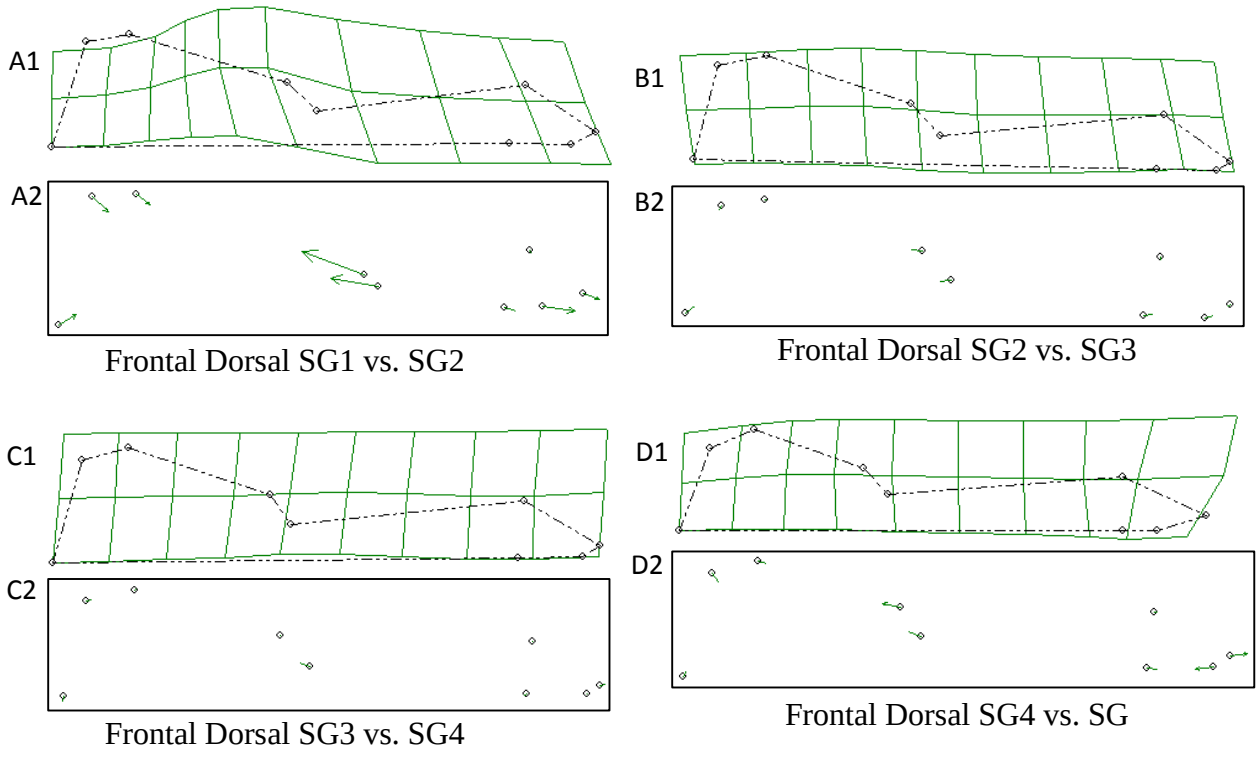

Figure 28 – Frontal Dorsal View Thin Plate Spline. Spline comparing SG1 and SG2 in (A1) grid and (A2) vector format. Spline comparing SG2 and SG3 in (B1) grid and (B2) vector format. Spline comparing SG3 and SG4 in (C1) grid and (C2) vector format. Spline comparing SG4 and SG5 in (D1) grid and (D2) vector format.

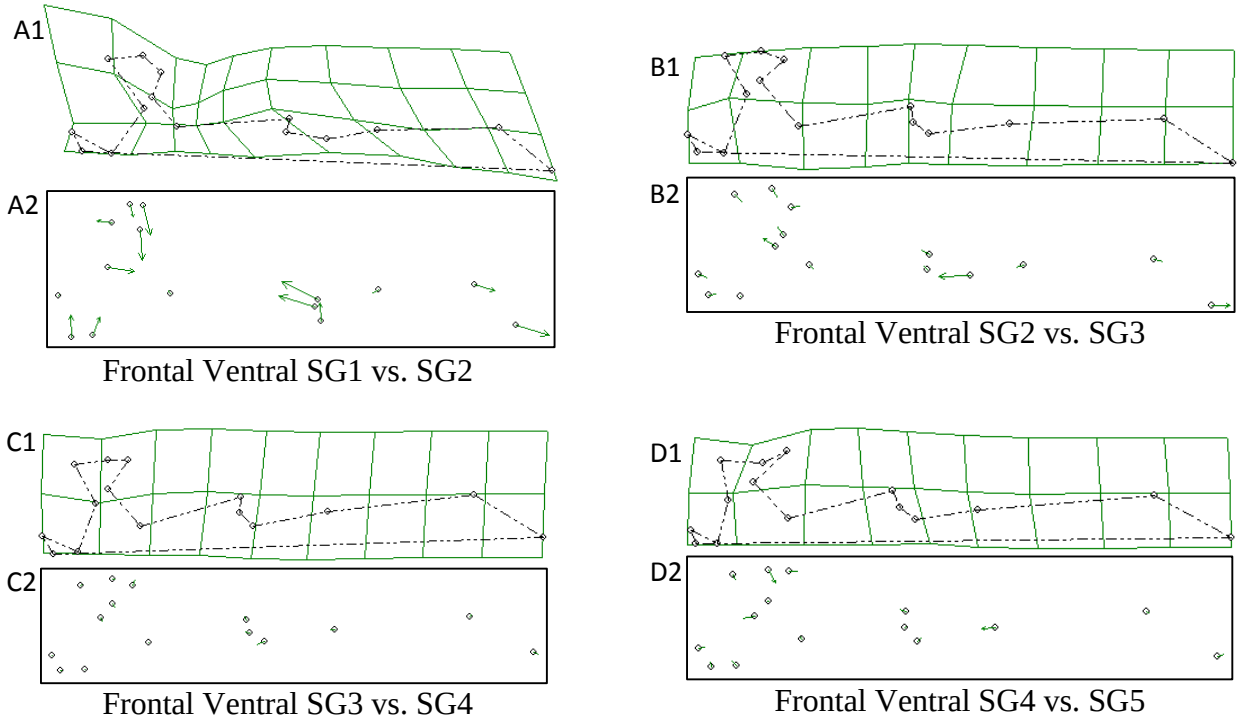

Figure 29 – Frontal Ventral View Thin Plate Spline. Spline comparing SG1 and SG2 in (A1) grid and (A2) vector format. Spline comparing SG2 and SG3 in (B1) grid and (B2) vector format. Spline comparing SG3 and SG4 in (C1) grid and (C2) vector format. Spline comparing SG4 and SG5 in (D1) grid and (D2) vector format.

The main changes noticeable in the spline for SG1 and SG2 were similar to the dorsal view (Fig. 29). A mediolateral narrowing of the posterior of the frontal, shortening of the orbital margin, and lengthening of the anterior points could be seen. The new changes visible in the view were in the ventral sutures. The lateral extent of the frontal-parietal suture moved posteriorly, the posterior extent of the frontal-lateral sphenoid suture moved anteriorly, and the medial-ventral extent of the frontal-prefrontal suture moved laterally. The orbital margin continued to shorten in the spline for SG2 and SG3 while the anterior – and posterior-most points moved anteriorly. The posterior and lateral extent of the frontal-laterosphenoid suture moved posterolaterally. The medial-ventral extent of the frontal-prefrontal suture now moved in a posterior direction. There were only small movements but none notable between SG3 and SG4.

Same results for SG4 and SG5 except for the anterior movements of the frontal-postorbital suture and posterior movement of the posterior extent of the frontal-laterosphenoid suture and anterioventral extent of the frontal-prefrontal suture.

Parietal—The parietal shifted its shape somewhat consistently but still most notably at the smaller sizes of SG1 and SG2 (Fig. 30). The largest changes were in the temporal foramens and overall shape of the bone. The anteromedial points moved laterally in the spline giving the bone a more box-like shape than the wedge shape of the juvenile bone. The posteromedial point moved further posteriorly. The medial points of the tempoorbital foramen and the dorsotemporal fossa moved medially, enlarging those openings. Finally the posterior extent of the dorsotemporal fenestra moved anteromedially. Many of the changes between SG2 and SG3 differed from those before them. The posteromedial point now moved anteriorly and the posterior extent of the parietal-squamosal suture moved posterolaterally, re-forming a similar shape from SG1. The dorsotemporal fenestra moved anteromedially a great degree. The lateral extent of the parietal-squamosal suture anterior to the tempoorbital foramen also extended laterally. SG3 and SG4 showed the least amount of change. The tempoorbital foramen deepened slightly further while the dorsotemporal fenestra changed direction, moving laterally this time. The medial extent of the parietal-squamosal suture moved anterolaterally. Only three landmarks showed significant movement for SG4 and SG5, all others were stationary or barely moved. This time the medial extent of the parietal-squamosal suture resumed its anteromedial movement and the Lateral extent of the parietal-squamosal suture posterior to the tempoorbital foramen extended posterolaterally. The posterior extent of the dorsotemporal fenestra again moved medially.

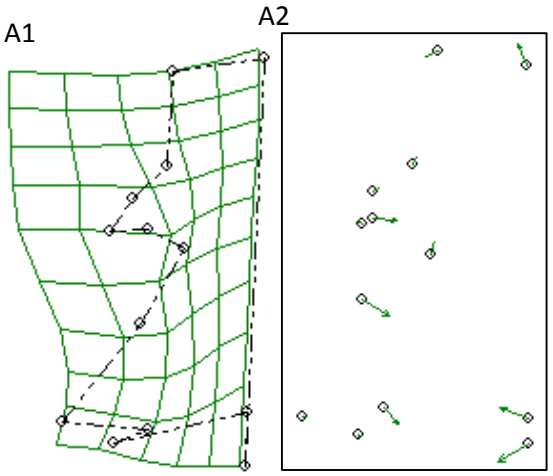

Parietal Dorsal SG1 vs. SG2

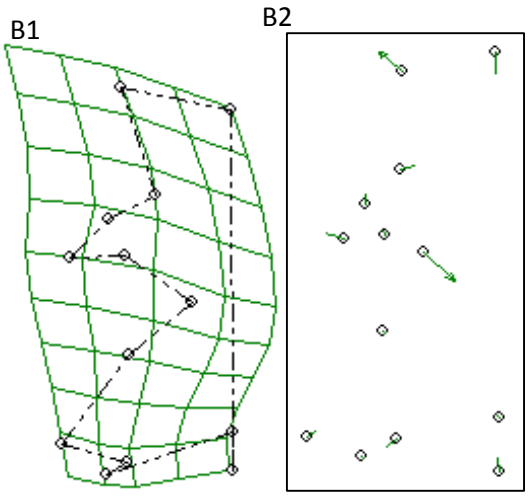

Parietal Dorsal SG2 vs. SG3

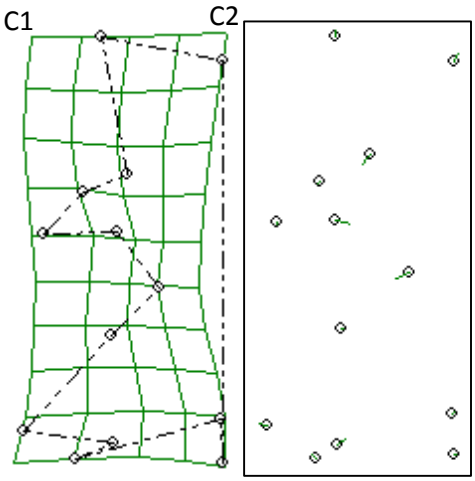

Parietal Dorsal SG3 vs. SG4

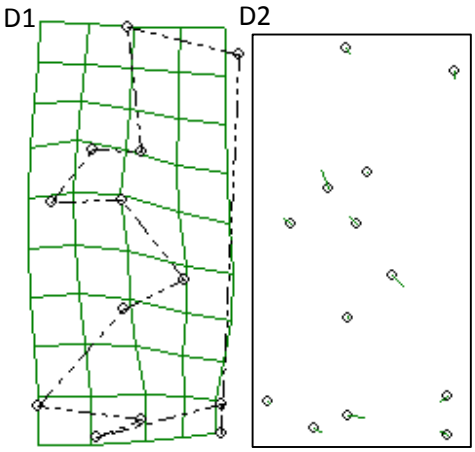

Parietal Dorsal SG4 vs. SG5

Figure 30 – Parietal Dorsal View Thin Plate Spline. Spline comparing SG1 and SG2 in (A1) grid and (A2) vector format. Spline comparing SG2 and SG3 in (B1) grid and (B2) vector format. Spline comparing SG3 and SG4 in (C1) grid and (C2) vector format. Spline comparing SG4 and SG5 in (D1) grid and (D2) vector format.

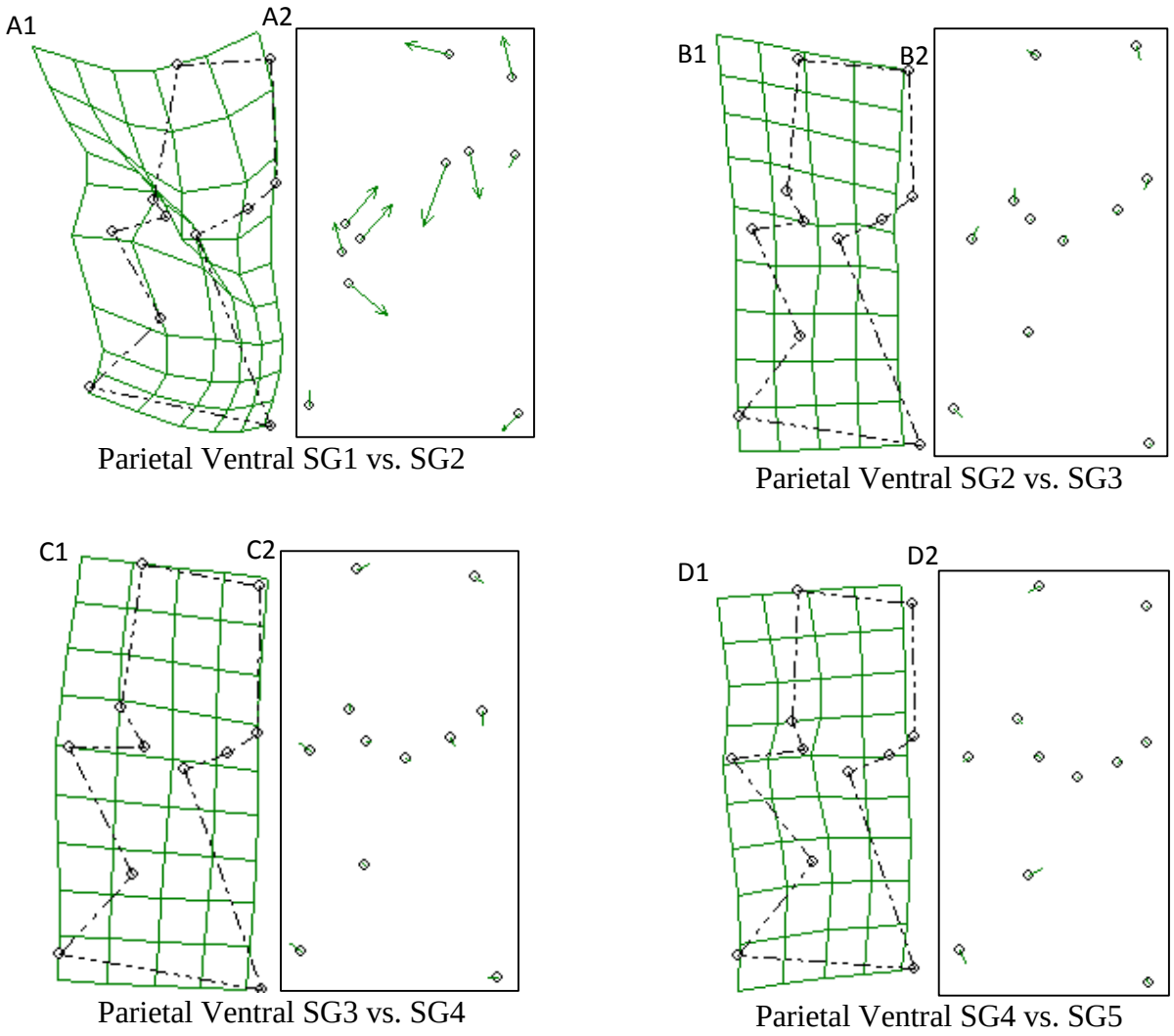

Figure 31 – Parietal Ventral View Thin Plate Spline. Spline comparing SG1 and SG2 in (A1) grid and (A2) vector format. Spline comparing SG2 and SG3 in (B1) grid and (B2) vector format. Spline comparing SG3 and SG4 in (C1) grid and (C2) vector format. Spline comparing SG4 and SG5 in (D1) grid and (D2) vector format.

The ventral movements of the parietal landmarks were much more stable, after the initial changed from SG1 to SG2, when compared to the dorsal view (Fig. 31). The posteromedial point moved posteriorly and the posterior extent of the parietal-squamosal suture moved laterally. The anteromedial point appeared to move laterally, again narrowing the anterior of the bone. The dorsotemporal fossa moved anteromedially a larger degree. The tempoorbital foramen moved in two directions, the posterior and medial points moved posteromedially and the anterior point

moved posterolaterally. The middle ear cavities moved anteriorly with the greatest movements being seen in the lateral cavities, which moved slightly away from each other in mediolateral directions. Almost all movements in the spline were large and dramatic. By contrast, the landmark movements all but stopped for SG2 and SG3. The posteromedial point once again reversed and moved anteriorly along with the anterior extent of medial foramen of the middle ear cavity. The lateral points of the tempoorbital foramen both moved posteriorly. A slight anteromedial movement of the lateral extent of the parietal-postorbital suture was the only other notable change between these SGs. The same lack of changes was seen through SG3, SG4, and SG5.

CHAPTER 4

DISCUSSION AND CONCLUSION

Discussion

Cranial Ontogenesis—Two main patterns were noticed in the analysis, the first being that the posterior bones of the cranium undergo more constant and noticeable ontogenetic change versus the rostral bones. Similar results were noticed by other studies on crocodilian ontogeny. Sadlier (2009) commented that the posterior portions of the skull experience large posterior movements while the rostrum experiences only small anterior movements. The bones of the rostrum (premaxilla, maxilla, and nasal) showed little change overall across the majority of SGs. The maxilla and nasal both showed noticeable landmark movement between SG1 and SG2 but then only minute shifts from there on. This early ontogenetic change is the result of the narrowing and elongating of the snout that has been consecutively noted in studies of crocodilian skull ontogeny (Mook 1921a; Mook 1921b; Dodson 1975; Hall and Portier 1994; Erickson et al. 2003; Wu et al. 2006; Platt et al. 2009; Sadleir 2009; Gignac and Erickson 2014). The rostrum of *A. mississippiensis*, as well as that of the majority of extant crocodilians, is noted to shift from a short, broad, and blunt snout as a juvenile to a relatively longer and more narrow form as an adult. This can be seen in the SG1 vs. SG2 splines of the maxilla where the medial landmarks appear to move laterally as the posterior of the maxilla's lateral edge shifts medially becoming more parallel with the maxillary suture (Fig. 24 and 25). The posteromedial points also move further, posteriorly lengthening the maxilla some. This continues slightly in the last of the splines but overall the maxilla stabilizes its shape and merely scales in size from then on. The nasal also parallels this—in the first spline it narrows considerably and then also stabilizes its overall shape. So though this seems to support the concept that the snout lengthens as the alligator grows, these

changes only happen early in life and the premaxilla shows almost no notable change during any of the SGs. The premaxilla retains its initial shape throughout all of the SGs, simply scaling up in size, showing consistent isometric growth.

The bones of the cranium that show much more consistent ontogenetic shape change are those posterior to the rostrum, the frontal and parietal, while the jugal is intermediate in these changes. The frontal and parietal both show slightly more noticeable change throughout their splines. The splines for SG1 vs. SG2 still show the majority of the changes, but instead of stabilizing, certain aspects of the bones continue to change in a definite pattern. With the frontal there is an increase in its overall length within the first two SGs and a large decrease in the length of the orbital margin. While the rest of the bone ceases to change for the rest of the SGs, the orbital margin continues to reduce in size. This reduction in the size of the orbits as the animal grows is common among many crocodilians (Mook 1921a; Mook 1921b; Dodson 1975; Hall and Portier 1994; Sadleir 2009). The bones that make up the margins of, and surround, the orbit must change shape to cause this shrinking. Notably the lachrymal and prefrontal move and extend posteriorly reducing the orbit to the posterior of the skull (Sadleir 2009). The anterior section of the jugal that forms the maxillary scarf joint widens dorsoventrally, constricting the orbit medially (Sadleir 2009). This widening is noticeable in the splines, especially in the first and last (Fig. 27). The parietal shifts from a more wedge-like shape, with the lateral edges converging posteriorly, from a juvenile to an adult shape with more irregular lateral margins to account for larger fenestra and anterior and posterior edges more equal in width. The most continuous change that can be seen throughout the splines is the widening of the dorsotemporal fenestra. This is commonly noted in *A. mississippiensis* and is a trait that is shared with the highly aquatic Indian Gharial, *Gavialis gangeticus* (Mook 1921a; Mook 1921b; Dodson 1975).

These observations make it seem that the shape change seen in the cranium is less due to the snout actually elongating and more due to the orbits reducing in size posteriorly (Fig. 32). Snout length in crocodilians is most often measured from the anterior of the orbits to the posterior of the nares, or anterior of the premaxilla (Dodson 1975; Flynt 2007; Platt et al. 2009). Since the orbits shift posteriorly as *A. mississippiensis* grows, this measuring technique could give the impression of the snout growing longer when that is not necessarily the case. Since the maxilla, the posterior most tooth bearing bone, does not allometrically lengthen throughout growth it seems misleading to claim the snout is lengthening.

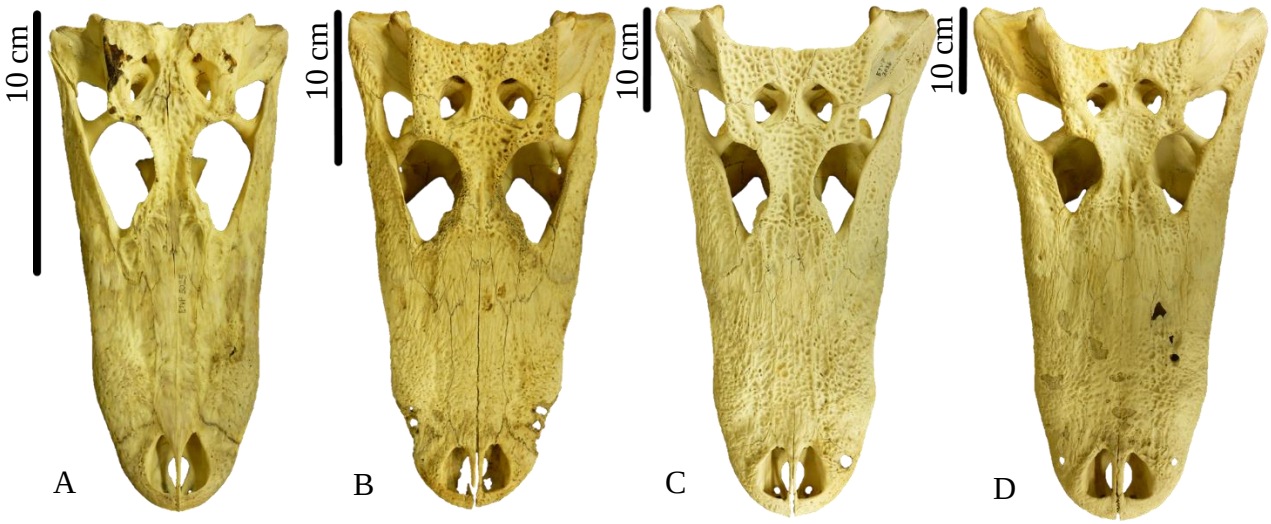

Figure 32 – Growth series of *A. mississippiensis* craniums: **A**, ETVP5025, SG2; **B**, ETVP7209, SG4; **C**, ETVP3036, SG6; **D**, NVPL265, SG6. The SGs for these skulls were achieved by measuring the premaxilla, being the most easily measured on an articulated skull. The two largest skull, ETVP3036 and NVPL265, are outside the size limits of SG5 and therefore would have created SG6 if they had been included in the study.

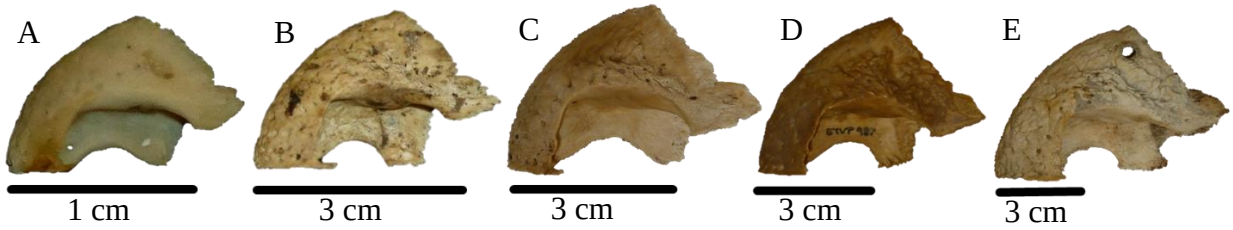

Figure 33 – Growth series of *A. mississippiensis* premaxillae: **A**, SG1, Specimen 7198PM204; **B**, SG2, Specimen 3235PM353; **C**, SG3, Specimen 7202APM749; **D**, SG4, Specimen 487PM702; **E**, SG5, Specimen 7205PML869.

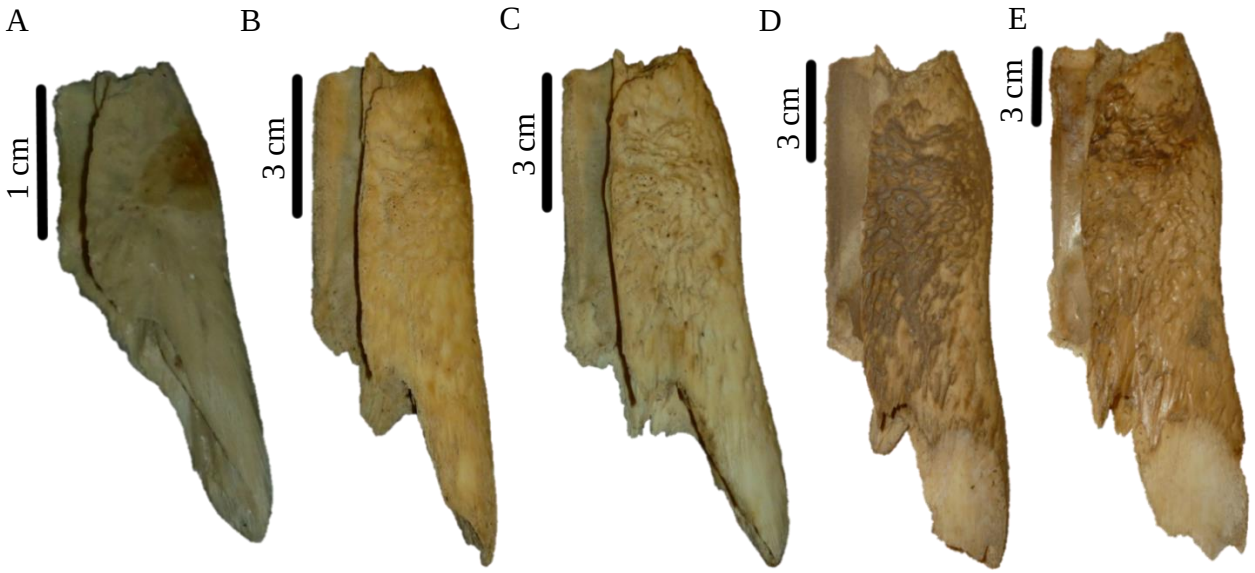

Figure 34 – Growth series of *A. mississippiensis* maxillae: **A**, SG1, Specimen 7198M195; **B**, SG2, Specimen 5000M494; **C**, SG3, Specimen 5000M484; **D**, SG4, Specimen 487M699; **E**, SG5, Specimen 7202MM795.

Figure 35 – Growth series of *A. mississippiensis* nasals: **A**, SG1, Specimen 7198N222; **B**, SG3, Specimen 3235N455, **C**; SG4, Specimen 487N136; **D**, SG5, Specimen 3235NL441.

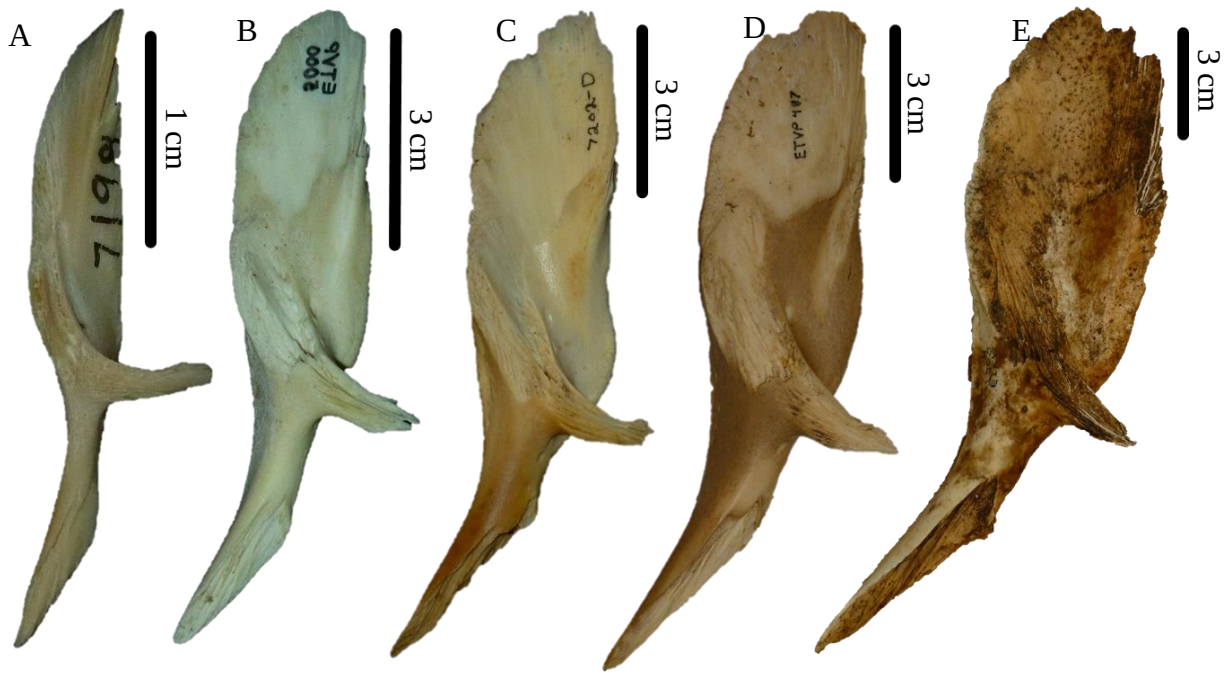

Figure 36 – Growth series of *A. mississippiensis* jugals: **A**, SG1, Specimen 7198J213; **B**, SG2, Specimen 5000JL551; **C**, SG3, Specimen 7202DJ593; **D**, SG4, Specimen 487J804; **E**, SG5, Specimen 7202NJL815.

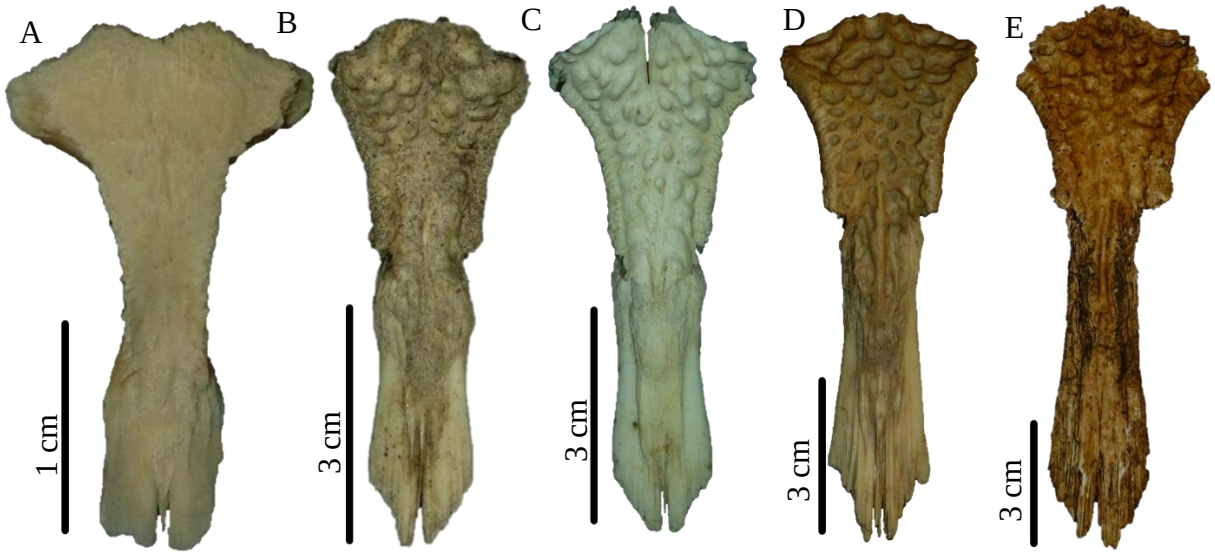

Figure 37 – Growth series of *A. mississippiensis* frontals: **A**, SG1, Specimen 7198F207; **B**, SG2, Specimen 5000F564; **C**, SG3, Specimen 5000F567; **D**, SG4, Specimen 487F133; **E**, SG5, Specimen 7202NF617. The reduction is the proportional size of the orbit is most notable in the shortening of the orbital margin.

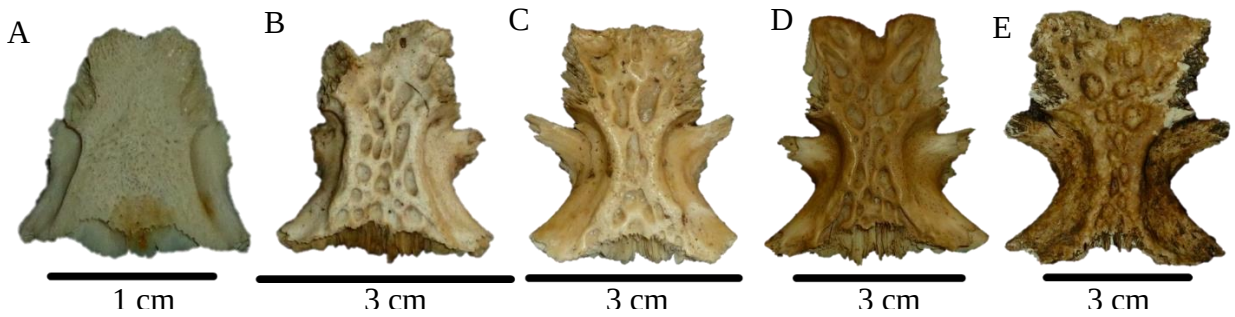

Figure 38 – Growth series of *A. mississippiensis* parietals: **A**, SG1, Specimen 7198P218; **B**, SG2, Specimen 3235P673; **C**, SG3, Specimen 3235P418; **D**, SG4, Specimen 487P144; **E**, SG5, Specimen 7202NP623.

Rate of Ontogenetic Change—The second pattern that emerged was that the majority of the shape change occurred early in the growth series, then essentially stops after that. Though there is variation, all of the bones follow a general pattern that can be seen in the splines and graphs. There is a large degree of shape change between SG1 and SG2—these splines always show the most landmark movement and in almost every PCA graph SG1 is separated from the rest of the SGs. Then after these initial early changes, the bones all become more stable. As discussed earlier, the posterior bones show more change in the later stages; however, the amount of landmark movement drops significantly here as well. It has been noted that *A. mississippiensis* acquires its rough adult cranial shape early in life (Dodson 1975). This accelerated rate of change early in life also makes sense when it is taken into consideration that *A. mississippiensis* grows fastest during its first six to eight years and then growth slows considerably until longitudinal growth effectively stops completely (Neill 1971; Dodson 1975; McIlhenny 1987; Brisbin 1988; Hall and Portier 1994;). With these observations it appears the cranium quickly takes its adult shape and then scales up in size. The orbits do continue to shrink throughout growth and there are small shifts in the bones at larger sizes but nothing compared to the extreme changes in SG1 vs. SG2.

Missing or Misleading Data—Another potential explanation for why the early life changes are as extreme as they are, and why SG1 is almost always separate from the other SGs in the graphs, is that there is a large size gap missing in the growth series between SG1 and SG2. This is blatantly notable in that SG2 is completely absent from the nasal bones. SG1 consists of two extremely young specimens that are significantly smaller than the smallest specimens in SG2. The largest of SG1 is a skull roughly 62 mm in length while the smallest specimen in SG2 was about 192 mm, over three times the length. On average, the bones of SG2 are 60% larger than SG1. This is why SG1 tends to fallout away from the other SGs, which tend to group closer together, in the PCA graphs. They represent a much more continuous growth series with smaller size gaps between the SGs, with the second largest between SG4 and SG5. These missing specimens definitely drove the analysis to a degree. The biggest issue caused by this gap is that the shape change that takes place between SG1 and SG2 cannot be seen in detail. Even having one specimen between these two points would shed some light. There was also uneven distribution of the bones among the SGs. There is definitely a bell curve effect in the distribution, with SG3 and SG4 always containing more than the rest. This could be remedied by adding in smaller and larger specimens to the study and thereby give a more complete and balanced ontogenetic view of alligator growth.

The other issue that could cause some error in the results is individual variation, which crocodilians are notorious for (Mook 1921a; Mook 1921b; Brongersma 1941; Busbey 1995; Platt et al. 2009). This was most noticeable in the jugal and nasal where the degree of variation made it difficult to choose consistent landmarks. It is not known to what degree, if any, individual variety may have affected this study but it is always an issue when working with such a plastic group. Phenotypic plasticity is easily notable in *A. mississippiensis* in comparisons between wild

and captive-raised individuals. Captive-reared alligators tend to develop a very different morphotype consisting of broader and shorter heads, splayed teeth, and more robust bodies (Erickson et al. 2004). Though physically distinct there is not any notable difference in bite force, with captive alligators possessing just as strong and at times stronger bite forces than their wild counterparts (Erickson et al. 2004). Yet another source of variation among crocodilians is sexual dimorphism. Size disparity is the most notable with the males growing much larger than the females. There are skeletal variations between the males and females, they are subtle but can be detected and even used to estimate sex (Brongersma 1941; Hall and Portier 1994; Bonnan et al. 2008; Platt et al. 2009)

Study Goals—Both ontogenetic and allometric change was evident. Every bone, except for the premaxilla, showed significant ontogenetic change especially in the smaller sizes. The allometric change was seen in the comparison of the anterior and posterior bones. The anterior bones of the snout show significant change early on but then cease to change while the posterior bones continue to change in noticeable ways throughout growth. This is not the first time this has been documented (Saldeir 2009). While most of the findings in this study parallel those of similar studies (Mook 1921a; Mook 1921b; Saldeir 2009), certain aspects have not been mentioned before, such as the lack of change seen in the premaxilla throughout ontogeny compared to the other bones. The rate of change of each bone was also much clearer in this study. Continued pursuit of this technique could reveal similar amounts of information about the remaining bones of the skull both in *A. mississippiensis* and other crocodilians, both extant and fossil. Also, using *A. mississippiensis* as a comparison to fossil crocodilians and archosaurs has been shown to be reliable source of data in many other studies and this technique could add new information to those comparisons (Brochu 1996; Farlow et al. 2005; Rayfield et al. 2007; Bonnan et al. 2008;

Holliday and Witmer 2008). In the future more bones as well other crocodilians, both fossil and extant, could be researched using this technique, and these results could be used to better understand alligator evolution.

Conclusions

- This study of isolated cranial material of *Alligator mississippiensis* documents ontogenetic and allometric change.
- Similar to other studies of *A. mississippiensis*, the orbits showed negative allometry while the maxilla shifts from a broader shape to be narrower.
- Posterior bones showed more consistent and noticeable shape change throughout ontogeny, while the anterior bones change early in life and then stabilize in overall morphology, showing isometry.
- The majority of the shape change in the cranium occurs early in life with the overall cranial shape reached at a young age, confirming earlier analyses.
- The isometric growth of the maxilla and reduction of the orbits in a posterior direction suggests that the common observation that the snout lengthens with age is a misconception brought on by the common method used to measure the snout.
- Unique to this study, the premaxilla of *A. mississippiensis* showed almost no shape change throughout the growth series.

REFERENCES

Bonnan MF, Farlow JO, Masters SL. 2008. Using linear and geometric morphometrics to detect intraspecific variability and sexual dimorphism in femoral shape in *Alligator mississippiensis* and its implications for sexing fossil Archosaurs. Journal of Vertebrate Paleontology 28(2):422-431.

Brisbin Jr., IL. 1988. Growth curve analyses and their application to the conservation and captive management of crocodilians. Working Meeting of Crocodile Specialist Group 9: 116-145.

Brochu CA. 1996. Closure of Neurocentral sutures during crocodilian ontogeny: implications for maturity assessment in fossil archosaurs. Journal of Vertebrate Paleontology 16(1):49-62.

Brongersma LD. 1941. Age variation in the skulls of crocodiles. Archives néerlandaises de zoologie 5:505.

Busbey AB. 1995. The structural consequences of skull flattening in crocodilians; pp. 173-192 in Functional Morphology in Vertebrate Paleontology. Press Syndicate of the University of Cambridge, New York, New York.

Dodson P. 1975. Functional and ecological significance of relative growth in *Alligator*. Journal of Zoology 175(3):315-355.

Erickson GM, Lappin AK, Vilet KA. 2003. The ontogeny of bite-force performance in American alligator (*Alligator mississippiensis*). Journal of Zoology 260:317-327.

Erickson GM, Lappin AK, Parker T, Vilet KA. 2004. Comparison of bite-force performance between long-term captive and wild American alligator (*Alligator mississippiensis*). Journal of Zoology 262:21-28.

Farlow JO, Hurlburt GR, Elsey RM, Britton ARC, Langston Jr., W. 2005. Femoral dimensions and body size of *Alligator mississippiensis*: estimating the size of extinct Mesoeucrocodylians. Journal of Vertebrate Paleontology 25(2):354-369.

Flynt R. 2007. Mississippi Wildlife, Fisheris, & Parks. Alligator Capture & Harvest Techniques. Available at http://www.mdwfp.com/wildlife-hunting/alligator-program.aspx. Accessed January 13, 2015.

Gignac PM. 2010. Biomechanics and the ontogeny of feeding in the American Alligator (Alligator Mississippiensis): reconciling factors contributing to intraspecific niche differentiation in a large-bodied vertebrate. Dissertation for The Florida State University.

Gignac PM, Erickson GM. 2014. Ontogenetic changes in dental form and tooth pressures facilitate developmental niche shifts in American alligators. Journal of Zoology.

Greer AE. 1974. On the maximum total length of the salt-water crocodile (*Crocodylus porosus*). Journal of Herpetology 8(4): 381-384.

Hall PM, Portier KM. 1994. Cranial morphometry of New Guinea crocodiles (*Crocodylus novaeguineae*): ontogenetic variation in relative growth of the skull and an assessment of its utility as a predictor of the sex and size of individuals. Herpetological Monographs 8:203-225.

Holliday CM. 2011. Vertebrate Functional Morphology & Evolution: 3D Alligator – Adult Skull. Program in Integrative Anatomy, Department of Pathology and Anatomical Sciences, University of Missouri School of Medicine. Available at web.missouri.edu. Accessed April 28, 2013.

Holliday CM, Witmer LM. 2008. Cranial kinesis in dinosaurs: intracranial joints, protractor muscles, and their significance for cranial evolution and function in diapsids. Journal of Vertebrate Paleontology 28(4):1073–1088.

Jacobsen T, Kushlan JA. 1989. Growth dynamics in the American alligator (*Alligator mississippiensis*). Journal of Zoology 219(2): 309-328.

Kardong KV, Zalisko EJ. 2012. Comparative Vertebrate Anatomy, A Laboratory Dissection Guide, Sixth Edition. McGraw Hill, New York, New York, 404 pp.

McIlhenny EA. 1987. The Alligator's Life History. Ten Speed Press, Berkley, California, 117 pp.

Mook CC. 1921a. Individual and age variations in the skulls of recent Crocodilia. Bulletin American Museum of Natural History 44(7):51–74.

Mook CC. 1921b. Skull characters of recent *Crocodilia*: with notes on the affinities of the recent genera. Bulletin American Museum of Natural History 44(13):123–167.

Neill WT. 1971. The Last of the Ruling Reptiles: Alligators, Crocodiles, and Their Kin. Columbia University Press, New York, 486 pp.

Pierce SE, Angielczyk KD, Rayfield EJ. 2008. Patterns of morphospace occupation and mechanical performance in extant crocodilian skulls: a combined geometric morphometric and finite element modeling approach. Journal of Morphology 269:840-864.

Platt SG, Rainwater TR, Thorbjarnarson JB, Finger AG, Anderson TA, McMurry ST. 2009. Size estimation, morphometrics, sex ratio, sexual size dimorphism, and biomass of Morelet's crocodile in northern Belize. Caribbean Journal of Science 45(1): 80-93.

Rayfield EJ, Milner AC, Xuan VB, Young PG. 2007. Functional morphology of spinosaur 'crocodile-mimic' dinosaurs. Journal of Vertebrate Paleontology 27(4): 892-901.

Rohlf FJ. 2009a. tpsDig. Stony Brook Mophometrics, Stony Brook, New York.

Rohlf FJ. 2009b. tpsUtil. Stony Brook Mophometrics, Stony Brook, New York.

Rohlf FJ. 2009c. tpsSuper. Stony Brook Mophometrics, Stony Brook, New York.

Rohlf FJ. 2009d. tpsSplin. Stony Brook Mophometrics, Stony Brook, New York.

Sadleir RW. 2009. A morphometric study of Crocodylian ecomorphology through ontogeny and phylogeny. Ph.D. dissertation, The University of Chicago, Chicago, Illinois, 242 pp.

SPSS Inc. 2007. SPSS 16.0. SPSS Inc., Chicago.

Snyder D. 2007. Morphology and systematics of two Miocene alligators from Florida, with a discussion of alligator biogeography. Journal of Paleontology 81(5):917-928.

Tsai HP, Holliday CM. 2011. Ontogeny of the alligator cartilago transiliens and its significance for sauropsid jaw muscle evolution. PLoS ONE 6(9):e24935.

Vickaryous MK, Hall BK. 2008. Development of the dermal skeleton in *Alligator* mississippiensis (archosauria, crocodylia) with comments on the homology of osteoderms. Journal of Morphology 269:398-422Woodward, A. R., J. H. White, and S. B. Linda. 1995. Maximum Size of the Alligator *(Alligator mississippiensis*). Journal of Herpetology 29(4): 507-513.

Woodward AR, White JH, Linda SB. 1995. Maximum Size of the Alligator (*Alligator mississippiensis*). Journal of Herpetology 29(4): 507-513.

Wu XB, Xue H, Wu LS, Zhu JL, Wang RP. 2006. Regression analysis between body and head measurements of Chinese alligators (*Alligator sinensis*) in the captive population. Animal Biodiversity and Conservation 29(1): 65-71.

APPENDICES

Appendix A

Bone Measurements

Premaxilla. All measurements are in mm.

Dorsal	Ventral	Measure 1	Measure 2	Measure 3	Measure	Size Group
7198PM204	7198PM200	10.88	10.98	10.58	10.81	1
7197PM249	7197PM250	11.28	11.27	11.24	11.26	1
5000PML534	-	28.98	29.08	28.87	28.98	2
3235PM353	3235PM380	31.38	31.38	31.33	31.36	2
7210PM850	7210PM852	34.98	34.96	34.91	34.95	2
5000PML526	5000PML539	39.73	39.70	39.46	39.63	3
7202APM749	7202AMP750	41.37	41.35	41.40	41.37	3
3235PML350	3235PML404	41.44	41.45	41.47	41.45	3
7144PM645	7144PM646	44.18	43.98	43.98	44.05	3
7202APM751	7202AMP752	46.04	46.18	46.28	46.17	3
3235PML357	3235PML399	46.61	46.59	46.60	46.60	3
3235PM374	3235PM375	48.47	48.45	48.45	48.46	3
7217PML687	7217PML688	52.00	52.07	51.92	52.00	4
3235PM369	3235PM387	52.11	52.13	51.98	52.07	4
509PM878	509PM879	52.74	52.65	52.72	52.70	4
3235PM372	3235PM398	53.95	53.96	53.96	53.96	4
7217PML686	7217PML689	54.23	53.97	53.99	54.06	4
487PM702	487PM705	54.24	54.18	54.19	54.20	4
3235PM345	3235PM385	54.21	54.21	54.21	54.21	4
3235PM368	3235PM381	55.51	55.65	55.80	55.65	4
3235PM671	3235PM672	56.28	56.52	56.54	56.45	4
3235PML348	3235PML383	56.79	56.72	56.59	56.70	4
508PM873	508PM874	56.77	56.76	56.76	56.76	4
3236PM303	3236PM304	58.00	58.00	58.00	58.00	4
3235PML365	3235PML406	58.31	58.09	57.77	58.06	4
5000PM524	5000PM537	62.57	62.55	62.54	62.55	4
3235PM344	3235PM377	69.51	69.32	69.52	69.45	5
7205PML869	7205PML870	74.71	74.67	74.67	74.68	5
7202NPM812	-	76.40	76.42	76.60	76.47	5

Maxilla. All measurements are in mm.

Dorsal	Ventral	Measure 1	Measure 2	Measure 3	Measure	Size Group
7198M195	7198M198	33.9	33.89	33.86	33.88	1
7197M242	7197M234	34.33	34.22	34.34	34.30	1
3235M331	3235M334	96.43	96.43	96.43	96.43	2
5000M494	5000M502	114.03	114.03	114.02	114.03	2
5000ML496	5000ML499	117.74	117.68	117.68	117.70	3
5000M484	5000M508	123.01	123.01	123.01	123.01	3
7210M839	7210M840	126.50	126.38	126.36	126.41	3
5000M488	5000M512	126.69	126.68	126.68	126.68	3
7144M647	7144M827	128.16	128.14	128.12	128.14	3
7202AM732	7202AM733	130.05	130.04	130.03	130.04	3
5000M485	5000M515	130.17	130.17	130.17	130.17	3
7206M818	7206M819	139.42	139.39	139.38	139.40	3
3232ML275	3232ML676	143.41	143.40	143.39	143.40	3
7202AM734	7202AM735	143.53	143.52	143.53	143.53	3
3235M314	3235M316	147.13	147.13	147.12	147.13	3
5020M831	5020M832	147.50	147.45	147.43	147.46	3
7202AM736	7202AM737	147.32	147.71	147.78	147.60	3
3235ML322	3235ML342	156.76	156.76	156.76	156.76	3
7202AM729	7202AM731	158.05	158.00	157.98	158.01	3
7217M682	7217M684	163.85	163.82	163.79	163.82	4
7202AM725	7202AM726	164.05	164.04	164.03	164.04	4
7218M658	7218M822	164.55	164.52	164.55	164.54	4
3235ML323	3235ML340	165.28	165.26	165.25	165.26	4
487M699	487M833	166.90	166.89	166.88	166.89	4
3232ML271	3232ML272	168.91	168.90	168.89	168.90	4
3235M327	3235M338	172.40	172.60	172.59	172.53	4
3235M330	3235M336	175.99	176.04	176.04	176.02	4
7202AM727	7202AM728	177.55	177.52	177.52	177.53	4
5000M493	5000M520	186.01	185.98	185.96	185.98	4
5000M491	5000M519	190.02	190.01	189.98	190.00	4
3236M299	3236M301	197.72	197.71	197.70	197.71	4
7202AM719	7202AM720	201.95	202.03	201.93	201.97	5
7202MM795	7202MM796	222.25	222.24	222.24	222.24	5
7202NM806	7202NM807	241.12	241.11	241.11	241.11	5

Nasal. All measurements are in mm.

Specimen ID	Measure 1	Measure 2	Measure 3	Measure	Size Group
7197N267	22.02	21.93	22.23	22.06	1
7198N222	25.56	25.59	25.66	25.60	1
7144N295	108.68	108.70	108.73	108.70	3
3235N447	114.61	114.63	114.64	114.63	3
5000NL544	121.84	121.87	121.87	121.86	3
7206N578	123.65	123.64	123.63	123.64	3
3235N461	125.56	125.53	125.52	125.54	3
3235N455	135.28	135.24	135.20	135.24	3
3235NL449	144.46	144.34	144.33	144.38	4
3235N451	144.54	144.53	144.51	144.53	4
7217N184	146.08	146.07	146.08	146.08	4
487N136	148.74	148.74	148.76	148.75	4
7218N159	149.92	149.92	149.93	149.92	4
3235N454	156.81	156.79	156.78	156.79	4
3235NL458	157.96	157.96	157.97	157.96	4
3235N459	167.20	167.19	167.20	167.20	4
7202LNL632	188.62	188.62	188.56	188.60	5
3235N444	200.70	200.68	200.72	200.70	5
3235NL441	207.47	207.46	207.47	207.47	5
7202NN627	218.41	218.59	218.57	218.52	5

Jugal. All measurements are in mm.

Specimen ID	Measure 1	Measure 2	Measure 3	Measure	Size Group
7198J213	30.02	30.05	30	30.02	1
7197J266	32.31	32.33	32.33	32.32	1
3235J430	78.64	78.62	78.66	78.64	2
3235JL434	80.59	80.57	80.59	80.58	2
3235J439	120.94	120.94	12.94	84.94	2
7210J881	85.76	85.85	85.86	85.82	2
5000JL551	93.57	93.6	93.59	93.59	2
7144J802	98.66	98.66	98.67	98.66	3
3235JL429	107.91	107.9	107.91	107.91	3
7206J821	117.18	117.17	117.17	117.17	3
7202AJ763	117.78	117.81	117.79	117.79	3
7202DJ593	124.24	124.24	124.21	124.23	3
3235J437	130.69	130.70	130.70	130.70	4
5000JL550	131.02	131.01	131.01	131.01	4
487J804	132.08	132.12	132.02	132.07	4
3235JL427	132.29	132.29	132.29	132.29	4
7217J801	133.87	133.89	133.89	133.88	4
7202KJ883	135.20	135.18	135.20	135.19	4
3232JL285	136.40	136.40	136.40	136.40	4
7202GJ880	136.51	136.49	136.50	136.50	4
3235JL422	137.26	137.25	137.26	137.26	4
7218J803	138.65	138.57	138.56	138.59	4
7202JJL882	141.59	141.60	141.56	141.58	4
7202AJ853	144.00	144.00	144.00	144.00	4
7202AJ759	148.69	148.69	148.70	148.69	4
7202IJL838	149.00	149.03	149.03	149.02	4
3235J432	149.81	149.81	149.80	149.81	4
3235J426	166.51	166.51	166.51	166.51	5
7202MJ800	182.31	182.28	182.29	182.29	5
7202AJ854	190.64	190.63	190.65	190.64	5
7202NJL616	195.24	195.02	195.03	195.10	5
7202NJL815	195.10	195.10	195.11	195.10	5

Frontal. All measurements are in mm.

Dorsal	Ventral	Measure 1	Measure 2	Measure 3	Measure	Size Group
7198F207	7198F210	25.55	25.40	25.40	25.45	1
7197F260	7197F261	28.46	28.33	28.30	28.36	1
3235F415	3235F417	62.00	62.00	61.91	61.97	2
5000F564	5000F565	70.67	70.71	70.68	70.69	2
5000F567	5000F569	76.76	76.86	76.24	76.62	3
3235F411	3235F413	79.77	79.79	79.78	79.78	3
7144F291	7144F293	83.31	83.31	83.30	83.31	3
5000F571	5000F572	84.17	84.20	84.19	84.19	3
7206F574	7206F576	86.16	86.16	86.16	86.16	3
7202EF596	7202EF598	86.42	86.36	86.31	86.36	3
7202CF587	7202CF588	90.60	90.80	90.43	90.61	3
5020F151	5020F152	93.15	93.15	93.15	93.15	3
7202DF590	7202DF591	93.19	93.21	93.23	93.21	3
3232PF286	-	97.22	97.64	97.31	97.39	4
7202FF604	7202FF605	98.57	98.64	98.63	98.61	4
7218F167	7218F168	99.38	99.40	99.42	99.40	4
7202GF680	7202GF681	99.63	99.78	99.70	99.70	4
7217F178	7217F180	100.61	100.36	100.41	100.46	4
7202BF612	7202BF613	102.70	102.30	102.53	102.51	4
7202KF668	7202KF669	104.16	104.16	104.15	104.16	4
487F133	487F135	107.19	107.41	107.49	107.36	4
7202JPF687	-	108.23	108.98	108.77	108.66	4
7202HPF683	-	111.56	111.44	111.53	111.51	4
7202IPF682	-	113.50	114.12	113.28	113.63	4
3236F310	3236F312	124.98	125.02	124.99	125.00	5
7202NF617	7202NF621	137.70	137.92	137.51	137.71	5
7202MPF685	-	139.30	139.01	139.14	139.15	5

Parietal. All measurements are in mm.

Dorsal	Ventral	Measure 1	Measure 2	Measure 3	Measure	Size Group
7197P253	7197P256	13.63	13.46	13.51	13.53	1
7198P218	7198P219	14.20	14.19	14.22	14.20	1
3235P673	3235P674	29.26	29.24	29.24	29.25	2
7210P170	7210P177	30.51	30.53	30.49	30.51	3
5020P154	5020P156	32.01	32.00	31.98	32.00	3
5000P559	5000P562	33.49	33.52	33.51	33.51	3
3235P418	3235P420	33.90	33.88	33.89	33.89	3
7202EP599	7202EP602	35.12	34.71	34.77	34.87	3
7202CP582	7202CP585	36.62	36.46	36.52	36.53	3
7202FP608	7202FP610	38.40	38.31	38.47	38.39	4
7202KP664	7202KP666	40.58	40.38	40.38	40.45	4
7202GP678	7202GP679	40.78	40.77	40.76	40.77	4
5020P642	5020P643	41.04	41.07	41.07	41.06	4
7218P162	7218P164	41.36	41.34	41.29	41.33	4
7206P684	-	41.52	41.82	41.68	41.67	4
7217P188	7217P183	41.72	41.85	41.70	41.76	4
3232P281	3232P282	42.10	42.13	42.09	42.11	4
487P144	487P146	43.81	43.82	43.82	43.82	4
-	3232PF288	45.26	45.09	45.59	45.31	5
3236P306	3236P309	49.23	49.05	48.94	49.07	5
7202NP623	7202NP626	52.93	52.92	52.91	52.92	5

Appendix B

DA, Stepwise, and Analysis Without SG1

Premaxilla Dorsal

DA

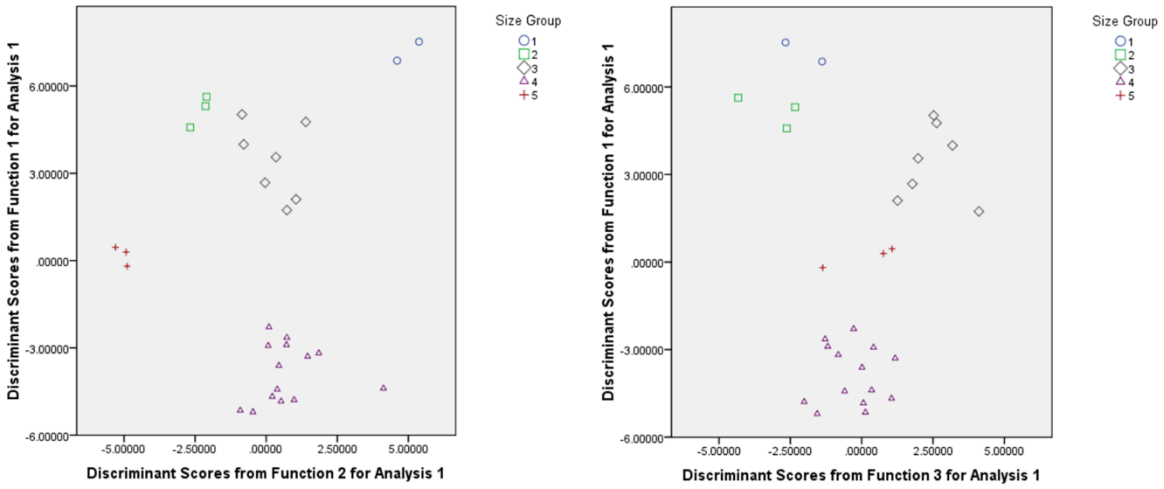

DA Stepwise

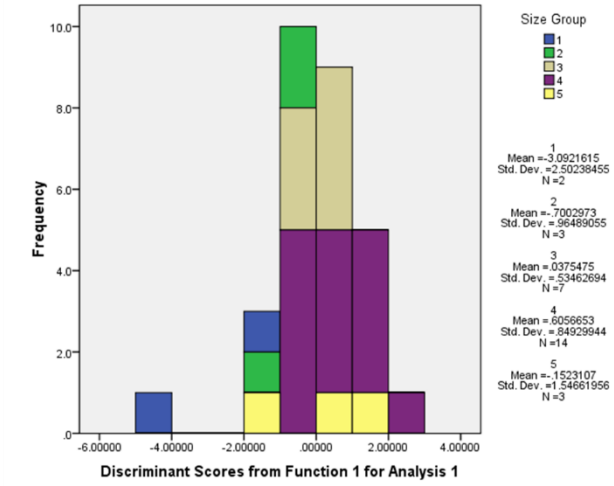

Minus Size Group 1

PCA

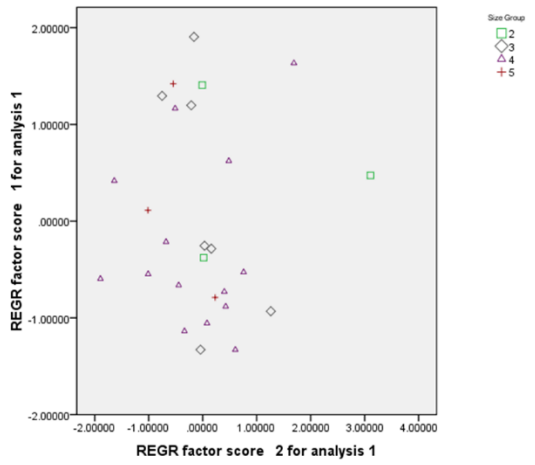

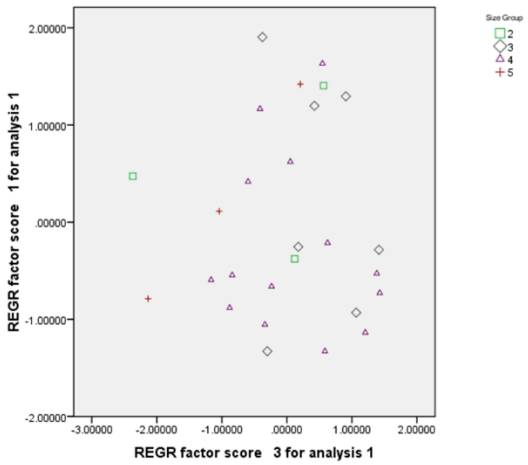

DA

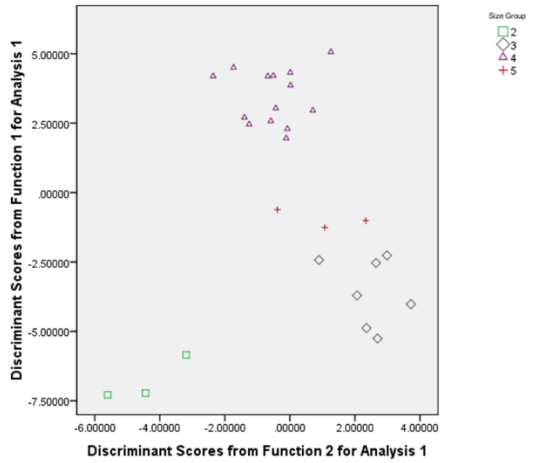

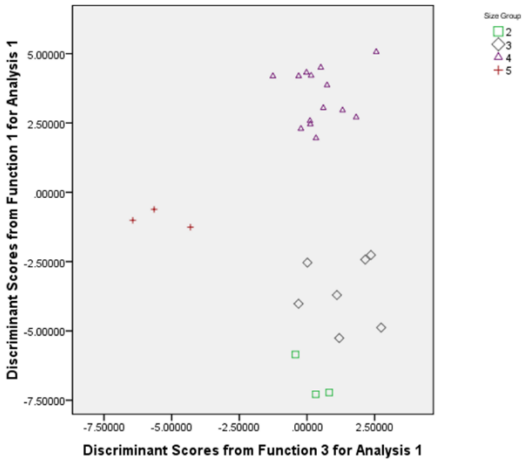

Premaxilla Ventral

DA

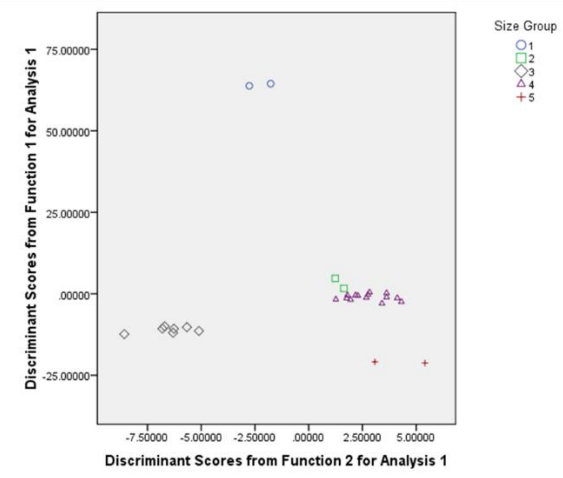

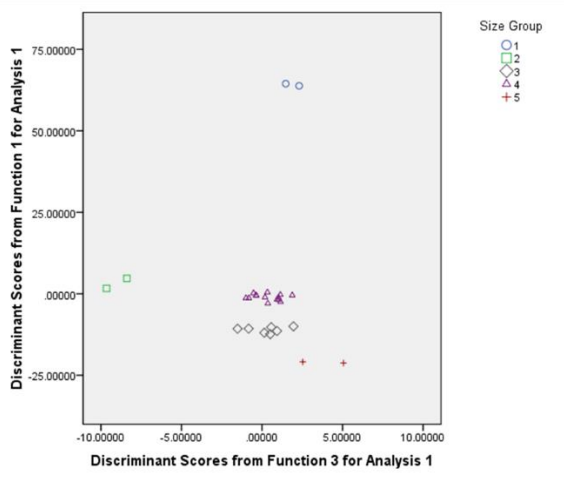

DA Stepwise

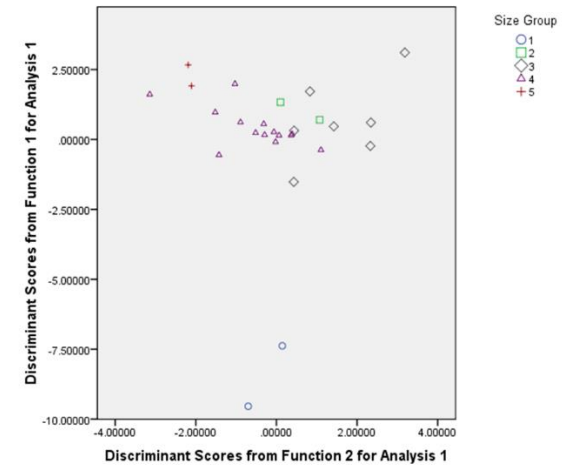

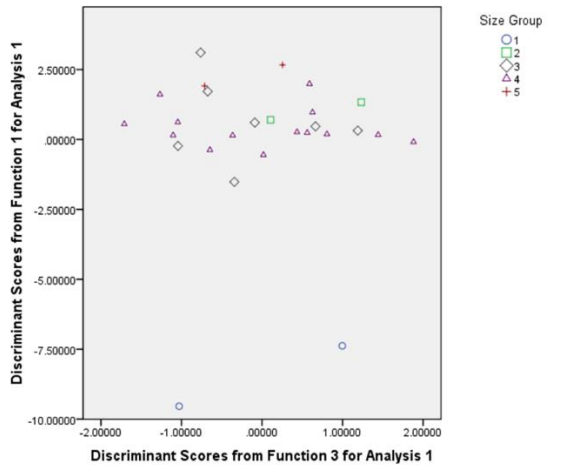

Minus Size Group 1

PCA

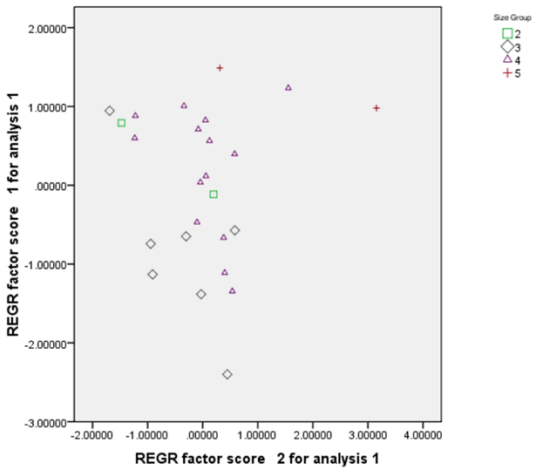

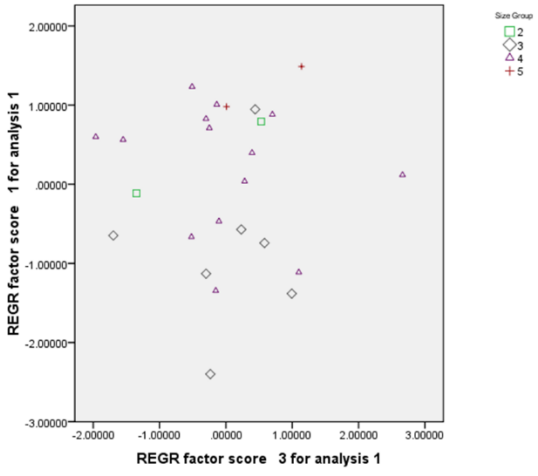

DA

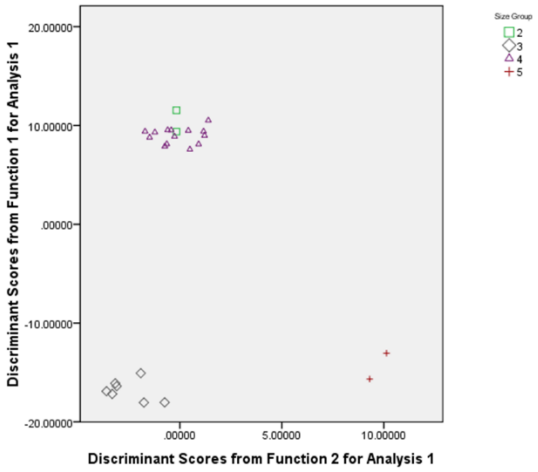

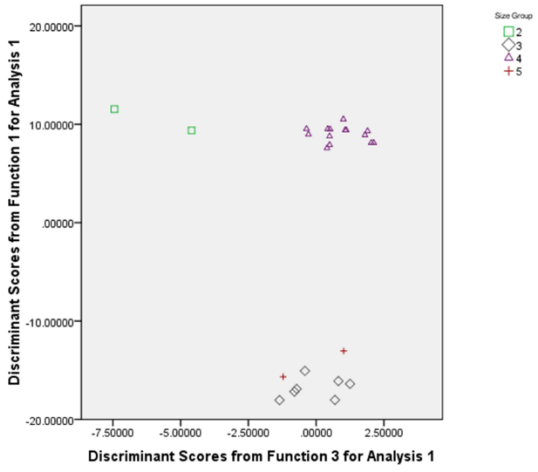

DA Stepwise

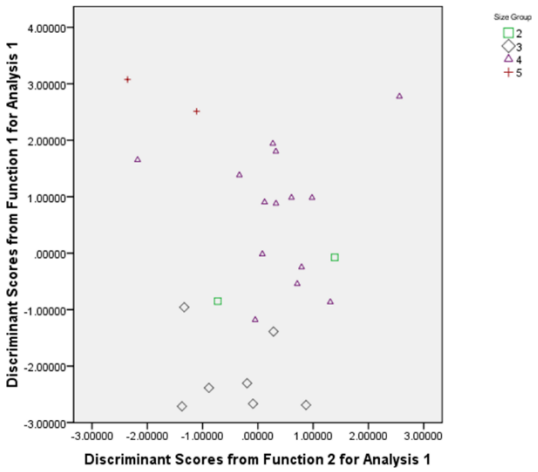

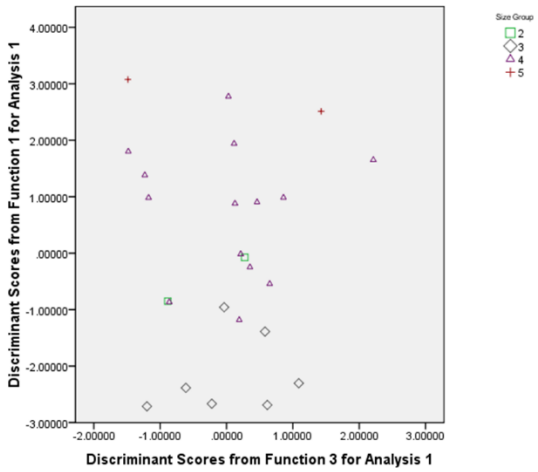

Maxilla Dorsal

DA

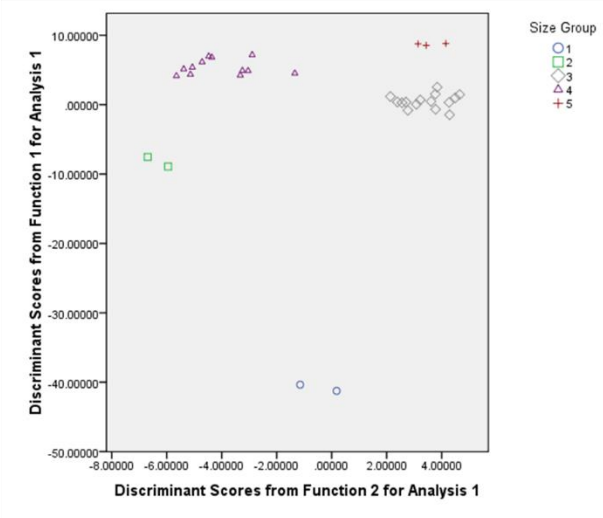

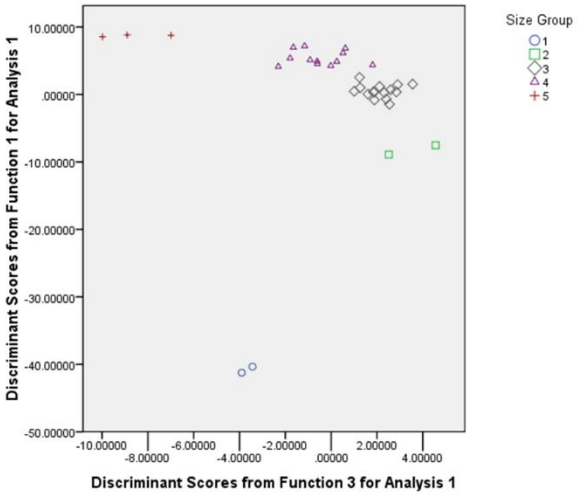

DA Stepwise

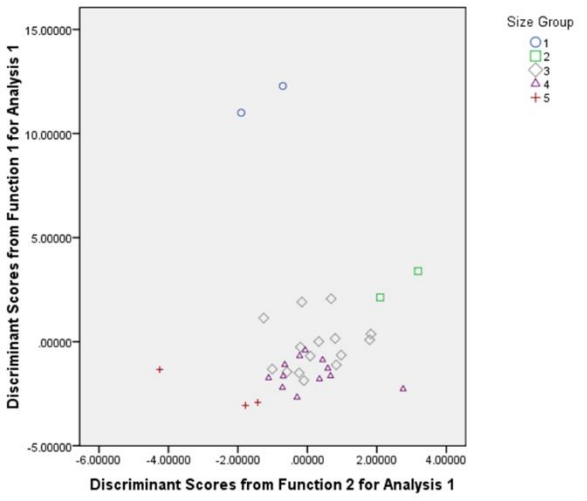

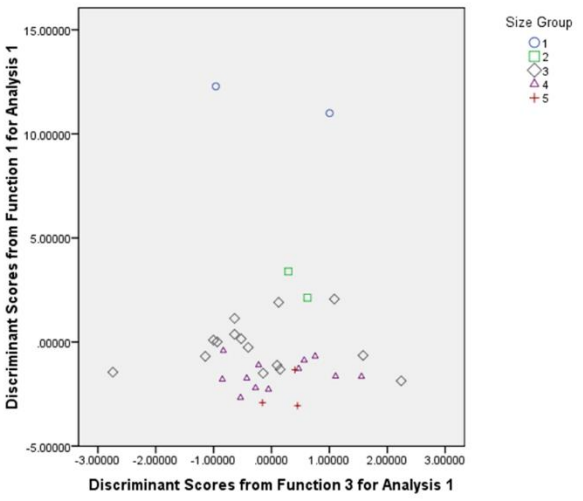

Minus Size Group 1

PCA

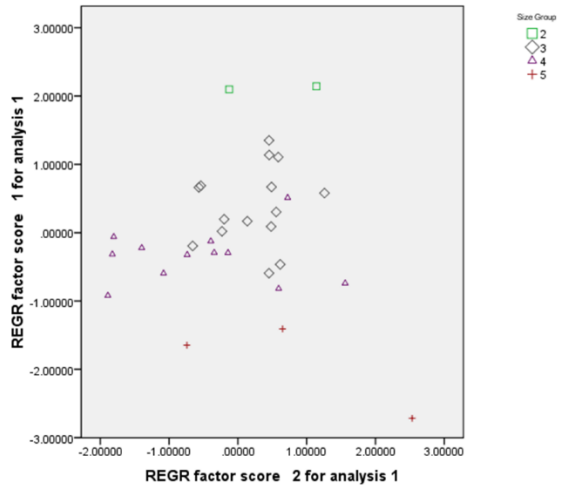

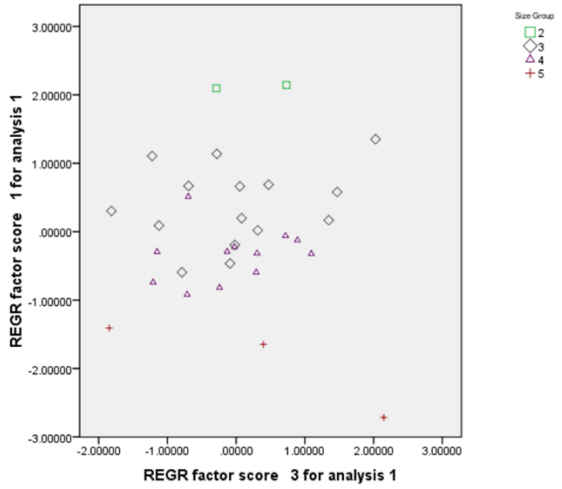

DA

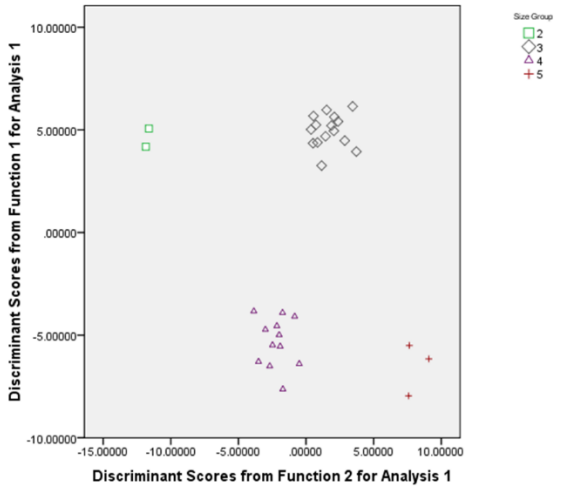

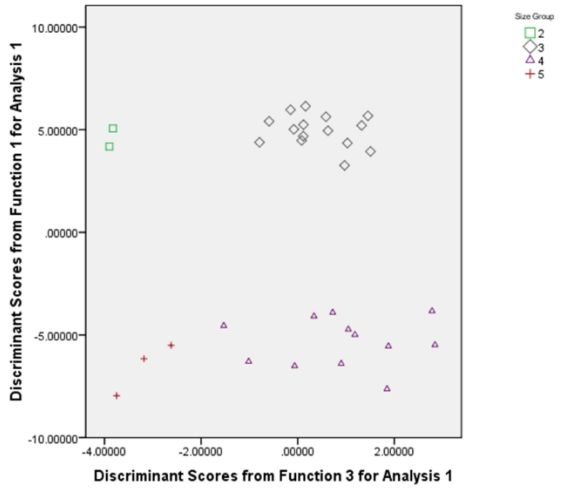

DA Stepwise

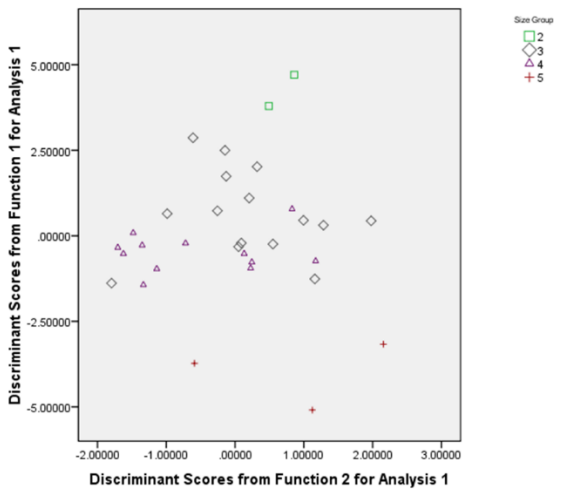

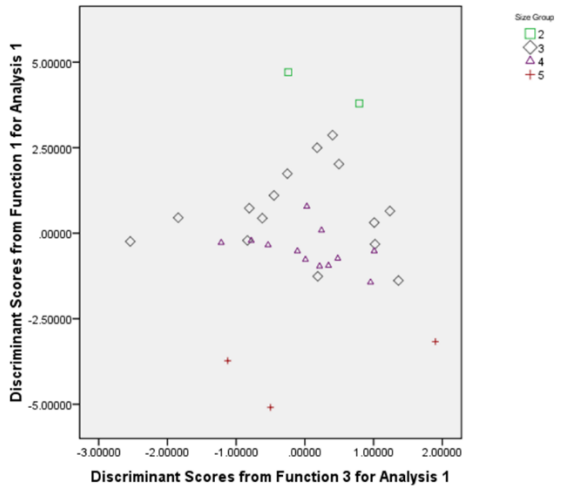

Maxilla Ventral

DA

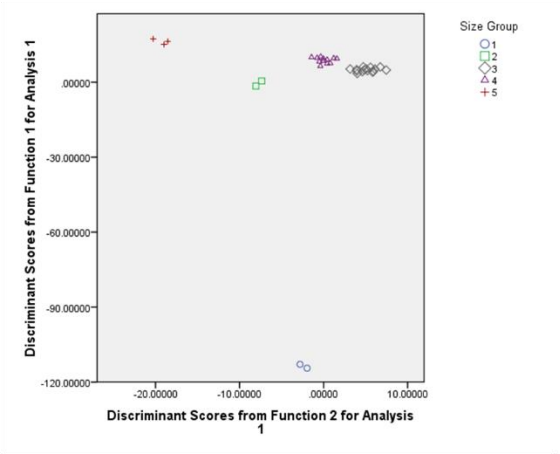

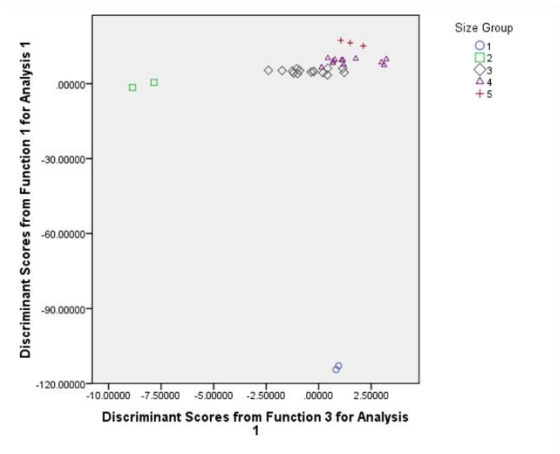

DA Stepwise

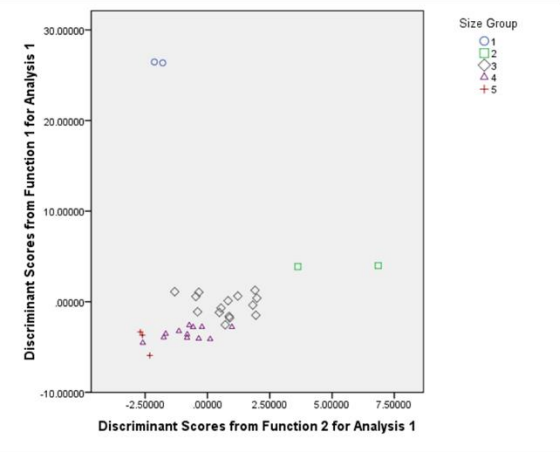

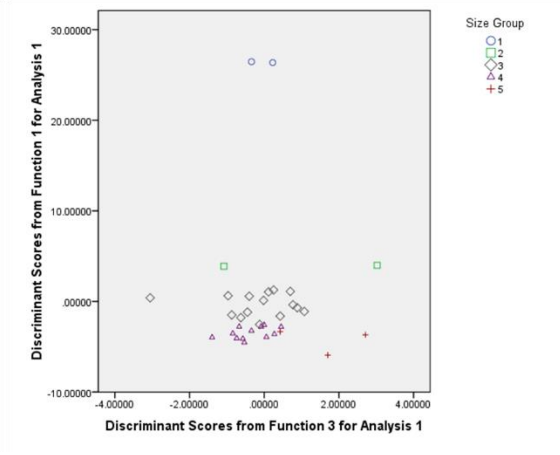

Minus Size Group 1

PCA

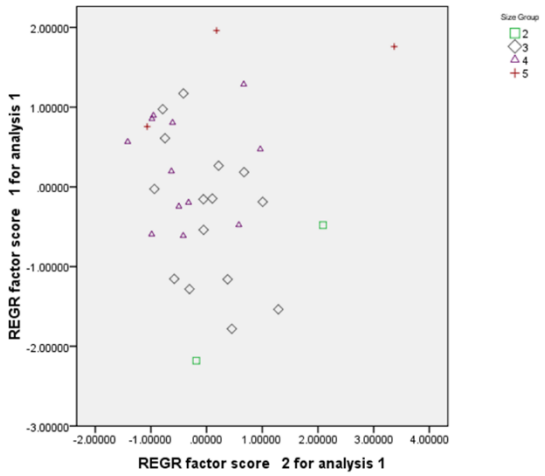

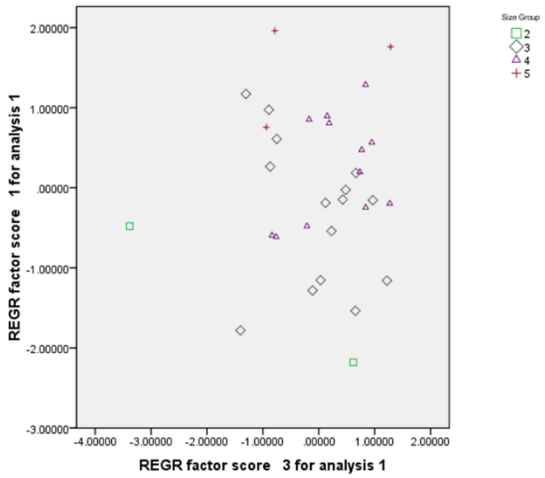

DA

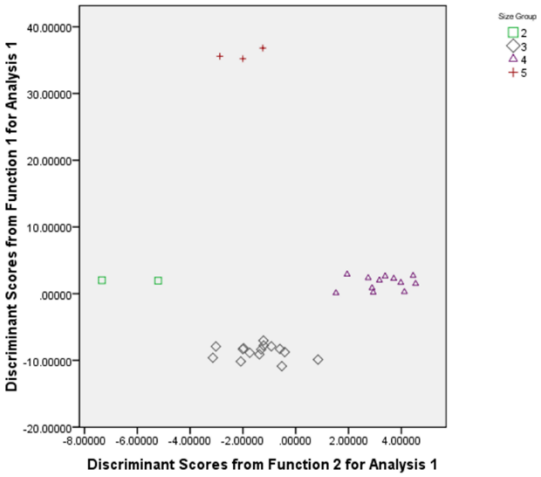

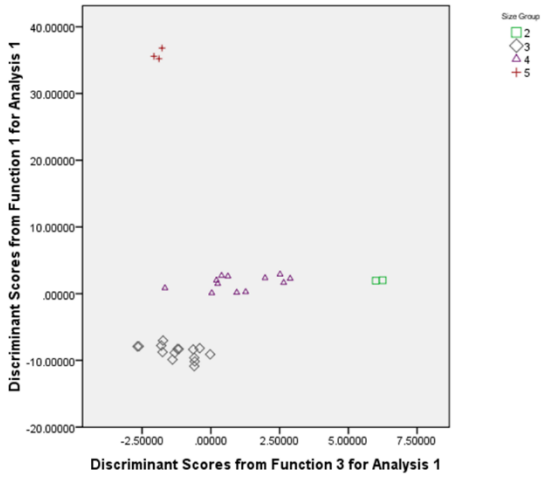

DA Stepwise

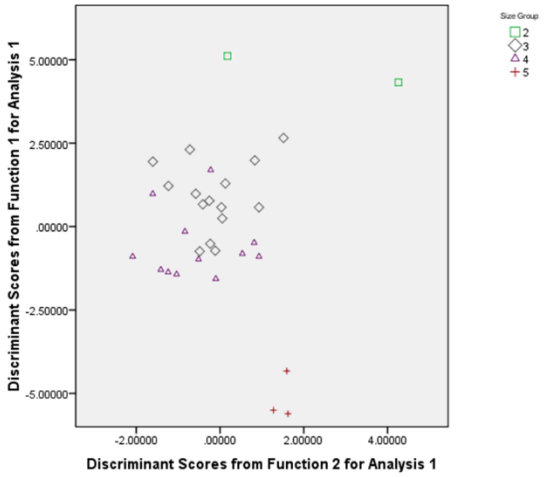

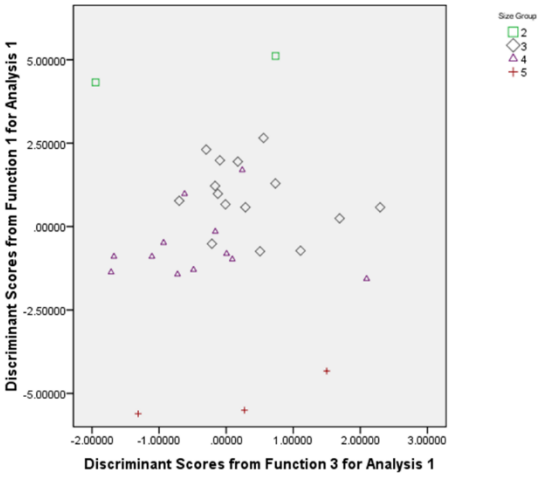

Nasal

DA

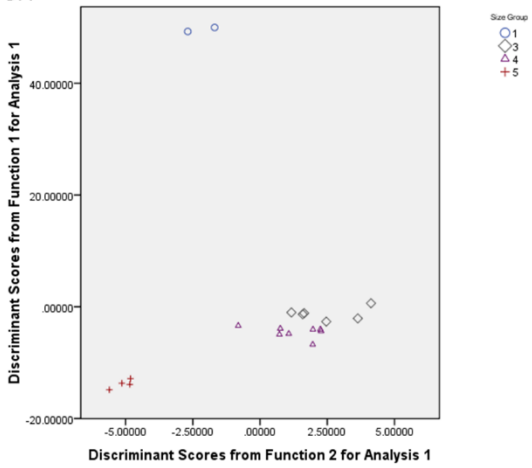

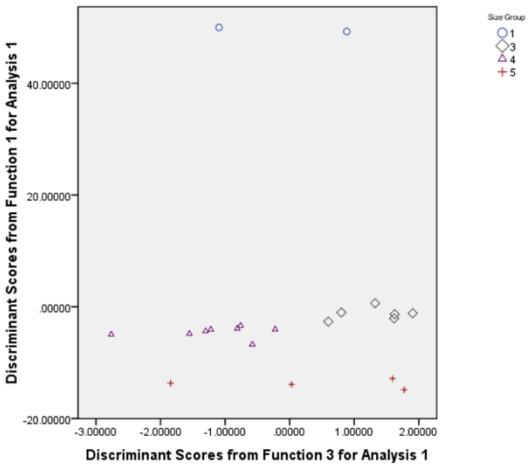

DA Stepwise

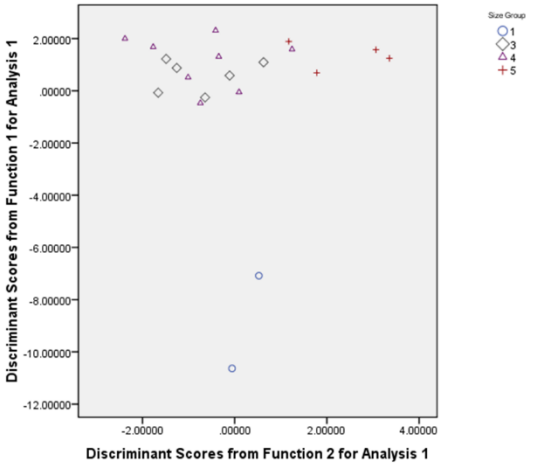

Minus Size Group 1

PCA

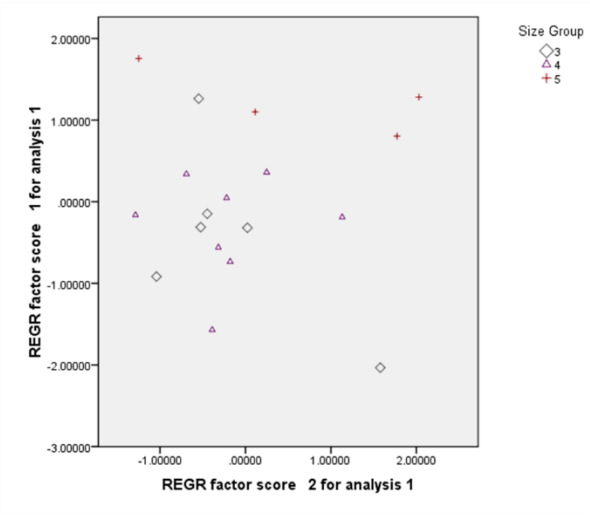

DA

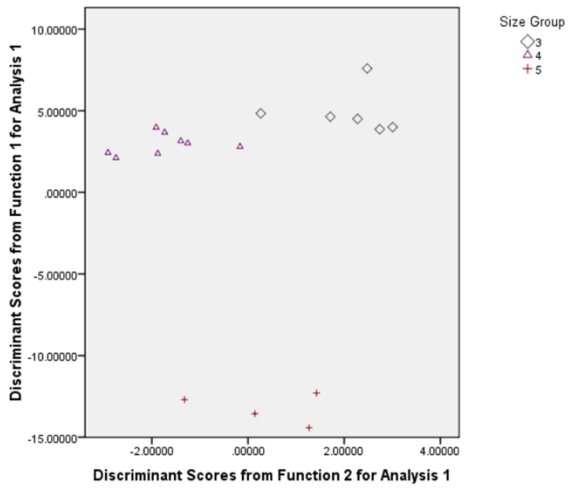

DA Stepwise

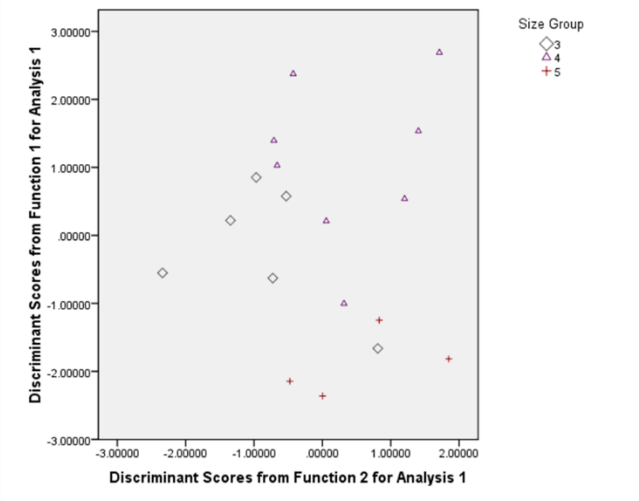

Jugal

DA

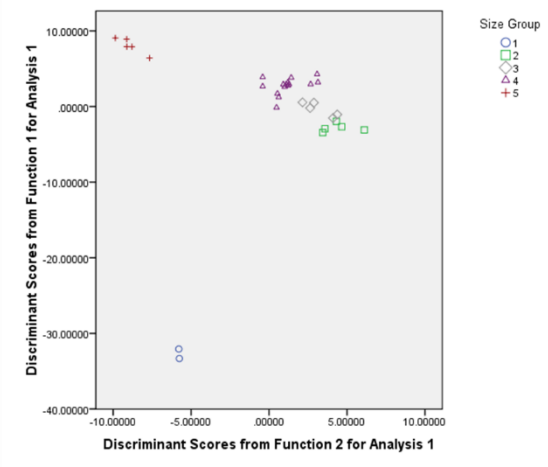

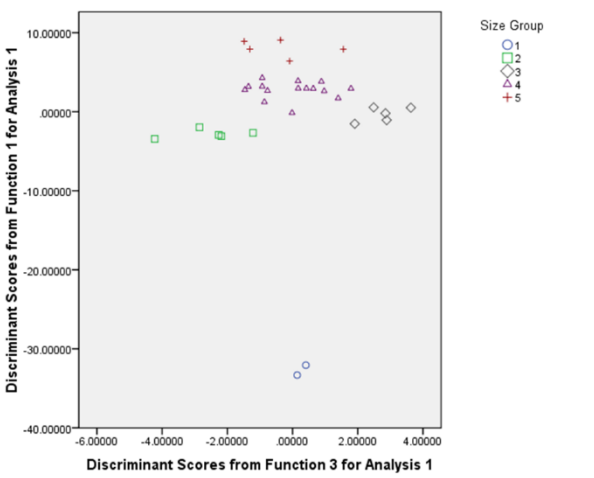

DA Stepwise

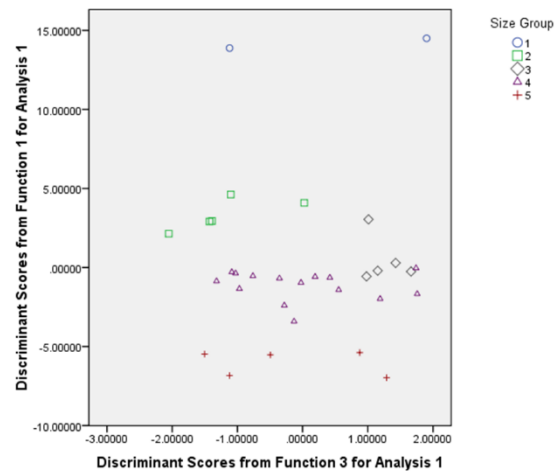

Minus Size Group 1

PCA

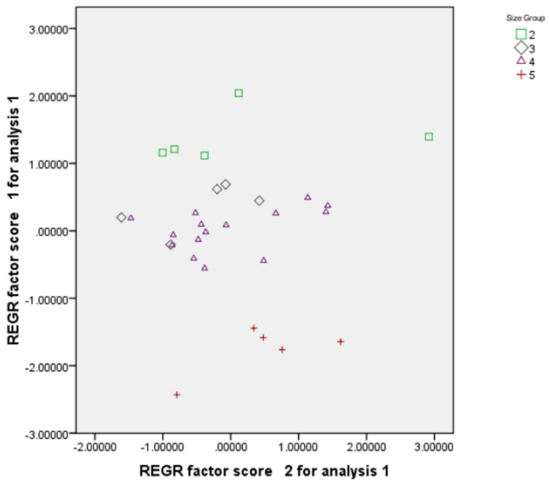

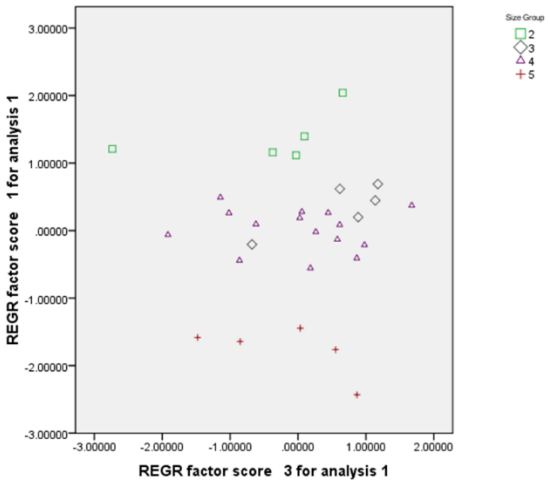

DA

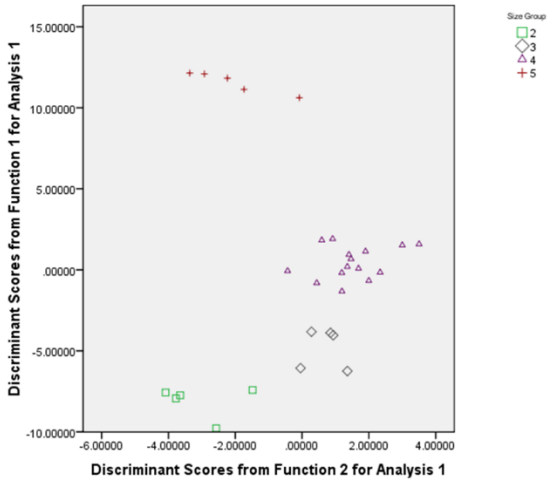

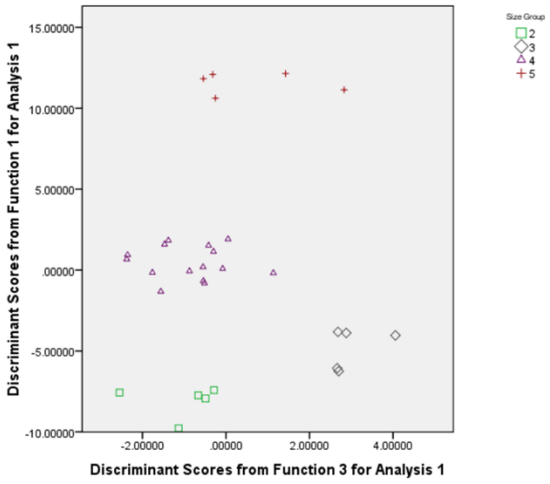

DA Stepwise

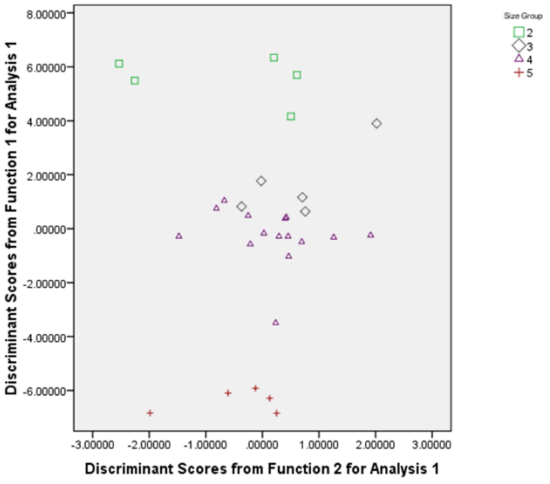

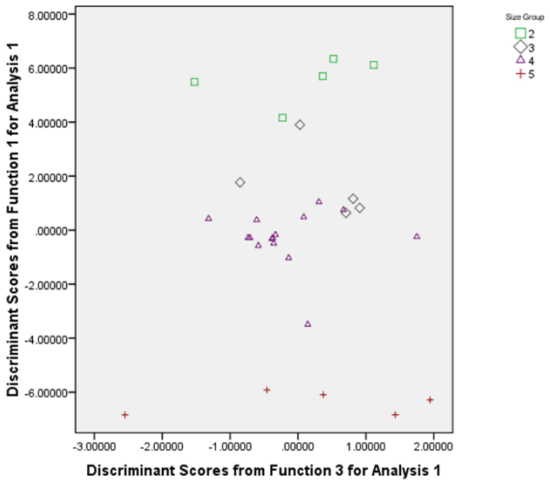

Frontal Dorsal

DA

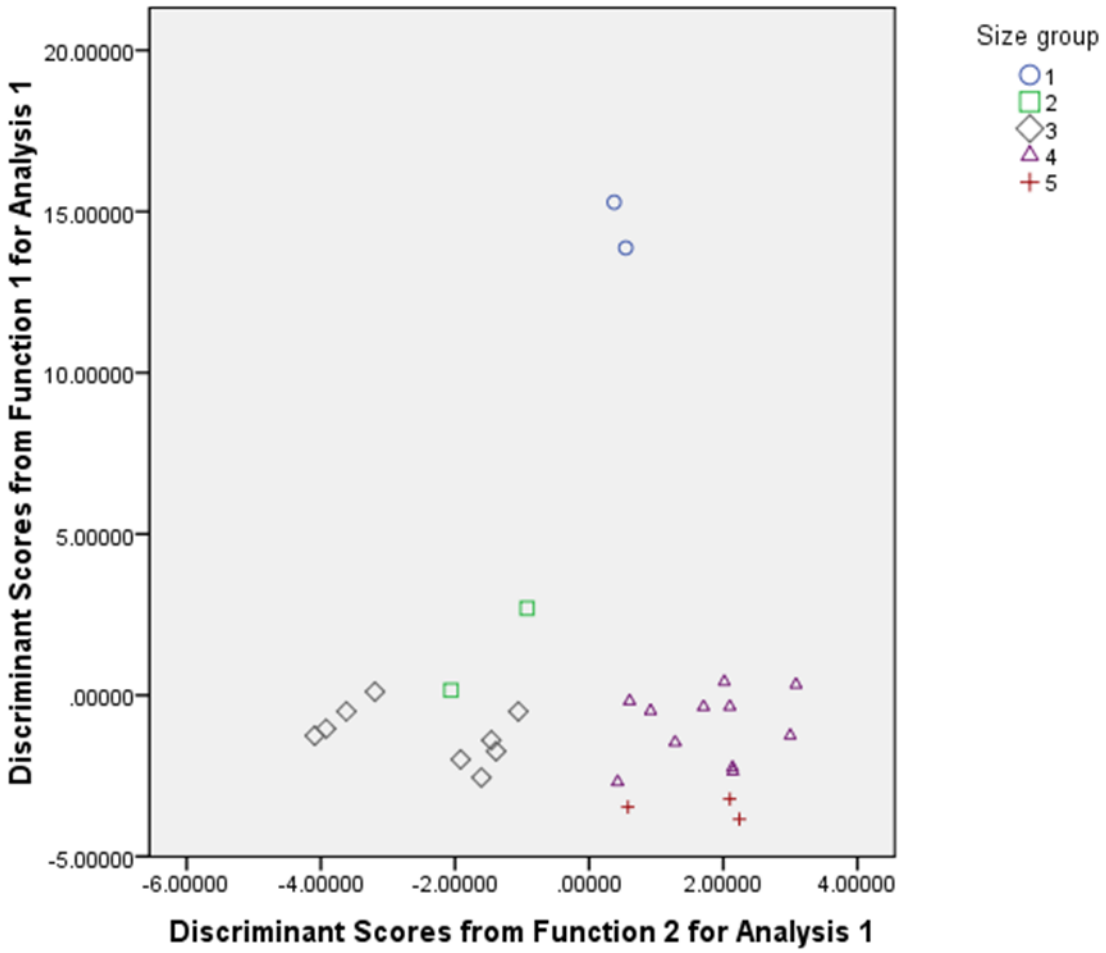

Minus Size Group 1

PCA

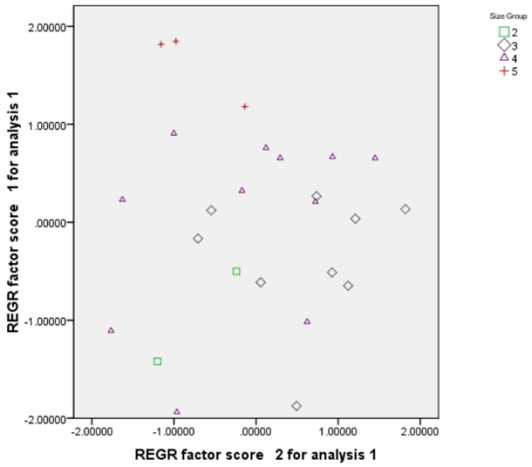

DA

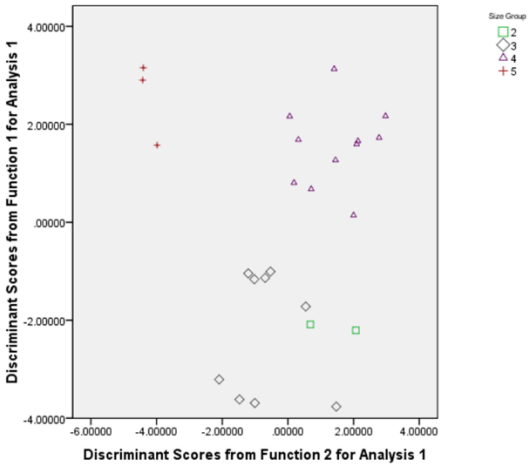

DA Stepwise

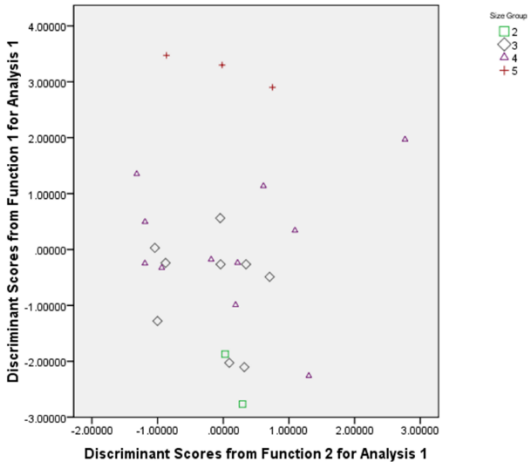

Frontal Ventral

DA

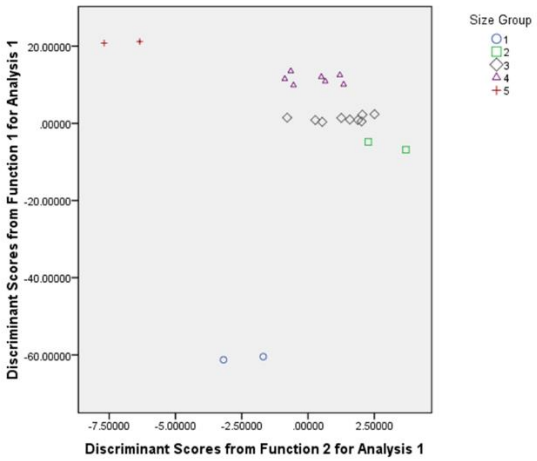

DA Stepwise

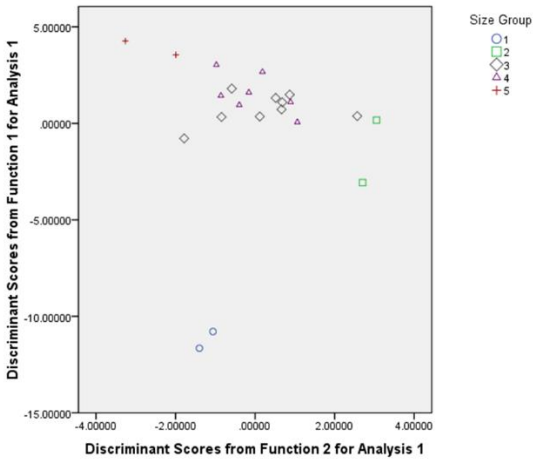

Minus Size Group 1

PCA

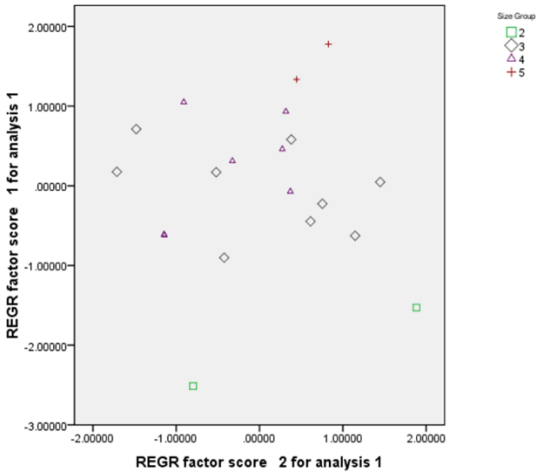

DA

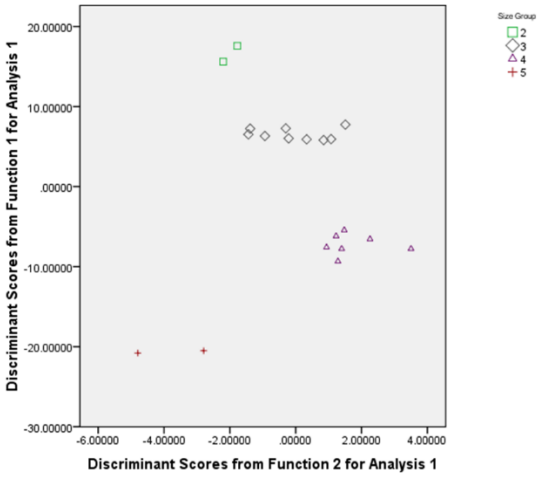

Parietal Dorsal

DA

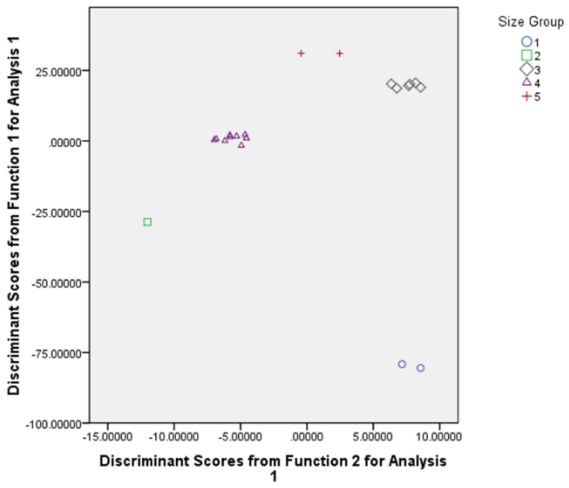

DA Stepwise

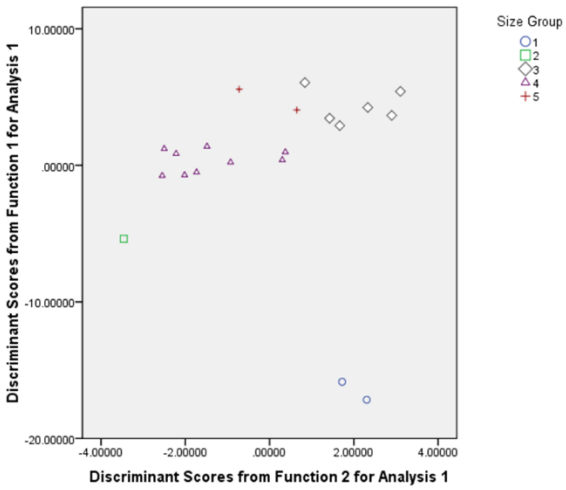

Minus Size Group 1

PCA

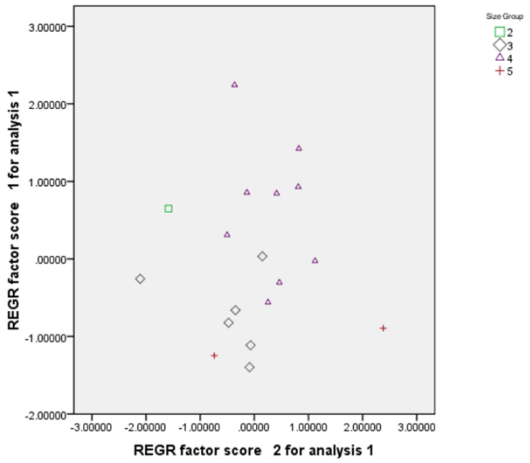

DA

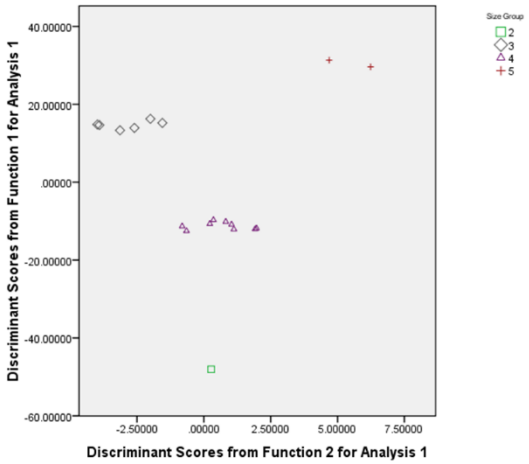

DA Stepwise

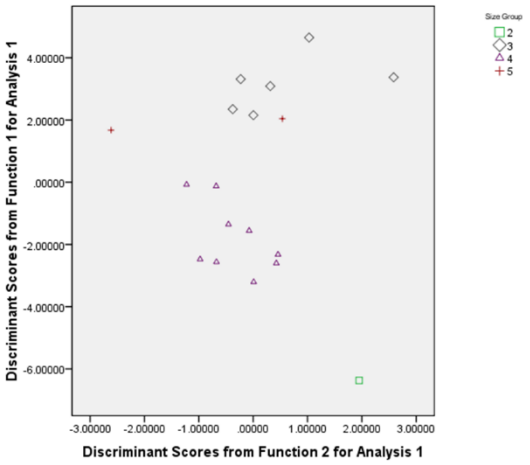

Parietal Ventral

DA

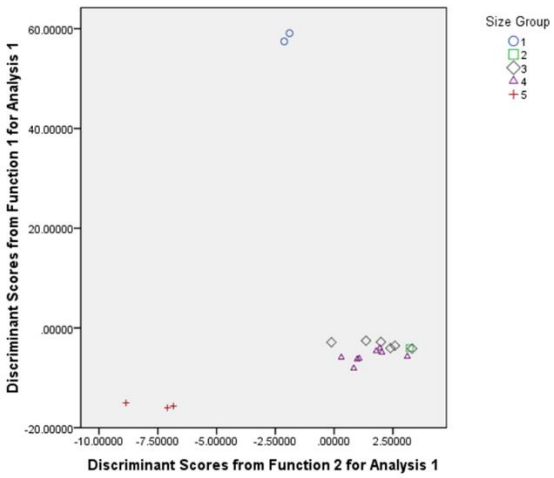

DA Stepwise

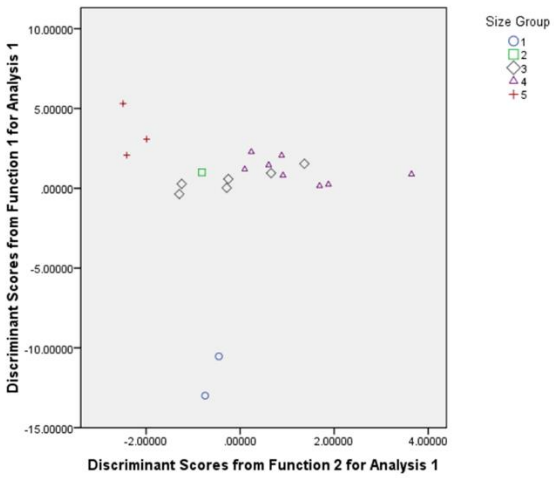

Minus Size Group 1

PCA

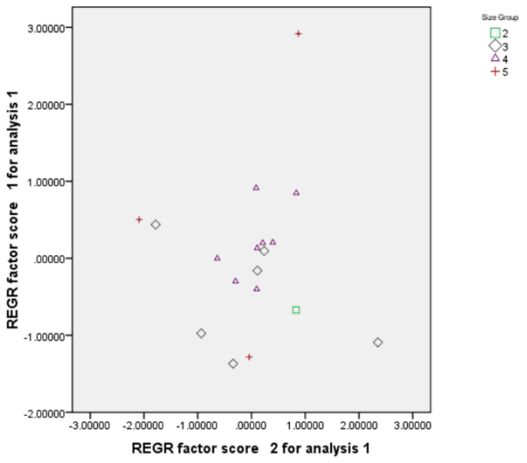

DA

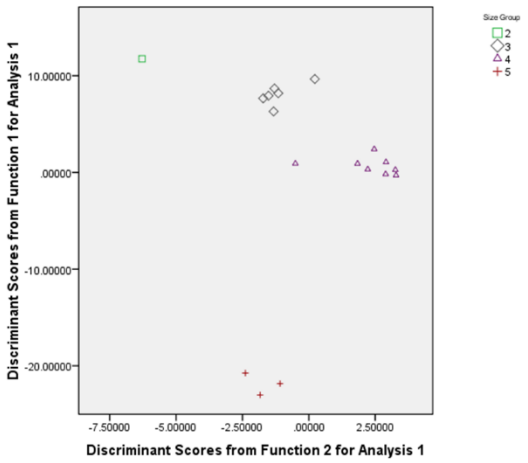

DA Stepwise

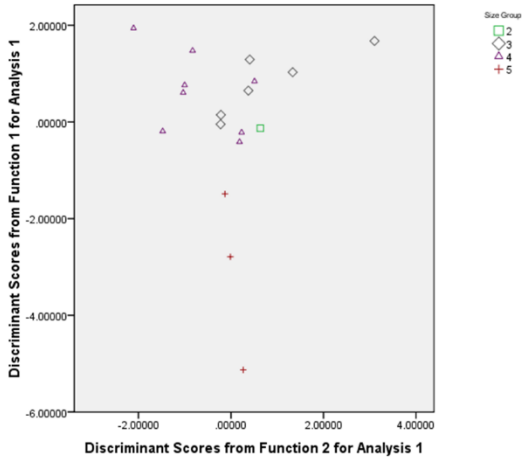

VITA

WILLIAM H HARRIS

Education:	Public Schools, Suwanee and Blairsville, Georgia
	B.A. Biology, Young Harris College, Young Harris, Georgia 2012
	M.S. Geosciences, East Tennessee State University, Johnson City, Tennessee 2015
Professional Experience:	Graduate Assistant, East Tennessee State University, Gray Fossil Site Museum, 2012 – 2014
Honors and Awards:	Who's Who in American Colleges